

THE ROLE OF SPHINGOLIPIDS IN RETINAL VASCULAR INTEGRITY

By

Nermin Mohammad Mohammad Kady

A DISSERTATION

Submitted to
Michigan State University
in partial fulfillment of the requirements
for the degree of

Genetics- Doctor of Philosophy

2017

ABSTRACT

THE ROLE OF SPHINGOLIPIDS IN RETINAL VASCULAR INTEGRITY

By

Nermin Mohammad Mohammad Kady

Diabetic retinopathy is a vision-threatening microvascular complication of diabetes mellitus. The increase in the prevalence of diabetes in the population will most likely lead to a higher incidence of diabetic retinopathy (DR), a devastating complication with limited treatment options. Years of investigations have yet to yield a fully understood mechanism for the causes of vascular dysfunction in DR. Dyslipidemia, as well as hyperglycemia, is a major metabolic insult of diabetes and is positively correlated with the development of DR. The objective of this study is to provide a mechanistic link between retinal dyslipidemia in diabetes and retinal vascular pathology in DR. Our studies revealed two main pathways of sphingolipid metabolism involved in the development of DR. The first pathway leads to disruption of blood retinal barrier (BRB) and thus increased vascular permeability-- an early sign of DR. The second pathway plays a role in retinal endothelial damage and its defective repair.

First, we addressed the link between dyslipidemia and BRB using both *in vitro* and *in vivo* experiments. We demonstrated that diabetes induces down regulation of an essential retinal fatty acid elongase enzyme, Elongation of very long chain fatty acids-4 (ELOVL4), in the diabetic retina. Down regulation of ELOVL4 plays a crucial role in diabetes-induced blood retinal barrier dysfunction. Overexpression of ELOVL4 in retinal endothelial cells enhances barrier properties of retinal vasculature. Ceramides were found to co-localize with tight junction complexes. Lipidomic analysis of tight junction isolates revealed the presence of ELOVL4-produced VLC ceramides, notably, omega-linked acyl-ceramides that were previously identified only in the skin

permeability barrier.

Second, we investigated the effect of dyslipidemia on the function of both cell types involved in revascularization; human retinal endothelial cells (HRECs) and circulating angiogenic cells (CACs). We demonstrated that diabetes induces activation of acid sphingomyelinase (ASM), a key enzyme of sphingolipid metabolism in human retinal endothelial cells (HRECs) and human CD34⁺ CACs. Diabetes induced ASM upregulation has deleterious effect on both retinal endothelial cell and CD34⁺ CAC function. Diabetic HRECs with high ASM showed defective ability to form blood-vessel-like tubular structure and diabetic CD34⁺ CACs with high ASM showed defective incorporation into endothelial tubes formed by HRECs.

Taken together, these findings indicate that modulation of sphingolipid metabolism to normalize retinal vascular dysfunction and improve retinal vascular repair can represent a novel therapeutic strategy for treating DR.

To the soul of my mother

ACKNOWLEDGEMENTS

I would like to express my deep appreciation to those who have contributed to my work and supported me in one way or the other during this exciting journey.

First of all, I would like to express my sincere gratitude to my mentor, Dr. Julia Busik, for her continuous support, motivation and wealth of knowledge. Dr. Busik has supported me not only by growing as a research scientist, but also academically and emotionally along the path to finish my doctorate degree. I greatly appreciate all of her contributions towards helping me find solutions in the lab and towards composing my doctorate literature. Outside of the lab, Dr. Busik and her husband, Dr. Denis, were truly kind and hospitable with their invitation to the whole Busik lab to spend time at their house up North. We all enjoyed their generosity and kindness. I do not exaggerate in the slightest when I say I was incredibly lucky to have the chance to join the Busik lab and have Dr. Busik as a mentor. The pleasure was truly mine.

I would like to thank my committee members Dr. Brian Schutte, Dr. Laura McCabe, Dr. Andras Komaromy and Dr. Simon Petersen-Jones for their support, valuable discussions and constructive criticism throughout all the committee meetings.

I would like to specially thank Dr. Brian Schutte for his tremendous support since day one when Dr. Sainan Wei introduced me to him. I am especially grateful to Dr. Schutte and his team consisting of Dr. Walid Fakhouri, Dr. Youssef Koussa, Dr. Tamer Mansour and Dr. Arianna Smith for their support, help and constructive feedback even during the harder times of my doctorate degree. Discussion with Dr. Schutte at committee meetings pushed me to approach all of my data more critically and with healthy skepticism. I am very grateful to Dr. Laura McCabe for her thorough questioning and gentle but firm encouragement during committee meetings. I

am very appreciative of Dr. Andras Komaromy and his expertise in all things retina related, he was invaluable to my doctorate study. Another special thanks must be made to Dr. Simon Petersen- Jones who not only served as my Genetics Program representative but also helped greatly with his famed experience in gene therapy. The success of my virus experiments is due in no small part to his consultation.

I would like to thank Dr. Barbara Sears, the former Genetics Graduate Program Director. When I applied to the PhD program, Dr. Sears was greatly concerned with the well-being of the graduate students and continued to be concerned throughout my years here at Michigan State University. My first year was quite a trial and Dr. Sears was fabulously supportive in helping me adjust.

I would like to thank Dr. Sainan Wei, the Director of DNA Diagnostics and Cytogenetics Lab in the Department of Pediatrics and Human Development. I first came to the United States as a visiting scholar to be trained by Dr. Wei on different molecular genetic techniques. Dr. Wei encouraged me to apply to the PhD program and introduced me to my future mentor, Dr. Busik. She opened my eyes and played an important role in changing my career. Thank you Dr. Wei.

I am deeply thankful to Dr. David Antonetti of the Kellogg Eye Center at the University of Michigan. His expertise in vascular permeability as well as his collaboration and invaluable scientific input were instrumental to my research. His generosity extended so far as to inviting me to do my in vitro experiments at his lab. The environment and guidance he provided helped me greatly in my research.

I would like to thank Dr. Xuwen Liu from Dr. Antonetti's lab. Dr. Liu taught me how to perform tricky permeability experiments. Dr. Liu also had a great impact on my research skills. He taught me how to stay organized under the culture hood, how to be prepared for my experiments more efficiently as well as teaching me better time management skills for lab. Thank you Xuwen!

I was blessed during this exciting journey to be surrounded by great people; Svetlana Navitskaya, Dr. Qi Wang, Dr. Sandra Hammer, Dr. Harshini Chakravarthy, Chao Huang, Yan Levitsky, Kiera Fisher, Maseray, Cassie Larrivee and Abid Ahmad. I would like to thank Svetlana, for working with me patiently and teaching me different lab techniques especially isolating retinal tissues and culturing cells. I would also like to thank her for her support during hard times. I would like to thank Qi, Harshini, Chao and Sandra for their help during my experiments, for their constructive discussions at lab meetings and for their friendship when we made trips to the MSU Dairy Store for ice cream.

I would like to thank Dr. Todd Lydic, our collaborator in the Department of Chemistry, for his expertise in mass spectrometry and for analyzing my lipid samples. I would also like to thank Dr. Maria Grant and Dr. Eleni Beli, our collaborators from Indiana University, for providing blood samples for my experiments.

I am deeply grateful to Dr. Sandra O'Reilly for teaching me how to handle mice with great confidence and for showing me different in vivo techniques. Thank you, Sandra, for taking time out of your busy schedule to teach me. I would also like to thank Dr. Melinda Frame for her assistance in confocal microscopy. I really enjoyed your class, Dr. Frame, which was of great help when scanning my images. I wish to express my deepest appreciation to Alicia Withrow for her skills with cutting, embedding and staining my retina samples for electron microscopy. I would also like to thank Amy Porter and Kathy Campbell for their help with my immunocytochemistry slides.

I would like to thank my undergraduate assistants Meesum Syed, John Jarad and Kent Gamber. They worked tirelessly on the project during the late part of my work, spending hours during

their weekends for tight junction isolations. Good luck on your next steps in your careers and educations!

I am forever grateful to my professors and friends back home at Mansoura University for their faith in my abilities and for their support.

I would like to thank my mother and father in law for their support and unconditional love and especially their encouragement in my doctoral pursuit.

I am deeply grateful to my father, Dr. Mohamed Kady, for shaping my interest in science—you are the greatest inspiration for me. Your emotional support, sacrifice, patience, encouragement and faith in my abilities have been a great pillar of strength for me throughout my PhD journey. I am truly thankful to my sisters, Eman and Aya, for always being there for me and showering me with support. To my father and sisters, thank you for helping fortify my career. And special thanks for your unconditional love.

Finally, I would like to thank my beloved husband, Amir Abougabal, for his constant, steady support and for his love.

I would not have made it this far without all of you. Thank you so much, I hope to make you all proud.

TABLE OF CONTENTS

LIST OF TABLES	xii
LIST OF FIGURES	xiii
KEY TO ABBREVIATIONS.....	xv
Chapter 1. Introduction.....	1
1.1 Background	1
1.2 Diabetic retinopathy	2
1.2.1 Introduction.....	2
1.2.2 Clinical classification of diabetic retinopathy	4
1.2.2.1 Pre-clinical diabetic retinopathy	5
1.2.2.2 Non-proliferative diabetic retinopathy	5
1.2.2.3 Diabetic macular edema	6
1.2.2.4 Pre-proliferative diabetic retinopathy	6
1.2.2.5 Proliferative diabetic retinopathy	7
1.2.3 Current treatment options	7
1.3 Diabetes induced blood retinal barrier breakdown.....	9
1.3.1 Retinal blood supply	9
1.3.2 Blood retinal barrier and tight junction	10
1.3.2.1 Proteins forming tight junction	14
1.3.2.2 A lipid-protein hybrid model of tight junction.....	17
1.3.3 Blood retinal barrier breakdown in diabetic retinopathy.....	18
1.3.3.1 Tight junction modulation	18
1.3.3.2 Endothelial cell loss.....	19
1.3.3.3 Pericyte loss	20
1.3.3.4 Leukostasis.....	21
1.3.3.5 Glial cell dysfunction	22
1.4 Diabetic dyslipidemia.....	23
1.4.1 Fatty acids.....	24
1.4.2 Dyslipidemia and diabetic retinopathy	26
1.4.3 Retinal lipid composition in diabetes	27
1.4.4 Fatty acid elongase, ELOVL4, and very long chain ceramides.....	28
1.4.5 ASM and short chain ceramides.....	33
1.5 Reparative circulating angiogenic cells	34
1.6 Objectives of the dissertation	36
1.7 Overview of chapters	38
REFERENCES.....	39

Chapter 2. Overexpression of ELOVL4 stabilizes tight junctions and prevents VEGF-induced vascular permeability in diabetic retina and retinal cells.....	58
2.1 Abstract.....	58
2.2 Introduction.....	60
2.3 Materials and methods	63
2.3.1 Cell culture	63
2.3.2 Virus-mediated hELOVL4 overexpression	63
2.3.3 siRNA transfection.....	64
2.3.4 Permeability assay in vitro	64
2.3.5 Western blotting.....	65
2.3.6 Quantitative real-time PCR	66
2.3.7 Immunocytochemistry	67
2.3.8 Immunogold electron microscopy	69
2.3.9 TJ isolation and mass spectrometry	69
2.3.10 Animal model	70
2.3.11 Retinal vascular permeability	71
2.3.12 Immunohistochemistry	72
2.3.13 Statistical analysis	72
2.4 Results	73
2.4.1 Expression level of ELOVL4 controls retinal endothelial permeability.....	73
2.4.2 ELOVL4 overexpression prevents VEGF- and IL-1 β induce increase in permeability.....	76
2.4.3 ELOVL4 overexpression increases the barrier properties of tight junction complex	78
2.4.4 Ceramide co-localizes with tight junction complex	81
2.4.5 Identification of VLC omega-linked acyl-ceramide species in the tight junction complex	85
2.4.6 Verification of AAV2 mediated expression of hELOVL4 in mouse retina	90
2.4.7 AAV2-hELOVL4 overexpression prevents diabetes-induced increase in retinal vascular permeability in vivo	94
2.5 Discussion.....	96
REFERENCES.....	101

Chapter 3. Increase in acid sphingomyelinase level in human retinal endothelial cells and CD34⁺ circulating angiogenic cells isolated from diabetic individuals is associated with dysfunctional retinal vasculature and vascular repair process in diabetes.....	109
3.1 Abstract.....	109
3.2 Introduction.....	111
3.3 Materials and methods	114
3.3.1 Circadian study of human CD34 ⁺ CACs	114
3.3.2 Postmortem imaging of human retina and cell culture.....	114
3.3.3 Human CD34 ⁺ CACs isolation.....	116
3.3.4 Tube formation assay	116
3.3.5 Quantitative real-time PCR	117

3.3.6 ELISA assay	117
3.3.7 Statistical analysis	117
3.4 Results	122
3.4.1 ASM expression level is increased in HREC, CD34 ⁺ CACs and blood plasma of diabetic donors.....	122
3.4.2 Diabetes induces decrease in HREC tube formation.....	123
3.4.3 Diabetes induced increase in ASM is associated with CD34 ⁺ CACs dysfunction.....	125
3.4.4 Diabetes induced increase in ASM is associated with loss of circadian release of CD34 ⁺ CACs	128
3.5 Discussion.....	130
REFERENCES.....	134
Chapter 4. Summary and future perspectives	141
4.1 Summary.....	141
4.2 Future perspectives	143

LIST OF TABLES

Table 1. Average body weights and non-fasting blood glucose level of control and diabetic mice.....	91
Table 2. Clinical characteristics of control and diabetic subjects involved in the circadian study	118
Table 3. Clinical characteristics of control and diabetic HRECs donors and CD34⁺ CACs subjects involved in the study	120

LIST OF FIGURES

Figure 1. Frequency of retinopathy by duration of diabetes in years.....	3
Figure 2. The anatomy of the retina.....	10
Figure 3. Intercellular Junctions	12
Figure 4. Morphology of the tight junction	13
Figure 5. Schematic representation of different constituents of tight junction.....	14
Figure 6. Schematic diagram of VLC-FA and VLC-PUFA biosynthetic pathways mediated a series of elongation and desaturation reactions	30
Figure 7. Synthesis of VLC ceramides	32
Figure 8. Acid sphingomyelinase (ASM) is a central enzyme of sphingolipid metabolism.....	34
Figure 9. Expression level of ELOVL4 controls retinal endothelial permeability	74
Figure 10. ELOVL4 overexpression block cytokine-induced retinal endothelial cell permeability.....	77
Figure 11. ELOVL4 overexpression increases the barrier properties of the tight junction complex	79
Figure 12. Ceramide co-localizes with tight junction complex	82
Figure 13. Tight junction ceramide content	87
Figure 14. Verification of AVV2 mediated expression of hELOVL4 in mouse retina	92
Figure 15. ELOVL4 overexpression prevents diabetes-induced vascular leakage in mice.....	95
Figure 16. Diabetes induced increase in ASM expression.....	122
Figure 17. Diabetes impairs tube formation capacity of HRECs	124
Figure 18. Reduced incorporation of diabetic CD34⁺ CACs into diabetic HRECs tubes	126

Figure 19. Loss of circadian release of diabetic CD34⁺ CACs..... 129

KEY TO ABBREVIATIONS

AAV2	Adeno-associated virus serotype 2
ACCORD	Action to Control Cardiovascular Risk in Diabetes
adMD	Autosomal dominant macular dystrophy
AGEs	Advanced glycation end products
AJ	Adherens junction
ALA	Alpha-linolenic acid
AP	Apical
ASM	Acid sphingomyelinase
Bl	Basolateral
BRB	Blood retinal barrier
BRECs	Bovine retinal endothelial cells
CACs	Circulating angiogenic cells
cDNA	Complementary deoxyribonucleic acid
Cer	Ceramides
CETP	Cholesteryl ester transfer protein
ChREBP	Carbohydrate-regulatory element binding protein
CMV	Cytomegalovirus
CSME	Clinically significant macular edema
CVD	Cardiovascular disease
CXCR-4	C-X-C chemokine receptor type 4

DAPI.....4', 6-Diamidino-2-phenylindole, Dihydrochloride
DCCTDiabetes Control and Complications Trial
DCCT/EDIC Diabetes Control and Complications Trial/ Epidemiology of Diabetes Interventions and Complications
DHA..... Docosahexaenoic acid
DM Diabetes mellitus
DME Diabetic macular edema
DPBS Dulbecco's phosphate-buffered saline
DR..... Diabetic retinopathy
DS Desmosome
ELISA..... Enzyme-linked immunosorbent assay
ELOVL.....Elongation of very long chain fatty acids
EPA.....Eicosapentaenoic acid
ETDRS Early Treatment of Diabetic Retinopathy Study
FA Fatty acid
FADS Fatty acid desaturases
FAS.....Fatty acid synthase
FBS Fetal bovine serum
FCS Fetal calf serum
FIELD Fenofibrate Intervention and Event Lowering in Diabetes
FITC-albuminFluorescein isothiocyanate-albumin
GAPDH Glyceraldehyde-3-phosphate dehydrogenase
GlcCer Glucosylceramides

GUK **Guanylate kinase domain**

HCD..... **High energy collisional dissociation**

HDL **High density lipoprotein**

hELOVL4 **Human elongation of very long chain fatty acid 4**

HRECs **Human retinal endothelial cells**

HSCs..... **Hematopoietic stem cells**

HSL..... **Hormone -sensitive lipase**

ICAM-1 **Intercellular adhesion molecule-1**

IDF..... **International Diabetes Federation**

IL-1 β **Interleukin-1 beta**

iNOS **Inducible nitric oxide synthase**

IRMA **Intraretinal microvascular abnormalities**

JAMs **Junctional adhesion molecule**

LA..... **Linoleic acid**

LDL **Low density lipoprotein**

LPL..... **Lipoprotein lipase enzymes**

LXR **Liver X receptor**

MA..... **Microaneurysm**

MAGUK..... **Membrane –associated guanylate kinase**

MDCK..... **Madin- Darby canine kidney cells**

MMPs **Matrix metalloproteinases**

MNCs **Mononuclear cells**

mRNA..... messenger ribonucleic acid
MUFAs Monounsaturated fatty acids
Mv.....Microvilli
NA.....Numerical aperture
NADPHNicotinamide adenine dinucleotide phosphate, reduced form
NEFA.....Non-esterified fatty acids
NO..... Nitric oxide
NPDR Non-proliferative diabetic retinopathy
OCTOptical coherence tomography
OsOS4..... Osmium tetroxide
PBS Phosphate buffer saline
PCs..... Phosphatidylcholines
PDGF- β Platelet-derived growth factor- β
PDGFR β Platelet-derived growth factor receptor- β
PDR Proliferative diabetic retinopathy
PDZ..... Postsynaptic density protein-95/Drosophila disc large tumor suppressor Dlg1/Zonula occludens-1
PKC Protein kinase C
PPAR- α Peroxisome proliferator-activated receptor alpha
qPCRquantitative polymerase chain reaction

PUFA Polyunsaturated fatty acid
RBC Red blood cell
RITC..... Rhodamine B isothiocyanate-Dextran
RPE..... Retinal pigment epithelia cells
S.E.M...... Standard error of the mean
SCDs Stearoyl-coA desaturases
SDF-1 Stromal cell-derived factor-1
SDSSodium dodecyl sulphate
SH3 Src homology 3 domain
siRNASmall interfering RNA
SM.....Sphingomyelin
smCBACMV-chicken - β actin
SREBP-1c..... Sterol regulatory element binding protein-1c
STGD3.....Stargardt-like macular dystrophy
STZ.....Streptozotocin
TBSTris-buffered saline
TER Transendothelial electrical resistance
TGF- β Transforming growth factor - β
TJ Tight junction
TNF- α Tumor necrosis factor- α
VEGFVascular endothelial growth factor

VLC-PUFA **Very long chain polyunsaturated fatty acid**
VLC **Very long chain**
VLCFA..... **Very long chain fatty acid**
VLDL**Very low-density lipoprotein**
WESDR.....**Wisconsin Epidemiologic Study of Diabetic Retinopathy**
WHO **World Health Organization**
ZO-1 **Zonula occludens-1**

Chapter 1. Introduction

1.1 Background

Diabetes mellitus (DM) is a serious endocrine disease characterized by chronic hyperglycemia--which results from defective insulin production or action. Defective insulin action leads to impaired carbohydrate, protein and fat metabolism. The American Diabetes Association diagnoses diabetes as fasting plasma glucose ≥ 126 mg/dl (7.0 mmol/l) or A1C $\geq 6.5\%$ (1).

Diabetes mellitus is classified into two major etiological categories; type 1 or type 2. Type 1 DM, previously defined as insulin-dependent DM, is characterized by absolute insulin deficiency due to autoimmune destruction of insulin secreting pancreatic β -cells of the islets of Langerhans. Insulin-dependent DM, generally occurring in children and adolescents, accounts for approximately 10 % of diabetic patients (1,2). Type 2 DM, previously designated as non-insulin -dependent DM, is due to insulin resistance in peripheral tissue and defective compensatory insulin secretion from β cells. Type 2 DM accounts for 90-95% of all cases of diabetes and occurs mostly in adults. Type 2 DM is normally correlated with obesity and a sedentary lifestyle (3-5).

Approximately 415 million people are estimated to currently have diabetes worldwide, this number is estimated to increase to approximately 642 million (or 1 in 10 adults) by 2040 (6).

The 2015 International Diabetes Federation (IDF) estimates 5 million deaths caused by diabetes every year (1 person every 6 seconds) (6-8). In addition, The World Health Organization (WHO) projects that diabetes will be the 7th main cause of death in 2030 (9). The estimated total medical cost of diagnosed diabetes is more than 300 billion dollars per year (10).

Complications of diabetes can be divided into macrovascular and microvascular disorders. The macrovascular complications include coronary heart disease, cerebrovascular disease and peripheral vascular disease. The microvascular complications include diabetic retinopathy (DR), diabetic nephropathy, and diabetic neuropathy. These complications highlight the importance of diabetes as a major public health problem.

1.2 Diabetic retinopathy

1.2.1 Introduction

Diabetic retinopathy (DR) is one of the most common and feared complications of diabetes, affecting approximately 93 million people worldwide. Of the 93 million, 28 million suffer from vision-threatening complications such as proliferative diabetic retinopathy (PDR) and /or diabetic macular edema (DME) (11). In both type 1 and type 2 DM, the prevalence of DR is strongly associated with the duration of diabetes. Nearly all patients with type 1 diabetes and > 60% of patients with type 2 diabetes have some degree of retinopathy after 20 years of the disease (12). In the Wisconsin Epidemiologic Study of Diabetic Retinopathy (WESDR), it was found that duration of diabetes is a strong predictor for development and severity of diabetic retinopathy. WESDR found that the frequency of any retinopathy among type 1 diabetes was 2% in those with < 2 years duration of diabetes, 25% after 5 years and 97.5% at 15 or more years of diabetes. Furthermore, frequency of PDR was very rare before 10 years of diabetes, nonexistent at 3 years, 4% after 10 years and 25% after 15 years of diabetes (Figure 1) (13). DR is the leading cause of visual impairment in the world; 3.6% of type 1 diabetics and 1.6% of type 2 diabetic individuals suffered from vision loss. In type 1 diabetes, 86% of the vision loss resulted in blindness from DR, mostly due to neovascularization of the proliferative stage (12,14). 33% of

vision loss in type 2 diabetic individuals resulted in complete vision loss from DR, mostly due to macular edema and very rarely PDR (12,14).

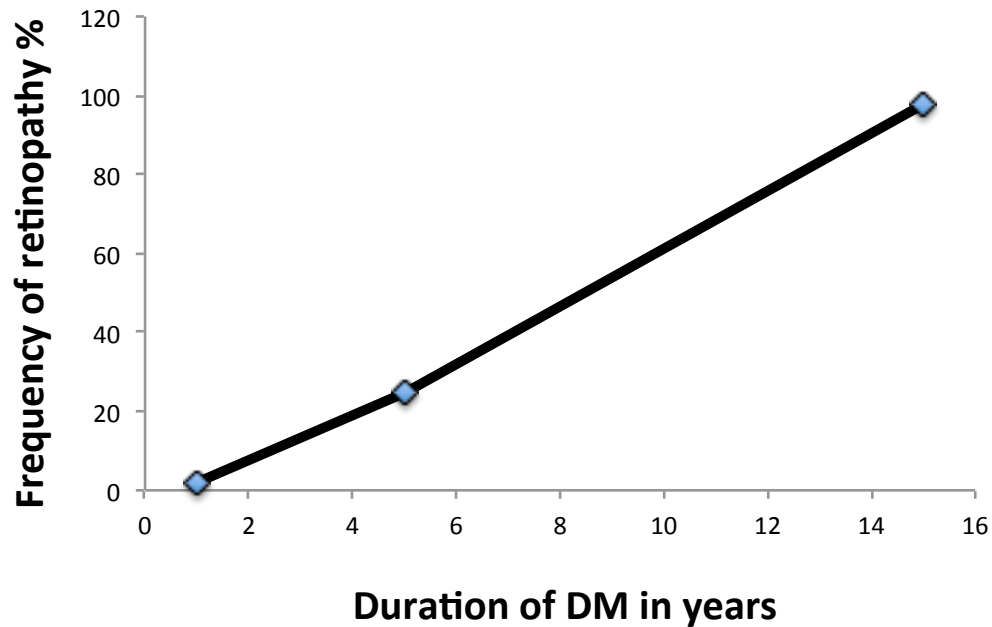


Figure 1. Frequency of retinopathy by duration of diabetes in years. The development and the severity of diabetic retinopathy is directly correlated with duration of diabetes (Modified form Klein et al., 1984) (13).

1.2.2 Clinical classification of diabetic retinopathy

Diabetic retinopathy is a chronic, progressive sight-threatening disease, with multiple retinal lesions accumulating along the course of the pathology. It is essential to classify and stage the severity of the disease in order to provide more effective therapeutic strategies to prevent the progression of DR. Retinal lesions seen in the fundus can be classified into 3 categories. Category 1 retinal lesions result from the breakdown of the blood retinal barrier and leaky vasculature (observed as hemorrhage, hard exudate, retinal edema). Category 2 retinal lesions result from structural changes in vascular wall (observed as microaneurysms). Lastly, category 3 retinal lesions result from ischemic changes (observed as soft exudate or cotton wool spots, intraretinal microvascular abnormalities (IRMA), neovascularization, vitreous hemorrhage and fibrous tissue formation) (15). Many attempts were made to develop standardized classification of DR. From 1968, there was the Airlie House Symposium classification that was modified for use in the Early Treatment of Diabetic Retinopathy Study (ETDRS). ETDRS was the gold standard classification system for DR. It graded retinopathy using 7 standard stereophotographic fields, classifying DR retinal lesions into 13 levels ranging from level 10 (no retinopathy) to level 85 (advanced proliferative diabetic retinopathy with vitreous hemorrhage, neovascularization or retinal detachment at the center of the macula). The term “clinically significant macular edema (CSME)” was first introduced by ETDRS, see below for details (16). The complexity of the ETDRS grading system rendered the scale to be clinically inapplicable. Another classification has been proposed by Wilkinson et al. 2003 in an attempt to simplify the classification of DR-- the International Clinical Disease Severity Scale of DR. It is based on WESDR and ETDRS classification, the retinopathy pathology is graded into 5 stages; (1) no apparent retinopathy; no diabetic fundus lesions, (2) mild non-proliferative diabetic retinopathy;

few microaneurysms, (3) moderate non-proliferative diabetic retinopathy; microaneurysm, hemorrhage or venous beading, (4) severe non-proliferative diabetic retinopathy; 4:2:1 rule, hemorrhages exist in the 4 quadrants, venous beading in 2 quadrants or more and IRMA in 1 quadrant or more, and finally, (5) proliferative diabetic retinopathy; neovascularization, vitreous hemorrhage or tractional retinal detachment (17). Stages of DR are listed below:

1.2.2.1 Pre-clinical diabetic retinopathy is characterized by subtle alterations that occur before ophthalmoscopic signs of DR. These alterations are not visible on fundus examination but they were demonstrated by histology and fluorescein angiography. Early alterations include pericyte loss, thickening of the blood vessel basement membrane, capillary occlusion and endothelial cell degeneration and loss (18,19).

Another prominent feature of this stage is diffuse mild BRB loss with increased vascular permeability (20,21). In addition, neurosensory dysfunction and altered color vision were also detected in this stage (22).

1.2.2.2 Non-proliferative diabetic retinopathy

This stage is characterized by visible retinal lesions upon fundus examination. Lesions include microaneurysms (MAs), intraretinal hemorrhage, hard exudates and altered blood retinal barrier (14).

MA is one of the earliest ophthalmoscopic signs, it appears as red dot with a well-defined border. With fluorescein angiography, MAs appear hyperfluorescent and leaky (23). MA is usually associated with loss of pericytes, thickening of the blood vessel basement membrane, capillary closure affecting both the arterial and venous side of the circulation at the posterior pole of

the retina (24,25). An interesting feature of MAs is that counting rate of MA formation and disappearance has been demonstrated as a good indicator of retinopathy progression (14,26).

Intraretinal hemorrhage results from breakdown of MAs or small vessels. Hard exudates result from extravascular leakage of lipids or lipoproteins into retinal tissue appearing as yellow glistening deposits close to the macula. Abnormal blood retinal barrier leads to accumulation of fluid in retinal tissue resulting in retinal edema.

1.2.2.3 Diabetic macular edema is the main cause of vision loss, particularly, in type 2 diabetes (27,28). Altered blood retinal barrier results in accumulation of fluid in the retinal tissue especially in macular area and is detected by optical coherence tomography (OCT). Progression of edema depends on Starling law, where the gradient induced between plasma blood pressure, tissue pressure and tissue osmotic pressure play important roles in controlling movement of fluids (29).

ETDRS introduced a definition for clinically significant macular edema, where the diagnosis mainly depends on the presence of retinal thickening or hard exudates at or within 500 microns of the center of the macula (16).

1.2.2.4 Pre-proliferative diabetic retinopathy Its name indicates increased risk of progression to proliferative retinopathy. This stage is characterized by signs of retinal ischemia: soft exudates or cotton wool spots, venous beading, IRMAs and several areas of capillary non-perfusion. Cotton wool spots are grayish white areas due to nerve fiber infarction which result from occlusion of pre-capillary arterioles (30). The presence of a high number of cotton wool spots (more than eight in one eye) is indicative of a severe case that may progress into the proliferative

stage (31). IRMAs represent non-leaky collaterals next to non-perfused areas (32).

1.2.2.5 Proliferative diabetic retinopathy is a vision threatening complication particularly in type 1 diabetes (14). It is characterized by neovascularization, that arise either from the optic disc, retina or iris. These new blood vessels are fragile and leaky with an abnormal blood retinal barrier. They pierce the internal limiting membrane causing vitreous hemorrhage, fibrosis and retinal detachment. These vessels usually arise secondary to massive areas of capillary occlusion and retinal ischemia, which in turn stimulates the production of angiogenic factors (33). Capillary occlusion usually results from inflammatory changes, microthrombosis and apoptosis (19).

In summary, impaired vision or vision loss usually takes place in the late stage of the disease, due to either macular edema or neovascularization.

1.2.3 Current treatment options

Diagnosis of patients in the very early stages of the disease (preclinical stage) before developing vision-threatening lesions provide the best window of opportunity for therapy, especially since this category of patients represent a majority and respond better to intensive diabetic therapy (34). Controlling diabetes-induced metabolic dysregulation is a milestone of DR treatment and can be achieved through optimizing blood-glucose levels (35). Tight glycemic control (HbA1C < 7 %) has become a standard intervention to slow down the development of DR. Several clinical trials (DCCT, UKPDS) have shown the benefit of intensive glycemic control in both type 1 and type 2 diabetic patients (36,37). However, maintaining the recommended blood-glucose level was found to be difficult in many patients. Moreover, tight glycemic control was associated with

critical complications such as hypoglycemic episodes and diabetic ketoacidosis. In the ACCORD clinical trial, intensive glycemic control was associated with increased mortality rate in type 2 diabetics especially those at high risk of cardiovascular events (38). Thus glycemic control should be aimed with great caution and each patient should be treated individually. Until recent years, laser photocoagulation was the only available therapeutic option for treating either proliferative diabetic retinopathy (PDR) or diabetic macular edema (DME) (39). Although proven beneficial, laser photocoagulation does not result in vision improvement but rather results in slowing the vision loss. It is also associated with some adverse effects: night blindness, color vision changes, reduced contrast sensitivity, acute glaucoma and worsening of macular edema (35).

These adverse effects of laser photocoagulation brought the need for new approaches in treating DR. Recently introduced intravitreal injection of anti-VEGF agents is considered a new modality in treating both PDR and diabetic macular edema. This class of drugs include: Pegaptanib (Macugen, RNA aptamer), Ranibizumab (Lucentis, recombinant antibody fragment (Fab)), Bevacizumab (Avastin, monoclonal antibody), and Aflibercept (Regeneron, fusion protein of VEGF receptors) (35,39,40). All these agents act by neutralizing the proangiogenic factor VEGF and inhibiting VEGF-induced blood retinal barrier breakdown and retinal neovascularization. However, this is an invasive approach of short duration, requiring repeated intravitreal injections with increasing incidence of local complications; endophthalmitis, vitreous hemorrhage and retinal detachment (40). Although, VEGF has been identified as playing an important role in the development of DR, endogenous VEGF is important for the survival and maintenance of retinal neurons (41) and photoreceptors (42), so great caution is required during long-term therapy. Other treatment options are also available as intravitreal injection of corticosteroids and

vitrectomy both are invasive with local complications. The currently available treatment options are highly invasive and only improve vision but do not restore it completely. Identification of novel therapeutic strategies aiming to prevent vision-threatening lesions of DR is crucial.

1.3 Diabetes induced blood retinal barrier breakdown

1.3.1 Retinal blood supply

The retina is a transparent multi-layer neural tissue (Figure 2). It is responsible for converting visible light into electrochemical impulses that are transmitted via the optic nerve to the cerebral visual cortex for interpretation of the image. This requires a protective environment with minimal interference to the passage of light which is supported by a unique vascular structure with restrictive or selective control of permeability for proper vision (34). Furthermore, the retina is a highly metabolically active tissue with the highest oxygen consumption per unit weight (43). In order to achieve this metabolic support with minimal interference to passage of light, the retina receives dual blood supply from the choriocapillaries and the retinal capillaries. The outer retina (photoreceptors) is supplied by the choriocapillaries while the inner retina is supplied by retinal capillaries originating from central retinal artery (44). The endothelium of choriocapillaries is highly fenestrated while that of retinal capillaries lack fenestration and possess selective barrier function.

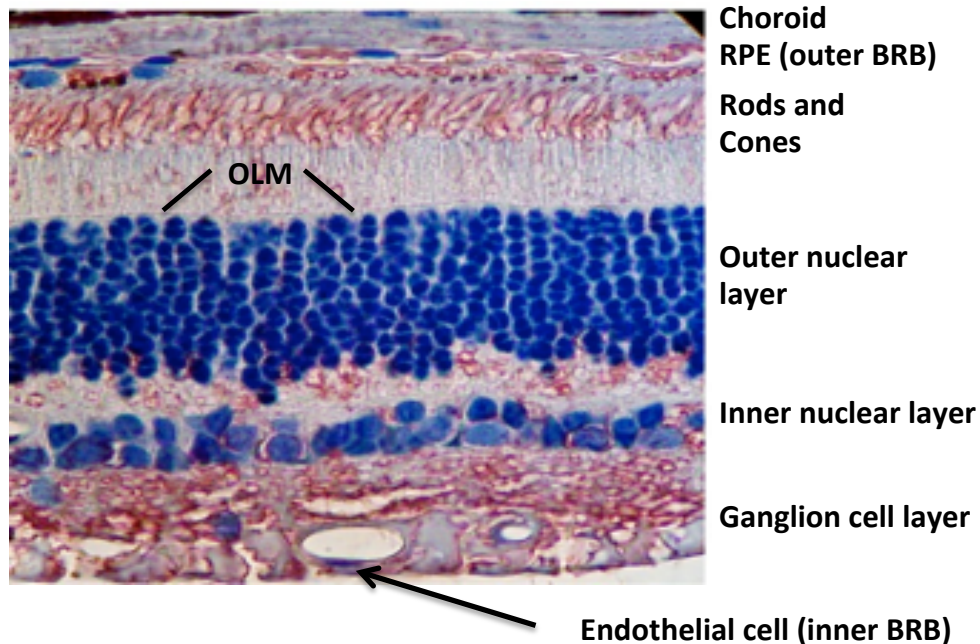


Figure 2. The anatomy of the retina. Image of rat retina showing the retinal layers. Anti-glucose transporter 1 staining (brick color) was used and nuclei were detected with DAPI (blue color). The blood retinal barrier (BRB) is formed of tight junctions, between retinal capillary endothelial cells (inner BRB) and retinal pigment epithelial cells (RPE, outer BRB). OLM: outer limiting membrane.

1.3.2 Blood retinal barrier and tight junction

The regulation of the flux of blood-born solutes and fluids into the retinal tissue is controlled by the outer and inner blood retinal barriers (BRB) (Figure 2). The outer BRB is formed by the tight junctions between retinal pigment epithelial cells (RPE) and the inner BRB is formed by the retinal neurovascular unit composed of tightly adherent retinal capillary endothelial cells surrounded by pericytes and glial cells (Muller and astrocytes) (45) . Pericytes and glial cells play an important role in the development and stabilization of the inner BRB through their direct

physical contact and intercellular signaling with the capillary endothelial cells. Pericyte recruitment to endothelial cells through PDGF- β /PDGFR β was found to be essential for tight junction formation (46). Another well-known pathway is Angiopoietin-1/Tie2, where pericytes secrete angiopoietin-1 inducing phosphorylation of Tie-2 on endothelial cells and promoting endothelial cell maturation (47), vessel integrity (48) and inducing tight junction occludin expression (49). The physical integrity of these cells is essential for regulating BRB; any disturbances by pathological condition, as in DR, will cause barrier integrity dysfunction.

Retinal capillary endothelial cells regulate the transport of the solutes through 2 pathways; the paracellular pathway and the transcellular pathway. Retinal endothelial cells are characterized by low rate of transcellular pathways (50) through membrane transporter, vesicle- (caveola), receptor- or carrier- mediated transport (51). The paracellular pathway is mostly regulated by the tight junction, the most apical part of inter-endothelial junctional complex, and also regulated by adherens junctions, desmosomes and gap junction (Figure 3).

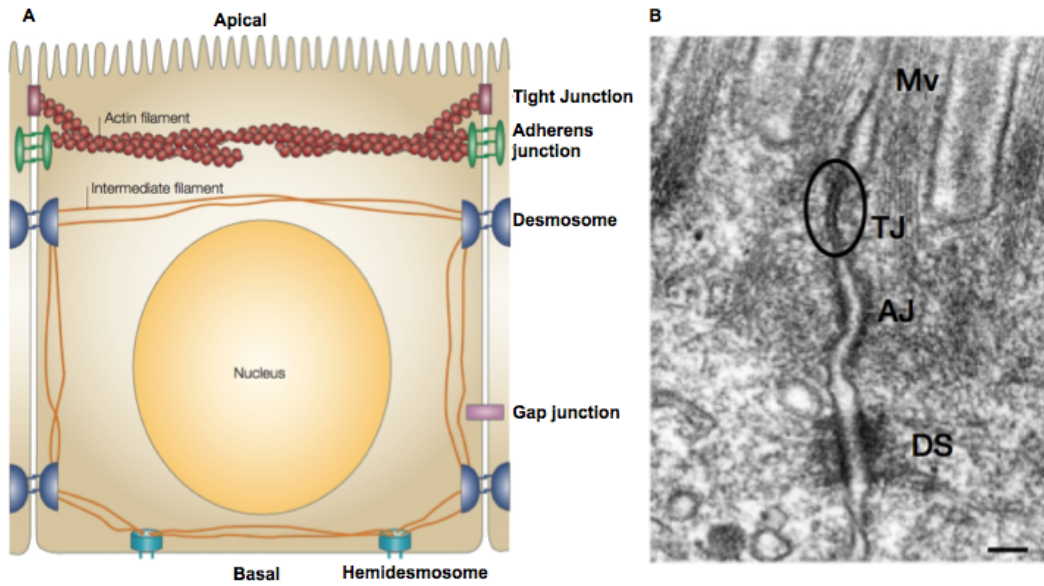


Figure 3. Intercellular Junctions. A. Schematic representation of different structures within the intercellular junctional complex (adapted from Matter and Balda, 2003) (52). B. Electron micrograph showing main structures of the intercellular junctional complex from apical to basolateral surface (adapted from Tsukita *et al.*, 2001) (53). Mv: microvilli, TJ: tight junction, AJ: adherens junction, DS: desmosome.

The tight junction is a multifunctional structure with (1) barrier functions regulating paracellular passage of water and water-soluble ions, (2) fence functions, preventing diffusion of lipid and proteins between the apical and basolateral membrane (54), (3) cell signaling functions, controlling cell proliferation and gene transcription (55). By electron microscopy, tight junctions appear as an area where the plasma membranes of two adjacent cells come together and fuse, obliterating the intercellular space (56). While by freeze –fracture microscopy they appear as anastomosing band-like mesh work (57) (Figure 4).

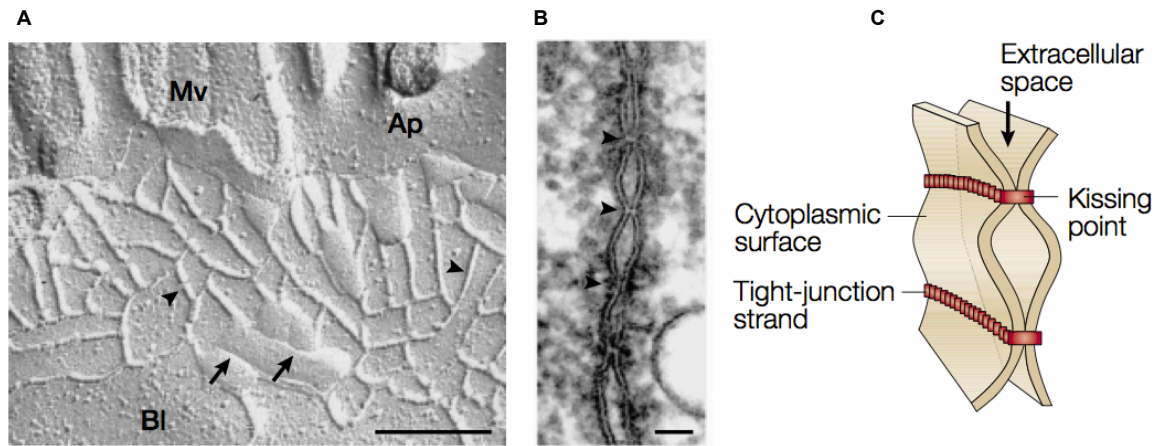


Figure 4. Morphology of the tight junction. A. Freeze-fracture replica electron microscope of the tight junction. Tight junction appears as continuous, anastomosing fibrils (arrowheads) on the P face with grooves on the E face (arrows). (Mv: microvilli, AP: apical membrane, Bl: basolateral membrane). B. Ultrathin sectional view of tight junctions, showing kissing points of tight junctions (arrowheads), where the intercellular spaces are obliterated. C. Schematic structure of tight junction strands (adapted from Tsukita *et al.*, 2001) (53).

Tight junctions are composed of distinct transmembrane proteins including claudin, occludin, and junctional adhesion molecule (JAMs) that are coupled to the intracellular anchoring or scaffolding protein zonula occludens (ZO) which is linked to the actin cytoskeleton (Figure 5). Some of these proteins are stable, while others cycle continuously between the plasma membrane and intracellular compartments and also along or within the plasma membrane. This cycling provides the dynamic nature of the junction; opening and closing in response to variable stimuli and regulating the inter-endothelial passage of different molecules (58,59).

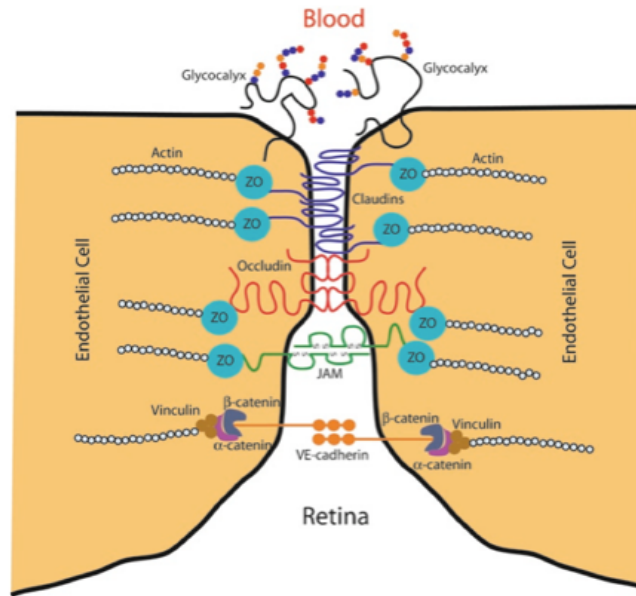


Figure 5. Schematic representation of different constituents of tight junction. Tight junctions are composed of several transmembrane proteins including, claudin, occludin, junctional adhesion molecule (JAMs) that are coupled to the intracellular scaffolding protein zonula occludens (ZO), which is linked to the actin cytoskeleton (adapted from Runkle and Antonetti, 2011) (45).

1.3.2.1 Proteins forming tight junction

- Occludin. Occludin, a 65 KDa transmembrane protein, was the first integral membrane protein identified as part of the tight junction of chicken liver by Furuse et al. (1993) (60). It is tetraspan transmembrane protein with two extracellular loops, one intracellular loop and cytoplasmic amino- and carboxy-termini. Occludin physically interacts with a number of proteins through its carboxy- and amino- termini. The carboxy terminus of occludin interacts with ZO-1 (61), ZO-2 (62), gap junction protein connexin 32 (63), or occludin itself (64). ZO-1 interaction with

occludin plays an important role in (1) connecting occludin with actin cytoskeleton (65) and (2) localization of occludin at the tight junction (61). Its amino- terminus was found to interact with Itch and E3 ubiquitin-protein ligase (59,66).

Occludin is expressed mainly at the tight junctions of endothelial and epithelial cells (60). Occludin is a functional constituent of the paracellular barrier, where its expression correlates with barrier properties of different tissues. Occludin is expressed at higher levels in endothelial cells with tight barrier property as in arterial, brain, and retinal endothelium compared to those with other barriers as in venous endothelium or endothelial cells of non-neuronal tissue (67,68). Moreover, increased expression of occludin in bovine retinal endothelial cells was associated with decreased paracellular permeability (69), while silencing of occludin decreased barrier property and increased permeability (67,70,71). Although occludin is an essential determinant of tight junction permeability, it is not required for tight junction formation (72,73).

- Claudins. Claudins, a large family of 24 transmembrane proteins (20-27 KDa) (53) , are tetraspan transmembrane proteins with two extracellular loops and cytoplasmic amino- and carboxy-termini. The carboxy termini interacts with ZO family protein (74) and was found to be essential in targeting claudin proteins into tight junctions (75). Claudin-1, -5,-15 are specifically expressed in endothelial cells and constitute blood retinal barrier (76). Unlike occludin, claudin was found to be an important regulator of tight junction formation. A number of studies showed expression of either claudin-1 and -2 or claudin-5 in fibroblast reconstituted tight junction strands (76,77).

In addition, claudin regulates barrier function of the tight junction, where overexpression of claudin in MDCK cells results in increased TER and decreased paracellular permeability (78).

In claudin-5 deficient mice paracellular permeability to small molecules was severely impaired (79). In retinal tissue, hypoxia-induced decrease in claudin-5 was associated with increased vascular permeability and impaired barrier function (80).

Collectively, Claudins play a critical role in tight junction formation and regulation of barrier function.

- The Zonula occludens family. ZO-1 (210-225 KDa) was the first protein to be discovered in association with tight junction (81). Later other members of the family were discovered, ZO-2 (160KDa) (82) and ZO-3 (130 KDa) (83), they were found to co-immunoprecipitate with ZO-1. ZO proteins belong to the membrane-associated guanylate kinase (MAGUK) homologue family and are present within tight junctions of endothelial cells and epithelial cells. In addition, they exist in adherens junction in those cells that lack tight junction formation as in fibroblast and cardiac myocytes (62). This family characterized by the presence of three PDZ domain, one Src homology 3(SH3) domain, guanylate kinase (GUK) domain and a proline-rich C-terminus (84). Through these multiple domains, ZO proteins bind to diverse set of junction proteins. ZO-1 interacts with other ZO proteins via the PDZ domain, forming heterodimer complexes (65,85), with claudin -1 through PDZ-1 domain (74). ZO-1 interacts with occludin via GUK domain (61) and cytoskeleton F-actin via proline-rich C-terminus (65). ZO proteins may serve as link connecting occludin and claudin 5 to the cytoskeleton. The ZO proteins family was demonstrated to have a functional role in tight junction organization and assembly. Silencing of either ZO-1 or ZO-2 in MDCK cells delayed tight junction assembly and formation (86,87). Other studies showed that ZO-1 and ZO-2 deficient mouse epithelial cells lacks tight junction completely and claudin fails to polymerize at tight junction, this was associated with decreased TER and increase

paracellular permeability (88). In vivo studies demonstrated that ZO-1 knockout mice possess a lethal phenotype due to developmental defects in the neural tube and yolk sac angiogenesis (89). In addition to their role in tight junction, ZO- proteins have been reported to play a role in gene transcription and cell differentiation (90).

1.3.2.2 A lipid-protein hybrid model of tight junction

Several studies have demonstrated the lateral diffusion of different molecules from one cell to its neighboring cell (91,92). Lee et al. (2008) explained that if the tight junction is formed of only transinteracting proteins across the intercellular space then such a structure would not allow these type of lateral movements (93). The tight junction represents fusion points between apposing plasma membranes, however there is no evidence for adhesion or fusion between extracellular components or membrane-bridging of any of the tight junction proteins (93). Therefore, the protein cannot be the only constituent of the tight junction.

The idea of the lipid-protein hybrid model is not recent. Lipidic nature of tight junction itself was first proposed more than 30 years ago (1980s) by Kachar et al. (1982). They showed that tight junction strands are formed of inverted lipid cylinders, where apposing cells get in contact with each other through fusion points between their exoplasmic leaflets (94). This was further supported by other studies - freeze fracture preparations demonstrated the presence of phospholipids and cholesterol particles in tight junction strands (95,96). The model of lipid bridges at tight junctions has been postulated as a route for lateral transfer of phospholipids and lipid-protein complex between neighboring cells (91,92). Collectively, these studies postulate that the tight junction is an assembly of lipid-protein interactions.

Although there is a good basis supporting the presence of lipids in the tight junction, the structural relationship between the proteins and the lipids in the junctional complex is not well understood.

1.3.3 Blood retinal barrier breakdown in diabetic retinopathy

Blood retinal barrier dysfunction and increased permeability is one of the earliest signs of DR even before any ophthalmoscopic signs are visible (20). Retinal vasculature forming the inner blood retinal barrier was demonstrated to be the primary site of leakage in diabetic patients (21,97). As mentioned above, the inner BRB is formed by what is called the retinal neurovascular unit; tightly adherent retinal capillary endothelial cells surrounded by pericytes and glial cells (Muller and astrocyte). The physical integrity of these cells is essential for regulating the BRB, any disturbances by pathological condition, as in DR, will cause barrier integrity dysfunction.

1.3.3.1 Tight junction modulation

Tight junctions (TJ) form a physical barrier regulating the flux of ions and molecules through the paracellular pathway into retinal tissue. Any changes in the content or localization of the tight junction proteins results in tight junction disruption and increased paracellular permeability. Among the different tight junction proteins, downregulation of occludin has been reported as a leading cause of the BRB breakdown particularly in association with VEGF. Induction of experimental diabetes and intravitreal injection of VEGF (71,98) were associated with either decreased occludin content or its dislocalization from the tight junction. This decreased occludin expression or dislocalization was associated with increased vascular permeability - an

observation mirrored by treatment of BRECs with VEGF (71). Molecular analysis suggests that VEGF activates downstream proteins, including protein kinase C(PKC) β , that induce Ser490 phosphorylation, ubiquitination, internalization and degradation of occludin. PKC β inhibitors were found to block VEGF-induced occludin phosphorylation and decrease paracellular permeability (59,99–101).

Alterations in other tight junction proteins have been associated with blood retinal barrier break down and increased vascular permeability. ZO-1 protein content has been shown to be reduced in the diabetic mouse retina, with concomitant increase in retinal vascular permeability (102). In addition, VEGF treatment of endothelial cells in vitro, results in significant decrease of ZO-1 content and immunoreactivity at the endothelial cell border (103,104). Intravitreal injection of VEGF caused tyrosine phosphorylation of ZO-1 in the rat retina (99). Claudin 5 transcript was reduced in the diabetic rat retina and in VEGF treated BRECs (105).

Taken together, altered expression, phosphorylation and localization of tight junction proteins affect tight junction function and the paracellular permeability.

1.3.3.2 Endothelial cell loss

Endothelial cell death and formation of acellular capillaries is one of the earliest signs of diabetic retinopathy (106). A chronic hyperglycemic environment, that results in accumulation of advanced glycation end products (AGEs) and oxidative stress, has been shown to be involved in the intracellular glucose toxicity and retinal endothelial cell injury (107,108). Moreover, leukostasis, an early feature of DR, may be a direct cause of retinal endothelial cell death. Inhibition of leukostasis by using intercellular adhesion molecule-1 (ICAM-1) and CD18

neutralizing antibodies prevent retinal endothelial cell loss (109). In combination with defective repair of impaired vessels due to diabetes induced endothelial progenitor dysfunction, leukostasis and chronic hyperglycemic environment (110,111) may result in endothelial cell damage.

Endothelial cell death may be a direct cause of BRB disruption.

1.3.3.3 Pericyte loss

The blood retinal barrier demands proper pericyte function, and loss of pericytes may lead to increased vascular permeability.

Several studies have shown that endothelial cell barrier property and permeability were directly correlated to the density of pericytes (112). In vitro studies have demonstrated that co-culturing of pericytes with endothelial cells enhances barrier property and decreases permeability (113,114). While endothelium-specific knockout of PDGF-B, an essential factor for pericyte survival, resulted in decreased pericyte density and increased retinal vascular regression (115).

Pericyte death has been observed as an early feature of DR in both diabetic humans and rats (106,116).

Diabetes induced pericyte loss may be attributed to many factors; hyperglycemia induced inhibition of PDGF signaling (117), increased expression of angiotensin 2 (118,119), or excessive production of AGEs and connective tissue growth factor (CTGF) (120,121). All these factors induce pericyte detachment from the endothelial cells and destabilization of the junctional complex (119,120,121).

Pericytes play an important role in providing physical support for endothelial cells and maintaining barrier properties.

1.3.3.4 Leukostasis

Leukostasis is increased adhesion of leukocytes to retinal vasculature and is an early event in the pathogenesis of diabetic retinopathy. Leukostasis correlates with the development of retinal capillary occlusion, death of retinal endothelial cells and breakdown of blood retinal barrier (122).

This process is mediated by expression of intercellular adhesion molecule-1 (ICAM-1) on endothelial cells and β 2 integrin CD18 on leukocytes (123,124). As diabetes progresses, expression of ICAM-1 increases which in turn correlates with retinal leukostasis (122). Inhibition of ICAM-1 and CD18 expression, by either using neutralizing antibodies (109,122,124) or by knockdown of ICAM-1 and CD-18 in mice (125), prevent diabetes induced leukostasis and retinal vascular leakage .

Many factors have been demonstrated to be involved in diabetes induced leukostasis; VEGF, PKC activation, and inducible nitric oxide synthase (iNOS). Lu et al. (1999) showed that intraocular injection of VEGF results in increased expression of ICAM-1 in retinal vasculature (126). While, inhibition of VEGF with neutralizing antibodies results in significant decrease in ICAM-1 expression and leukocyte adhesion (127). It was found that PKC activation is also involved in retinal leukostasis; oral administration of PKC β inhibitor, LY333531, decreases leukocyte adhesion to retinal circulation (128). iNOS has also been considered to have role in leukostasis, mice treated with iNOS inhibitor and iNOS knock out mice prevented diabetes

induced increase in leukostasis and BRB permeability (102). Leukocyte adhesion has been correlated with blood brain barrier dysfunction through disorganization of tight junctions and adherens junction (129).

Taken together, these studies show that leukostasis has a role in retinal vascular damage and BRB dysfunction.

1.3.3.5 Glial cell dysfunction

As mentioned above, retinal glial cells (Muller and astrocytes) participate in the establishment of BRB. Astrocytes have been shown to be restricted to the vascularized area of the retina, coexisting with the retinal blood vessels (130–132). More interestingly, they have been found to enhance the formation of the blood retinal barrier (130,133).

Gardner et al. (1997) demonstrated that astrocyte conditioned media increased expression of tight junction protein ZO-1 and the barrier property of BRECs (134). In vivo studies also showed that astrocytes play a critical role in maintaining tight junction complex, where astrocyte loss coincides with the loss of occludin, claudin-5 and Zo-1 localization in brain tight junction (135).

In the in vitro co-culture model, Muller cells were also shown to enhance barrier properties of BRECs and its dysfunction lead to break down of the blood retinal barrier (136). Muller dysfunction by glial toxin or siRNA results in excessive production of VEGF and reduced expression of claudin-5, which was associated with increased vascular leakage (137).

It has also been suggested that Muller cell activation under pathological conditions result in overexpression of a number of cytokines e.g. TGF- β and VEGF which may induce breakdown of

the BRB via proteolytic degradation of occludin by matrix metalloproteinases (MMPs) (138,139). Of particular relevance to diabetes, diabetic rats show evidence of reactive gliosis of muller cells with excessive expression of glial fibrillary acidic protein (GFAP), this was accompanied by reduced and redistributed occludin in retinal endothelial cells (140).

Retinal microglia have also been reported to be activated in early diabetes with excessive production of proinflammatory cytokines IL-1 β and TNF- α (141) which are important mediators of leukostasis and increased permeability (142,143).

All together, this demonstrates the importance of glial cells in maintenance of BRB.

1.4 Diabetic dyslipidemia

Dyslipidemia can be defined as abnormal serum level of lipids due to disordered or disrupted lipid metabolism; release or uptake by either adipose or hepatic tissue. In adipose tissue, during the postprandial period, insulin inhibits fat mobilization and stimulates fat deposition through suppression of hormone -sensitive lipase (HSL) and activation of lipoprotein lipase enzymes (LPL) (144–146). In hepatic tissue, following food intake and increase in the carbohydrate flux into the liver, insulin stimulates fatty acid synthesis (de novo lipogenesis) which in turn get esterified into triglycerides (147). Therefore, abnormalities in insulin, as in in type 1 diabetes (dependence) and in type 2 diabetes (resistance), are expected to have a profound effect on lipid profile. In poorly controlled type 1 diabetes, elevated triglycerides and LDL cholesterol commonly occur (148–150). Type 2 diabetes have high levels of free fatty acids, triglycerides, atherogenic lipoproteins (small dense LDL) and reduced high density lipoprotein (HDL) cholesterol (148,151–153). Type 1 diabetes differs from type 2 diabetes in that lipid

abnormalities in the former are reversible and can be corrected by insulin replacement while in the latter these abnormalities cannot be fully corrected (148).

Dyslipidemia is a disorder of lipid metabolism with altered production of different lipid classes. Diabetes associated alteration in fatty acid class is discussed below.

1.4.1 Fatty acids

In type 2 diabetes, Insulin resistance coupled with increased release of non-esterified fatty acids (NEFA) from adipose tissue and decreased clearance of circulating triacylglycerol results in elevated blood level of both esterified and non-esterified fatty acids (NEFA) (146). Moreover, the uncontrolled release of NEFA leads to increased fatty acid flux to the liver, which in turn stimulates hepatic synthesis of triglycerides and thus VLDL secretion (147,148,151). The accumulated VLDL leads to the generation of atherogenic lipoprotein (small dense LDL) and the reduction of HDL cholesterol through the action of cholesteryl ester transfer protein (CETP) (147,148).

Several studies have demonstrated the effect of fatty acids content on serum low density lipoprotein (LDL), where saturated fatty acids have been associated with increased concentration of small, dense LDL in plasma and unsaturated fatty acids decreased the concentration of these atherogenic lipoprotein particles (154,155).

Diabetes is characterized by altered saturation and elongation of fatty acids with increased level of saturated, short chain fatty acids and decreased polyunsaturated, long chain fatty acids (156,157). Fatty acids that are either synthesized by the cytosolic enzyme fatty acid synthase (FAS) or derived from the diet undergo series of desaturation and elongation reactions by

physically associated, membrane-bound enzymes localized in the endoplasmic reticulum called desaturases and elongases enzymes (158–160). Fatty acid desaturases and elongases play an essential role in hepatic and whole body lipid composition.

Desaturases are enzymes that introduce double bonds at certain positions on the acyl chain of fatty acids. According to the position at which the double bond is introduced, desaturases are divided into 2 groups; stearoyl-coA desaturases (SCDs) including the $\Delta 9$ desaturases and fatty acid desaturases (FADS) including $\Delta 6$, 5 desaturases (161). Previous studies have revealed defective desaturase activity in type 1 diabetes, which can be reverted by insulin treatment (162–165).

Elongase enzymes are believed to perform the first condensation (regulatory) step in the four-step fatty acid (FA) elongation cycle, which takes place in the endoplasmic reticulum with the help of 3-ketoacyl-CoA reductase, 3-hydroxyacyl-CoA dehydratase, and 2,3- trans-enoyl-CoA reductase. Fatty acid elongation is a complex reaction involving the addition of two carbons to the fatty acyl-CoA using malonyl-CoA as the carbon donor. To date, seven elongases, termed ELOVL 1-7 (elongation-of-very-long-chain-fatty acids) have been identified in mammals. ELOVLs exhibit tissue-specific distribution and have distinct substrate specificities. ELOVL1, ELOVL5 and ELOVL6 are ubiquitously expressed among tissues, while ELOVL2, ELOVL3 and ELOVL4 are highly expressed in liver/testis (166), skin/liver (159,167) and retina/brain/skin (159,167–169), respectively. ELOVL1, ELOVL3 and ELOVL6 are responsible for the elongation of both saturated and monosaturated FAs, while ELOVL2 and ELOVL5 elongate polyunsaturated FAs (PUFAs). ELOVL4 utilizes both saturated and polyunsaturated long fatty acids ($C \geq C_{24}$) to synthesize very long chain fatty acids ($C \geq C_{26}$) (158–160). Elongases are well

controlled enzymes, they are regulated at a transcriptional level where different cellular stimuli have been shown to alter their expression (158). Wang et al. (2006) have demonstrated that ELOVLs are regulated in hepatic tissue by hormones (insulin), transcriptional factors (SREBP-1c, LXR and PPAR- α), and nutrients (glucose, fat). Insulin, liver X receptor (LXR) and glucose induce ELOVL-6 expression through the induction of the transcription factors: sterol regulatory element binding protein-1c (SERBP-1c) and carbohydrate-regulatory element binding protein (ChREBP), respectively (165). Lipolytic transcription factor PPAR- α induces both ELOVL5 and ELOVL6. Interestingly, Jakobsson et al. (2005) revealed differential regulation of ELOVL3 in brown adipocyte where ELOVL3 expression was induced in activated adipocyte cells by glucocorticoids, norepinephrine and PPAR- α treatment but was inhibited by LXR (170). Although activated brown adipose tissue is associated with increased lipolysis, fatty acid β oxidation and turn over, ELOVL3 was still induced to replenish tissue pools of specific fatty acids. Similar to desaturases, elongases are suppressed in diabetes due to reduced insulin and insulin-induced SREBP (165,171).

1.4.2 Dyslipidemia and diabetic retinopathy

Clinical data support a possible role of dyslipidemia in the development of diabetic retinopathy in both type 1 and type 2 diabetes. Small early clinical trials revealed that a lipid lowering diet could reduce the amount of retina hard exudates (172) and a diet rich in unsaturated fatty acids (linoleic acid) delay the development and the progression of DR (173). Augustin et al. (1993) demonstrated that lipid peroxide levels were significantly elevated in the vitreous of patients with proliferative diabetic retinopathy (174). Data from the Early Treatment Diabetic Retinopathy Study (ETDRS) showed that severity of retinal hard exudate was positively

associated with serum level of total cholesterol and LDL cholesterol (175–177). Moreover, the DCCT/EDIC cohort study revealed a positive correlation between severity of DR in type 1 diabetes with the small size of lipoprotein subclasses (VLDL, LDL, HDL) and with increased LDL concentration (178). A prospective analysis of the DCCT data indicates strong association between clinically significant macular edema (CSME) and elevated serum lipids in particular high triglycerides and total -to -HDL cholesterol ratio (179). Recent intervention studies performed by ACCORD Eye study group in type 2 diabetes have determined that intensive dyslipidemia therapy with combination of PPAR α activator fenofibrate and HMG-CoA reductase inhibitor simvastatin, significantly slowed the progression of diabetic retinopathy (180).

Taken together, these studies revealed that dyslipidemia is highly associated with the development of diabetic retinopathy.

1.4.3 Retinal lipid composition in diabetes

Fatty acid composition of any particular tissue is determined by complex interplay among two metabolic pathways; de novo lipogenesis using glucose as substrate and polyunsaturated fatty acid (PUFA) biosynthesis (Sprecher) pathway using essential fatty acids, i.e., linoleic acid (LA, C18:2n-6) or α -linolenic acid (ALA, C18:3n-3) (Figure 6). (181,186). Excessive carbohydrate, glucose, or dietary fatty acid precursors undergo a series of desaturation and elongation reactions resulting in the production of either saturated, monounsaturated (MUFAs) or polyunsaturated fatty acids (PUFAs).

The retina possesses a unique lipid profile, it is highly enriched in n-3 PUFA, docosahexaenoic acid (DHA, 22:6n-3) (182,183) and very long chain polyunsaturated fatty acids (VLC-PUFA,

C28-38) (184,185). This is concomitant with the high expression of Elongases 4, 2, 1 and 6 (186). ELOVL4 shows the greatest expression level among retinal elongases. ELOVL4 is known for its substrate specificity for long chain fatty acids ($\geq C24$) with synthesis of very long chain fatty acids (VLCFA), which may explain the high content (or abundance) of VLC-PUFA in retinal tissue. Our lab has previously demonstrated that diabetes-induced down regulation of retinal elongases resulted in significantly different retinal lipid profiles, including higher saturation index, shorter fatty acid chains, and decreased long-chain-to-short-chain polyunsaturated fatty acids (PUFA) ratio and n3-to-n6 PUFA ratio, with a significant decreases in DHA and VLC-PUFA (186).

Apart from diabetes induced retinal fatty acid remodeling, we have previously demonstrated dysregulation of sphingolipid metabolism in the diabetic retina with pathological activation of the acid sphingomyelinase (ASM) enzyme and increased acid sphingomyelinase-mediated production of pro-inflammatory and pro-apoptotic ceramides (187).

These changes in retina lipid metabolism were associated with higher expressions of pro-inflammatory cytokines, adhesion molecules and retinal vascular degeneration (186,188,189). This evidence suggests that lipid metabolism may play an important role in pathogenesis of DR.

1.4.4 Fatty acid elongase, ELOVL4, and very long chain ceramides

Elongation of very long chain fatty acids-4 (ELOVL4) belongs to a seven-member elongase (ELO) family that is involved in the synthesis of very long chain fatty acids (VLCFA). ELOVL4 was identified by genetic linkage and haplotype analysis in families with two dominant forms of macular dystrophy; Stargardt-like macular dystrophy (STGD3) and autosomal dominant macular

dystrophy (adMD). Genetic mapping revealed that a 5-base pair deletion mutation in the protein-coding region of a newly discovered retinal gene called ELOVL4 was found in all affected members. The new protein, ELOVL4, had a homology with a group of yeast proteins involved in the synthesis of VLCFA, Zhang et al. (2001) suggested that this enzyme may be involved in the elongation of long chain fatty acids (168).

ELOVL4 is restricted to the tissues where extremely long fatty acids ($\geq C_{24}$) exist. With the highest expression of ELOVL4 in the retinal tissue (168,169,190–192), followed by the skin, brain and testis (167,169). In the human retina, ELOVL4 is mainly expressed in the inner segment of photoreceptors and their cell bodies in the outer nuclear layer, with some expression in the ganglionic cell layer (192). ELOVL4 seems to be the only elongase that is involved in the biosynthesis of both saturated and polyunsaturated very long chain fatty acids ($C \geq 26$). Agbaga et al. (2008) revealed the metabolic function of ELOVL4, demonstrating that ELOVL4 is involved in the synthesis of both saturated (VLC-FA, $C \geq 26$) and polyunsaturated (VLC-PUFA, C_{28-36}) very long chain fatty acids in cultured cells that have been transfected with mouse ELOVL4 (Figure 6) (193).

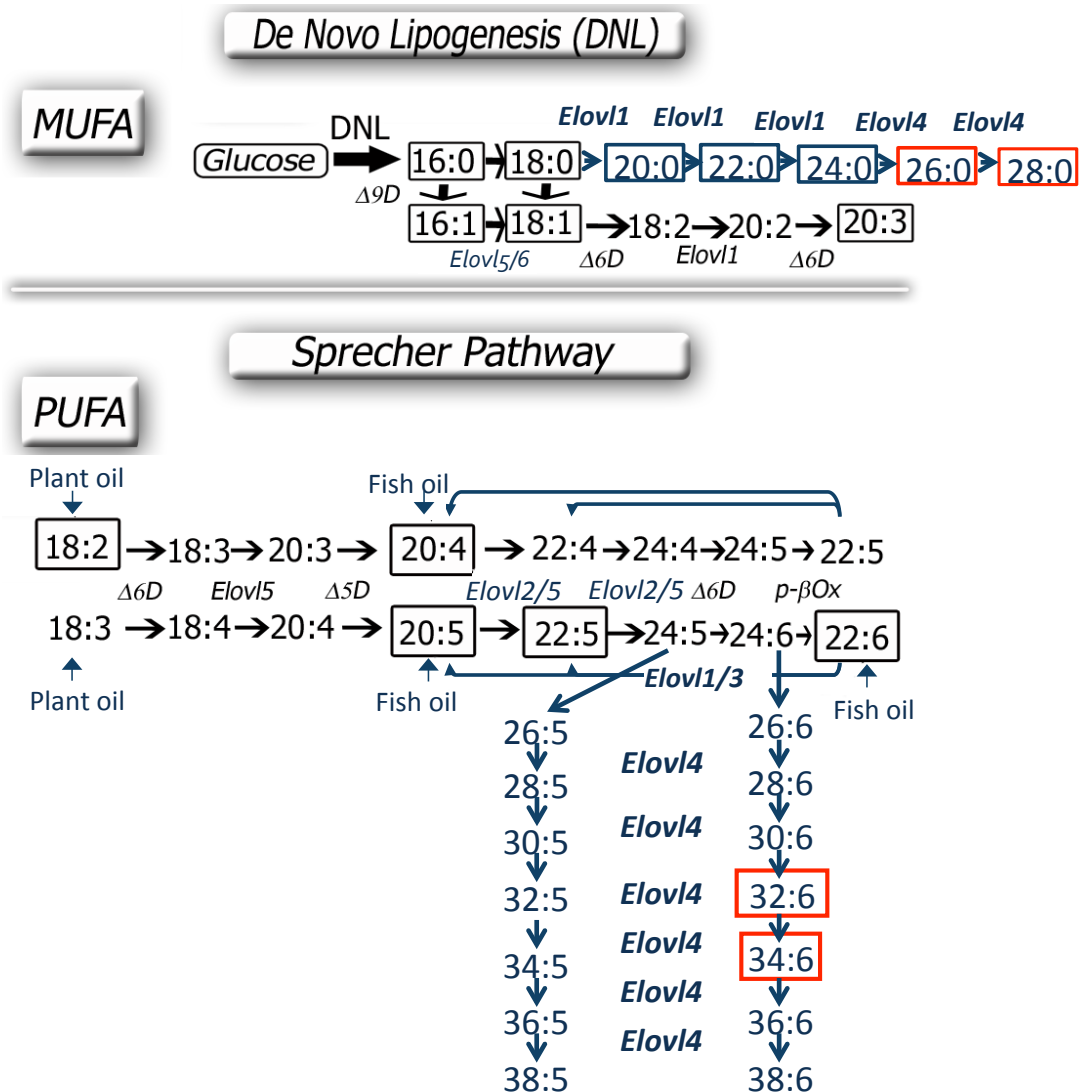


Figure 6. Schematic diagram of VLC-FA and VLC-PUFA biosynthetic pathways mediated a series of elongation and desaturation reactions. Fatty acids are synthesized through either de novo lipogenesis pathway using glucose as substrate or polyunsaturated fatty acid (PUFA) remodeling pathway (Sprecher) using essential fatty acids, i.e., linoleic acid (LA, C18:2n-6) or α -linolenic acid (ALA, C18:3n-3). ELOVL4 is necessary for elongating long chain fatty acids generating VLC-FA and VLC-PUFA (C \geq 26). Fatty acids in solid boxes, those that accumulate in animal and human tissues (modified from Tikhonenko *et al.*, 2010) (186).

Moreover, retinas of heterozygous *Stgd3* mice carrying the pathogenic 5 base pair deletion in exon 6 of the *ELOVL4* gene (194) and photoreceptor-specific homozygous *ELOVL4* knock-out mice (195) showed a significant decrease in VLC-PUFA-containing phosphatidylcholines (PCs, C28-C36) that have been shown to interact with rhodopsin (184). This decrease was associated with retinal manifestations similar to those seen in *STGD3* patients. *STGD3* is an autosomal dominant Stargardt – like macular degeneration characterized by the accumulation of lipofuscin, RPE atrophy, degeneration of macular photoreceptor and reduced vision (196,197). The disease is caused by 5 base pair deletion in exon 6 of *ELOVL4* gene, resulting in C- terminal truncated *ELOVL4* with its mislocalization and aggregation outside the endoplasmic reticulum. Moreover this mutant *ELOVL4* exerts a dominant negative effect on the wild type *ELOVL4*, changing its subcellular distribution. The presence of the misfolded mutant protein leads to photoreceptor degeneration and vision loss (192). As this misfolding is not a problem in DR, the role or the function of *ELOVL4* in BRB maintenance rather than photoreceptor damage is observed in DR. While, mice homozygous for either *Stgd3* (167,197) or *ELOVL4* null mutations (198) exhibit neonatal lethal phenotype due to defective skin permeability barrier, excessive water loss and dehydration. The homozygous and null mutation mice were found to have complete absence of epidermal VLC-FA- containing acylceramides (VLCFA, $C \geq 28$), these phenotypes were rescued by epidermal –specific expression of wild-type (WT) *ELOVL4* transgene (199).

We can conclude that *ELOVL4* plays a major role in the biosynthesis of VLC-PUFAs which are esterified into PCs in the retina, and in the biosynthesis of saturated or monounsaturated VLC-FAs which are incorporated into skin ceramides (Figure 7).

The Function of VLC-PUFAs in the retina is not known but they are mainly present in the retinal outer segment in PCs and are able to span both leaflets of the lipid bilayer. VLC-PUFAs may

play a role in the stability of highly curved cell membranes, such as the rims of photoreceptors disk membranes (193). Karan et al. (2005) has found that photoreceptor-specific overexpression of mutant ELOVL4 was associated with irregularities in disk membrane organization (196).

Most of the identified retinal fatty acids are VLC-PUFAs (C28-C36) with six double bonds. However, Brush et al. (2010) has demonstrated the presence of saturated and monounsaturated VLC-FAs (C 26-30), with C26:0 is the most abundant VLC-FA incorporated into retinal ceramides (185). The role of these VLC-FAs in the retina is largely unknown.

ELOVL4 was initially discovered as the etiological gene of STGD3 (168). It has also been shown to be associated with other retinal diseases. Abcouwer et al. (2010) demonstrated that ELOVL4 is one of the enzymes that was found to be down regulated by ischemia-reperfusion in the retina (200).

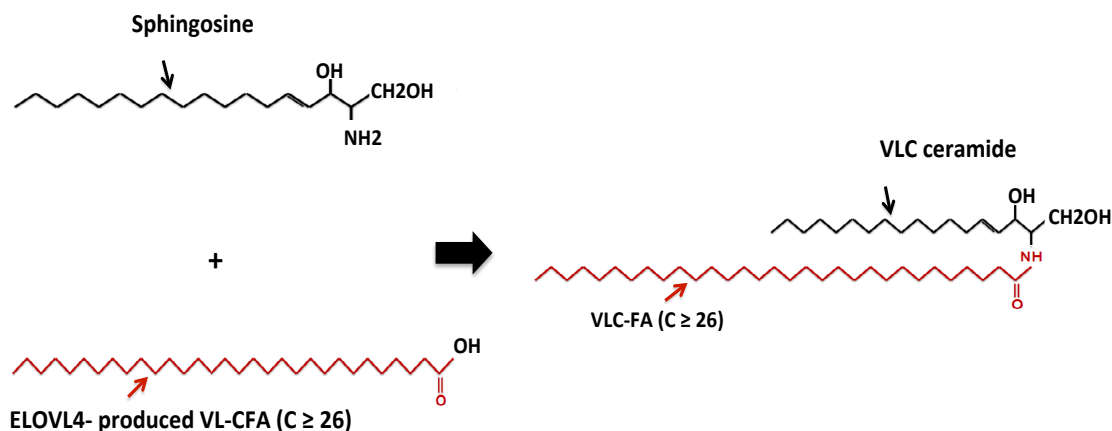


Figure 7. Synthesis of VLC ceramides. ELOVL4-produced VLC-FA incorporates into the structure of VLC-ceramides.

We have previously demonstrated that expression level of elongases and desaturases

in the liver and retina is affected by diabetes with dramatic downregulation of elongases, including ELOVL4 in the retina (165,171,186), this may be attributed to the reduced level (type 1 DM) or reduced action (type 2 DM) of insulin, the well-known regulator of the elongases. Diabetes-induced down regulation of elongase in the retina was associated with significant decrease in total retinal DHA and VLC-PUFA incorporated into retinal phosphatidylcholine. These changes of retinal lipid metabolism were associated with higher expressions of pro-inflammatory cytokines, adhesion molecules and retinal vascular injury (186,188,189). According to these data, it is conceivable that ELOVL4 plays a critical role in maintaining retinal homeostasis.

1.4.5 ASM and short chain ceramides

Acid sphingomyelinase (ASM) is the key enzyme of sphingolipid metabolism. ASM exists in two cellular components; the intracellular lysosome and the outer leaflet of the cell membrane. Activation of acid sphingomyelinase by either receptor (CD95) (201) or stress stimuli (UV radiation) (202) results in its translocation from the lysosome to the outer leaflet of the cell membrane catalyzing the hydrolysis of membrane sphingomyelin (SM) into ceramides (Figure 8). The produced ceramide molecules self-associate into ceramide-enriched membrane domains and result in reorganization of membrane rafts, aggregation of signaling proteins, receptor clustering and enhanced cellular signal transduction (203,204). We have previously demonstrated that ASM exhibits distinct substrate specificity towards short saturated acyl chains (SM) with the production of pro-inflammatory and pro-apoptotic short chain ceramides ($C \leq 16$) when it gets activated in different pathological conditions such as diabetes (187). ASM was found to be highly activated in diabetic retinal vasculature (189), inhibition of ASM exhibits a

protective effect-- preventing diabetes induced retinal inflammation and vascular degeneration (187–189).

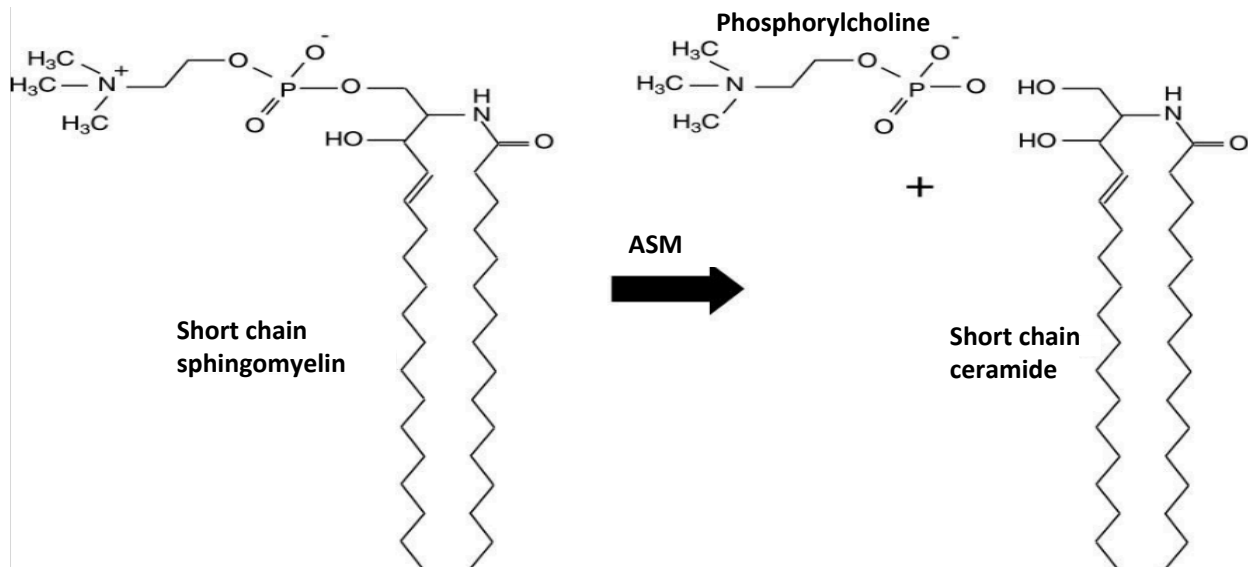


Figure 8. Acid sphingomyelinase (ASM) is a central enzyme of sphingolipid metabolism.

ASM hydrolyzes SM to pro-apoptotic and pro-inflammatory short chain ceramides.

1.5 Reparative circulating angiogenic cells

Circulating angiogenic cells (CACs), a population of vascular progenitors originated from hematopoietic stem cells (HSCs) (205) in the bone marrow, are now recognized as key regulators for vascular repair. HSCs isolated from bone marrow or CACs from peripheral blood of control animals have been shown to repair ischemic damage and aid in reperfusion of ischemic tissues (205–207). This reparative process takes place through a series of orchestrated steps: mobilization of CACs from bone marrow, their recruitment and extravasation to the sites of damaged vessels.

CACs mobilize in response to a number of physiological or pathological stimuli to the site of injury (208) promoting the repair of the damaged endothelium, either by incorporation and differentiation into mature endothelial cells (205,209) or by secretion of paracrine factors that enhance the integrity of the resident endothelium (210–212) . CACs mobilization is regulated by sympathetic signaling to bone marrow stromal cells, which results in stromal cell-derived factor-1 (SDF-1) down regulation and progenitor egress from the bone marrow (213,214).

In diabetes bone marrow-derived CACs are dysfunctional, with defective proliferation, migration, adhesion and differentiation potential (110,215,216). Several studies have shown an association between DR risk and both reduced number (217–219) and function of CACs (187,220,221). We have previously demonstrated that the defective release of BM-derived CACs in T2D rat model precedes the development of DR (217). The impaired release of CACs to the site of injury is due to defective migration of these cells in response to ischemic induced factors; SDF-1 and VEGF (222). The blunted response of CACs is due to reduced bioavailability of nitric oxide (NO) in diabetes, essential for CACs migration (223–225) and survival (226).

Our laboratory identified marked increase in ASM expression in diabetic CACs (187,227). Increase in ASM activity in CACs in diabetic animal models was associated with ceramide accumulation in the cell membrane, and thereby increasing membrane rigidity and impairing migration (227). Interestingly, we demonstrated that inhibition of ASM in diabetic CACs decreased membrane rigidity and improved the migration of these cells to damaged retinal vasculature, preventing diabetes induced increase in retinal vascular permeability and retinal capillary loss (227).

1.6 Objectives of the dissertation

Diabetic retinopathy (DR) is a microvascular disease that results from diabetes-induced retinal damage. The underlying mechanisms of vascular dysfunction in diabetes are yet to be fully understood. Dyslipidemia, as well as hyperglycemia, is a major metabolic insult of diabetes and is positively correlated with the development of DR. We previously explored the novel concept that altered retinal lipid metabolism and dyslipidemia leads to retinal inflammation and vascular degeneration (186–189). We found that early - stage diabetes induced marked decrease in the expression of many retinal fatty acid elongases, in particular severe downregulation of the most abundant elongase; elongation of very long chain fatty acids 4 (ELOVL4). Downregulation of elongases in the diabetic retina lead to significant remodeling of retinal fatty acids with decreased long-chain-to-short-chain fatty acids ratio and n3-to-n6 PUFA ratio, and higher saturation index with significant decrease in n3-DHA and n3 VLCPUFA. These changes were associated with increased expression of adhesion molecules, pro-inflammatory cytokines, and retinal vascular pathology (186).

ELOVL4 was initially discovered as the etiological gene of STGD3 retinal disease with association to a significant decrease in VLC-PUFA-containing phosphatidylcholines. It has also been shown to be essential in maintenance of the water permeability barrier in skin (197,198). To date, no studies have approached the direct role of ELOVL4 in retinal vascular permeability.

In addition to ELOVL4, we have previously demonstrated activation of the central enzyme of sphingolipid metabolism, acid sphingomyelinase (ASM), as the key metabolic abnormality in diabetic retinal vasculature and CACs (188,189).

Thus, the central hypothesis of this dissertation is as follows:

Diabetes-induced disruption of retinal lipid metabolism plays a critical role in retinal vascular dysfunction through two pathways

- **Down regulation of ELOVL4-produced very long chain ceramides, contribute to diabetes induced retinal vascular permeability.**
- **Up regulation of ASM-produced short chain ceramides, contribute to retinal endothelial damage and defective function of the reparative progenitor cells.**

Thus normalizing the ratio between pro-barrier long chain ceramides and pro-inflammatory and pro-apoptotic short chain ceramides could prevent diabetes-induced retinal damage and progression of DR.

1.7 Overview of chapters

Chapter I is a review of the relevant literature addressing diabetic retinopathy disease, Blood retinal barrier break down in DR, diabetic dyslipidemia and its contribution to retinal vascular degeneration.

Chapter II investigates the role of ELOVL4 and VLC ceramides in diabetes-induced increase in retinal vascular permeability and to identify if lipids in particular VLC ceramides localize in the tight junction and play a role in controlling the paracellular permeability of retinal endothelial cells. Experiments described in this chapter demonstrate that ELOVL4-mediated production of VLC-ceramides is necessary for retinal endothelial barrier function and normalization of retinal ELOVL4 expression may provide a potential therapeutic strategy for the prevention of diabetes-induced early breakdown of the blood-retina barrier by modulating retinal sphingolipid metabolism.

Chapter III investigates the effect of diabetes-induced ASM activity on the function of both cell types involved in revascularization; retinal endothelial cells and circulating angiogenic cells (CACs). Experiments described in this chapter demonstrate that ASM has deleterious effect on the vascular repair potential of both mature retinal endothelial cells and circulating angiogenic cells in diabetes and correcting this defect could treat vasodegeneration, enhancing vessel repair and thus preventing progression into PDR stage. This study is published in Journal of Clinical Lipidology.

Chapter IV summarizes the obtained data, the conclusions that can be reached from the studies included in the thesis and suggests directions for future research related to the present study.

REFERENCES

REFERENCES

1. American Diabetes Association. Diagnosis and classification of diabetes mellitus. *Diabetes Care*. 2014;37(SUPPL.1):81–90.
2. Williams R, Airey M, Baxter H, Forrester J, Kennedy-Martin T, Girach a. Epidemiology of diabetic retinopathy and macular oedema: a systematic review. *Eye (Lond)*. 2004;18(10):963–83.
3. Stumvoll M, Goldstein B, van Haeften T. Type 2 diabetes: principles of pathogenesis and therapy. *Lancet*. 2005;365:1333–46.
4. Olokoba AB, Obateru OA, Olokoba LB. Type 2 diabetes mellitus: A review of current trends. *Oman Med J*. 2012;27(4):269–73.
5. Lin Y, Sun Z. Current views on type 2 diabetes. *J Endocrinol*. 2010;204(1):1–11.
6. International Diabetes Federation. *IDF Diabetes Atlas 7th edn* <http://www.diabetesatlas.org> (2016).
7. Zimmet P, Alberti KG, Magliano DJ, Bennett PH. Diabetes mellitus statistics on prevalence and mortality: facts and fallacies. *Nat Rev Endocrinol*. 2016;12:616–22.
8. Kanguru L, Bezawada N, Hussein J, Bell J. The burden of diabetes mellitus during pregnancy in low- and middle-income countries: a systematic review. *Glob Health Action*. 2014;7:23987.
9. Mathers CD, Loncar D. Projections of global mortality and burden of disease from 2002 to 2030. *PLoS Med*. 2006;3(11):2011–30.
10. American Diabetes Association. Economic costs of diabetes in the U.S. in 2012. *Diabetes Care*. 2013;36(4):1033–46.
11. Yau JWY, Rogers SL, Kawasaki R, Lamoureux EL, Kowalski JW, Bek T, et al. Global prevalence and major risk factors of diabetic retinopathy. *Diabetes Care*. 2012;35(3):556–64.
12. Fong DS, Aiello L, Gardner TW, King GL, Blankenship G, Cavallerano JD, et al. Retinopathy in Diabetes. *Diabetes Care*. 2004;27(SUPPL. 1): s84-s87
13. Klein R, Klein BEK, Moss SE, Davis MD, Demets DL. The Wisconsin Epidemiologic Study of Diabetic Retinopathy. *Arch Ophthalmol*. 1984;102:520–6.
14. Cunha-Vaz J, Bernardes R. Nonproliferative retinopathy in diabetes type 2. Initial stages and characterization of phenotypes. *Prog Retin Eye Res*. 2005;24(3):355–77.

15. Wong K. Defining diabetic retinopathy severity. *Diabet Retin Evidence-Based Manag.* 2010;(10):105–20.
16. Early Treatment Diabetic Retinopathy Study Research Group. Grading Diabetic Retinopathy from Stereoscopic Color Fundus Photographs-an Extension of the Modified Airlie House Classification. *Ophthalmology* [Internet]. 1991;98(5):786–806.
17. Wilkinson CP, Ferris FL, Klein RE, Lee PP, Agardh CD, Davis M, et al. Proposed international clinical diabetic retinopathy and diabetic macular edema disease severity scales. *Ophthalmology.* 2003;110(9):1677–82.
18. Hammes HP, Feng Y, Pfister F, Brownlee M. Diabetic retinopathy: Targeting vasoregression. *Diabetes.* 2011;60(1):9–16.
19. Lorenzi M, Gerhardinger C. Early cellular and molecular changes induced by diabetes in the retina. *Diabetologia.* 2001;44(7):791–804.
20. Cunha-Vaz J, Faria de Abreu JR, Campos AJ. Early breakdown of the blood-retinal barrier in diabetes. *Br J Ophthalmol.* 1975;59(11):649–56.
21. Viores S a, McGehee R, Lee a, Gadegbeku C, Campochiaro P a. Ultrastructural localization of blood-retinal barrier breakdown in diabetic and galactosemic rats. *J Histochem Cytochem.* 1990;38(9):1341–52.
22. Daley ML, Watzke RC, Riddle MC. Early loss of blue-sensitive color vision in patients with type I diabetes. *Diabetes Care.* 1987;10(6):777–81.
23. Kohner EM, Henkind P. Correlation of fluorescein angiogram and retinal digest in diabetic. *Am J Ophthalmol.* 1970;69(3):403-14.
24. Ashton N. Studies of the Retinal Capillaries in Relation To Diabetic and Other Retinopathies. *Br J Ophthalmol.* 1963;47:521–38.
25. Cunha-Vaz JG. Pathophysiology of Diabetic Retinopathy. *Br J Ophthalmol.*1978;62:351-55
26. Klein R, Moss SE, Klein BEK. Retinal Microaneurysm counts and 10-year progression of diabetic retinopathy. *Arch Ophthalmol.*1995; 113:1386-91.
27. Klein R, Klein BE, Moss SE, Cruickshanks KJ. The Wisconsin Epidemiologic Study of Diabetic Retinopathy. XV. The long-term incidence of macular edema. *Ophthalmology* [Internet]. 1995;102(1):7–16.
28. Aiello LP, Gardner TW, King GL, Blankenship G, Cavallerano JD, et al. Diabetic retinopathy. *Diabetes Care.* 1998;21(1):143-56.
29. Cunha-Vaz J, Travassos A. Breakdown of the blood-retinal barriers and cystoid macular

- edema. *Surv Ophthalmol.* 1984;28(SUPPL. 2):485–92.
30. Kohner EM, Dollery CT, Bulpitt CJ. Cotton-wool spots in diabetic retinopathy. *Diabetes.* 1969;18(10):691–704.
 31. Kohner EM, oakley NW. Diabetic Retinopathy. *Metabolism.* 1975; 24(9):1085-102.
 32. Frank RN. Diabetic retinopathy. *Prog Retin Eye Res.* 1995;14(2):361–92.
 33. Aiello LP, Avery RL, Arrigg PG, Keyt BA, Jampel HD et al. Vascular endothelial growth factor in ocular fluid of patients with diabetic retinopathy and other retinal disoredrs. *N Engl J Med.* 1994; 331: 1480-7.
 34. Antonetti DA, Barber AJ, Bronson SK, Freeman WM, Gardner TW, Jefferson LS, et al. Diabetic retinopathy: Seeing beyond glucose-induced microvascular disease. *Diabetes.* 2006;55(9):2401–11.
 35. Simó R, Hernández C. Advances in the medical treatment of diabetic retinopathy. *Diabetes Care.* 2009;32(8):1556–62.
 36. The Diabetes Control and Complications Trial Research Group. The effect of intensive treatment of diabetes on the development and progression of long-term complications in Insulin- dependent diabetes mellitus. *N Engl J Med.* 1993; 329:977-86.
 37. UK Prospective Diabetes Study (UKPDS) Group. Intensive blood-glucose control with sulphonylureas or insulin compared with conventional treatment and risk of complications in patients with type 2 diabetes (UKPDS 33). *Lancet.* 1998; 352 (9131): 837–53.
 38. The Action of Control Cardiovascular Risk in Diabetes Study Group. Effect of intensive glucose lowering in type 2 diabetes. *N Engl J Med.* 2008; 358: 2545-59.
 39. Mohamed Q, Gillies MC, Womg TY. Management of diabetic retinopathy. *JAMA.* 2007;298(8):902-16.
 40. Osaadon P, Fagan XJ, Lifshitz T, Levy J. A review of anti-VEGF agents for proliferative diabetic retinopathy. *Eye (Lond).* 2014;28(5):510–20.
 41. Nishijima K, Ng Y-S, Zhong L, Bradley J, Schubert W, Jo N, et al. Vascular Endothelial Growth Factor-A Is a Survival Factor for Retinal Neurons and a Critical Neuroprotectant during the Adaptive Response to Ischemic Injury. *Am J Pathol.* 2007;171(1):53–67.
 42. Saint-Geniez M, Maharaj ASR, Walshe TE, Tucker BA, Sekiyama E, Kurihara T, et al. Endogenous VEGF is required for visual function: Evidence for a survival role on Muller cells and photoreceptors. *PLoS One.* 2008;3(11):e3554.
 43. Arden GB, Arden GB, Sidman RL, Sidman RL, Arap W, Arap W, et al. Spare the rod and spoil the eye. *Br J Ophthalmol.* 2005;89(August):764–9.

44. Klaassen I, Van Noorden CJF, Schlingemann RO. Molecular basis of the inner blood-retinal barrier and its breakdown in diabetic macular edema and other pathological conditions. *Progress in Retinal and Eye Research*. 2013;34: 19–48.
45. Runkle EA, Antonetti DA. The blood-retinal barrier: structure and functional significance. *Methods Mol Biol*. 2011;686: 133-48.
46. Kim JH, Kim JH, Yu YS, Kim DH, Kim KW. Recruitment of pericytes and astrocytes is closely related to the formation of tight junction in developing retinal vessels. *J Neurosci Res*. 2009;87(3):653–9.
47. Davis S, Aldrich TH, Jones PF, Acheson A, Compton DL, Jain V, et al. Isolation of angiopoietin-1, a ligand for the TIE2 receptor, by secretion-trap expression cloning. *Cell*. 1996;87(7):1161–9.
48. Sato TN, Tozawa , Deutsch U, Wolburg-Buchholz K, Fujiwara Y, et al. Distinct roles of the receptor tyrosine kinases Tie-1 and Tie-2 in blood vessel formation. *Nature*. 1995;376(6535):70-4.
49. Hori S, Ohtsuki S, Hosoya KI, Nakashima E, Terasaki T. A pericyte-derived angiopoietin-1 multimeric complex induces occludin gene expression in brain capillary endothelial cells through Tie-2 activation in vitro. *J Neurochem*. 2004;89(2):503–13.
50. Sagaties MJ, Raviola G, Schaeffer S, Miller C. The structural basis of the inner blood-retina barrier in the eye of *Macaca mulatta*. *Investig Ophthalmol Vis Sci*. 1987;28(12):2000–14.
51. Zlokovic B V. The blood-brain barrier in health and chronic neurodegenerative disorders. *Neuron*. 2008;57(2):178–201.
52. Matter K and Balda MS. Signaling to and from tight junctions. *Nature Reviews Molecular Cell Biology*. 2003;4: 225-37.
53. Tsukita S, Furuse M, Itoh M. Multifunctional strands in tight junctions. *Nat Rev Mol Cell Biol*. 2001;2(4):285-93.
54. Van Meer G, Simons K, Simons K. The function of tight junctions in maintaining differences in lipid composition between the apical and the basolateral cell surface domains of MDCK cells. *EMBO J*. 1986;5(7):1455–64.
55. González-Mariscal L, Lechuga S, Garay E. Role of tight junctions in cell proliferation and cancer. *Prog Histochem Cytochem*. 2007;42(1):1–57.
56. Farquhar MG, Palade GE. Junctional complexes in various epithelia. *J cell Biol*. 1963;17(2):375–412.
57. Staehelin L.A. Further observations on the fine structure of freeze-cleaved tight junctions. *J Cell Sci*. 1973;13:763–86.

58. Shen L, Weber CR, Turner JR. The tight junction protein complex undergoes rapid and continuous molecular remodeling at steady state. *J Cell Biol.* 2008;181(4):683–95.
59. Murakami T, Felinski EA, Antonetti DA. Occludin phosphorylation and ubiquitination regulate tight junction trafficking and vascular endothelial growth factor-induced permeability. *J Biol Chem.* 2009;284(31):21036–46.
60. Furuse M, Hirase T, Itoh M, Nagafuchi A, Yonemura S, Tsukita S, et al. Occludin: A Novel Integral Membrane Protein Localizing at Tight Junctions. *J cell Biol.* 1993;123(6):1777–88.
61. Furuse M, Itoh M, Hirase T, Nagafuchi A, Yonemura S, Tsukita S, et al. Direct association of occludin with ZO-1 and its possible involvement in the localization of occludin at tight junctions. *J Cell Biol.* 1994;127(6 I):1617–26.
62. Itoh M, Morita K, Tsukita S. Characterization of ZO-2 as a MAGUK Family Member Associated with Tight as well as Adherens Junctions with a Binding Affinity to Occludin and α Catenin. *J Biol Chem.* 1999;274(9):5981–6.
63. Kojima T, Sawada N, Chiba H, Kokai , Yamamoto M, . Induction of tight Junctions in human connexin 32 (hCx32) -transfected mouse hepatocytes : Connexin 32 interacts with occludin. *Biochem Biophys Res Commun.* 1999;266(1):222–9.
64. Nusrat A, Chen JA, Foley CS, Liang TW, Tom J, Cromwell M, et al. The coiled-coil domain of occludin can act to organize structural and functional elements of the epithelial tight junction. *J Biol Chem.* 2000;275(38):29816–22.
65. Fanning AS, Jameson BJ, Lynne a, Anderson JM, Jesaitis L a, Melvin J. The Tight Junction Protein ZO-1 Establishes a Link between the Transmembrane Protein Occludin and the Actin Cytoskeleton. *J Biol Chem.* 1998;273(45):29745–53.
66. Traweger A, Fang D, Liu YC, Stelzhammer W, Krizbai IA, Fresser F, et al. The tight junction-specific protein occludin is a functional target of the E3 ubiquitin-protein ligase itch. *J Biol Chem.* 2002;277(12):10201–8.
67. Kevil CG, Okayama N, Trocha SD, Kalogeris TJ, Coe LL, et al. Expression of zonula occludens and adherens junctiona proteins in human venous and and arterial endothelial cells: role of occludin in endothelial solute barriers. *Microcirculation.* 1998;5(2-3)197–210.
68. Hirase T, Staddon JM, Saitou M, Ando-Akatsuka Y, Itoh M, Furuse M, et al. Occludin as a possible determinant of tight junction permeability in endothelial cells. *J Cell Sci.* 1997;110 (Pt 14):1603–13.
69. Antonetti DA, Wolpert EB, DeMaio L, Harhaj NS, Scaduto RC. Hydrocortisone decreases retinal endothelial cell water and solute flux coincident with increased content and decreased phosphorylation of occludin. *J Neurochem.* 2002;80(4):667–77.

70. Phillips BE, Cancel L, Tarbell JM, Antonetti DA. Occludin independently regulates permeability under hydrostatic pressure and cell division in retinal pigment epithelial cells. *Invest Ophthalmol Vis Sci.* 2008;49(6):2568-76.
71. Antonetti DA, Barber AJ, Khin S, Lieth E, Tarbell JM, Gardner T. Vascular permeability in experimental diabetes is associated with reduced endothelial occludin content: vascular endothelial growth factor decreases occludin in retinal endothelial cells. *Diabetes.* 1998;47(12):1953-9.
72. Saitou M, Fujimoto K, Doi Y, Itoh M, Fujimoto T, Furuse M, et al. Occludin-deficient embryonic stem cells can differentiate into polarized epithelial cells bearing tight junctions. *J Cell Biol.* 1998;141(2):397-408.
73. Saitou M, Furuse M, Sasaki H, Schulzke JD, Fromm M, Takano H, et al. Complex phenotype of mice lacking occludin, a component of tight junction strands. *Mol Biol Cell.* 2000;11(12):4131-42.
74. Itoh M, Furuse M, Morita K, Kubota K, Saitou M, Tsukita S. Direct binding of three tight junction-associated MAGUKs, ZO-1, ZO-2 and ZO-3, with COOH termini of claudins. *J Cell Biol.* 1999;147(6):1351-63.
75. Ruffer C, Gerke V. The C-terminal cytoplasmic tail of claudins 1 and 5 but not its PDZ-binding motif is required for apical localization at epithelial and endothelial tight junctions. *Eur J Cell Biol.* 2004;83(4):135-44.
76. Morita K, Sasaki H, Furuse M, Tsukita S. Endothelial Claudin: Claudin-5/TMVCF constitutes tight junction strands in endothelial cells. *J Cell Biol.* 1999;147(1):185-94.
77. Furuse M, Sasaki H, Fujimoto K, Tsukita S. A single gene product, claudin-1 or -2, reconstitutes tight junction strands and recruits occludin in fibroblasts. *J Cell Biol.* 1998;143(2):391-401.
78. Inai T, Kobayashi J, Shibata Y. Claudin-1 contributes to the epithelial barrier function in MDCK cells. *Eur J Cell Biol.* 1999;78(12):849-55.
79. Nitta T, Hata M, Gotoh S, Seo Y, Sasaki H, Hashimoto N, et al. Size-selective loosening of the blood-brain barrier in claudin-5-deficient mice. *J Cell Biol.* 2003;161(3):653-60.
80. Koto T, Takubo K, Ishida S, Shinoda H, Inoue M, Tsubota K, et al. Hypoxia disrupts the barrier function of neural blood vessels through changes in the expression of claudin-5 in endothelial cells. *Am J Pathol.* 2007;170(4):1389-97.
81. Stevenson BR, Siliciano JD, Mooseker MS, Goodenough DA. Identification of ZO-1: a high molecular weight polypeptide associated with tight junction (zonula occludens) in a variety of epithelia. *J Cell Biol.* 1986;103(September):755-66.
82. Gumbiner B, Lowenkopf T, Apatira D. Identification of a 160-kDa polypeptide that binds to the tight junction protein ZO-1. *Proc Natl Acad Sci U S A* [Internet].

- 1991;88(8):3460–4.
83. Haskins J, Gu L, Wittchen ES, Hibbard J, Stevenson BR. ZO-3, a novel member of the MAGUK protein family found at the tight junction, interacts with ZO-1 and occludin. *J Cell Biol.* 1998;141(1):199–208.
 84. Woods DF, Bryant PJ. ZO-1, DlgA and PSD-95/SAP90: homologous proteins in tight, septate and synaptic cell junctions. *Mech Dev.* 1993;44(2–3):85–9.
 85. Wittchen ES, Haskins J, Stevenson BR. Protein Interactions at the Tight Junction. Actin has multiple binding partners, and ZO-1 forms independent complexes with ZO-2 and ZO-3. *J Biol Chem.* 1999;274(49):35179–85.
 86. McNeil E, Capaldo CT, Macara IG. Zonula occludens-1 function in the assembly of tight junctions in Madin-Darby canine kidney epithelial cells. *Mol Biol Cell.* 2006;17(4):1922–32.
 87. Hernandez S, Chavez Munguia B, Gonzalez-Mariscal L. ZO-2 silencing in epithelial cells perturbs the gate and fence function of tight junctions and leads to an atypical monolayer architecture. *Exp Cell Res.* 2007;313(8):1533–47.
 88. Umeda K, Ikenouchi J, Katahira-Tayama S, Furuse K, Sasaki H, Nakayama M, et al. ZO-1 and ZO-2 Independently Determine Where Claudins Are Polymerized in Tight-Junction Strand Formation. *Cell.* 2006;126(4):741–54.
 89. Katsuno T, Umeda K, Matsui T, Hata M, Tamura A, Itoh M, et al. Deficiency of zonula occludens-1 causes embryonic lethal phenotype associated with defected yolk sac angiogenesis and apoptosis of embryonic cells. *Mol Biol Cell.* 2008;19(6):2465–75.
 90. Balda MS, Matter K. The tight junction protein ZO-1 and an interacting transcription factor regulate ErbB-2 expression. *EMBO J.* 2000;19(9):2024–33.
 91. Laffafian I, Hallett MB. Lipid-Protein Cargo Transfer : A Mode of Direct Cell-to-Cell Communication for Lipids and Their Associated Proteins. *J cell Physiol.* 2007 ;210(2):336–42.
 92. Grebenkfinper K. Translational diffusion measurements of a fluorescent phospholipid between MDCK-I cells support the lipid model of the tight junctions. *Chem Phys Lipids.* 1994;71(94):133–43.
 93. Lee DBN, Jamgotchian N, Allen SG, Abeles MB, Ward HJ. A lipid-protein hybrid model for tight junction. *Am J Physiol Renal Physiol.* 2008 ;295(6):F1601-12.
 94. Kachar B, Reese TS. Evidence for the lipidic nature of tight junction strands. *1982 Nature.* 1982;296:464-6.
 95. Kan FW. Cytochemical Evidence for the Presence of Phospholipids in Epithelial Tight

- Junction Strands. *J Histochem Cytochem.* 1993;41(5):649-56.
96. Feltkamp CA, Van der waerden AW. Junction formation between cultured normal rat hepatocytes. An ultrastructural study on the presence of cholesterol and the structure of developing tight- junction strands. *J Cell Sci.* 1983;63:271–86.
 97. Viores SA, Gadegbeku C, Campochiaro PA, Greent WR. Immunohistochemical localization of blood-retinal barrier breakdown in human diabetics. *Am J Pathol* 1989;134(2):231–5.
 98. Barber AJ, Antonetti DA. Mapping the Blood Vessels with Paracellular Permeability in the Retinas of Diabetic Rats. *Investig Ophthalmol Vis Sci.* 2003;44(12):5410–6.
 99. Antonetti DA, Barber AJ, Hollinger LA, Wolpert EB, Gardner TW. Vascular Endothelial Growth Factor Induces Rapid Phosphorylation of Tight Junction Proteins Occludin and Zonula Occluden 1. *J Biol Chem.* 1999;274(33):23463–7.
 100. Harhaj NS, Felinski EA, Wolpert EB, Sundstrom JM, Gardner TW, Antonetti DA. VEGF activation of protein kinase C stimulates occludin phosphorylation and contributes to endothelial permeability. *Investig Ophthalmol Vis Sci.* 2006;47(11):5106–15.
 101. Murakami T, Frey T, Lin C, Antonetti DA. Protein kinase C β phosphorylates occludin regulating tight junction trafficking in vascular endothelial growth factor - Induced permeability in vivo. *Diabetes.* 2012;61(6):1573–83.
 102. Leal EC, Manivannan A, Hosoya K, Terasaki T, Cunha-Vaz J, Ambrósio AF, et al. Inducible nitric oxide synthase isoform is a key mediator of leukostasis and blood-retinal barrier breakdown in diabetic retinopathy. *Invest Ophthalmol Vis Sci.* 2007;48(11):5257–65.
 103. Ghassemifar R, Lai CM, Rakoczy PE. VEGF differentially regulates transcription and translation of ZO-1 α and ZO-1 β and mediates trans-epithelial resistance in cultured endothelial and epithelial cells. *Cell Tissue Res.* 2006;323(1):117–25.
 104. Peters S, Cree IA, Alexander R, Turowski P, Ockrim Z, Patel J, et al. Angiopoietin modulation of vascular endothelial growth factor: Effects on retinal endothelial cell permeability. *Cytokine.* 2007;40(2):144–50.
 105. Klaassen I, Hughes JM, Vogels IMC, Schalkwijk CG, Van Noorden CJF, Schlingemann RO. Altered expression of genes related to blood-retina barrier disruption in streptozotocin-induced diabetes. *Exp Eye Res.* 2009;89(1):4–15.
 106. Mizutani M, Kern TS, Lorenzi M. Accelerated death of retinal microvascular cells in human and experimental diabetic retinopathy. *J Clin Invest.* 1996;97(12):2883–90.
 107. Hammes HP, Du X, Edelstein D, Taguchi T, Matsumura T, Ju Q, et al. Benfotiamine blocks three major pathways of hyperglycemic damage and prevents experimental diabetic

- retinopathy. *Nat Med.* 2003;9(3):294-9.
108. Brownlee Michael. The pathobiology of diabetic complications. A unifying mechanism. *Diabetes.* 2005;54(6):1615-25.
 109. Jousseaume AM, Murata T, Tsujikawa A, Kirchhof B, Bursell S-E, Adamis AP. Leukocyte-Mediated Endothelial Cell Injury and Death in the Diabetic Retina. *Am J Pathol* [Internet]. 2001;158(1):147–52.
 110. Chen Y, Lin S, Lin F, Wu T, Tsao C. High Glucose Impairs Early and Late Endothelial Progenitor Cells by Modifying Nitric Oxide – Related but Not Oxidative Stress – Mediated Mechanisms. *Diabetes.* 2007;56(6):1559–68.
 111. Churdchomjan W, Kheolamai P, Manochantr S, Tapanadechopone P, Tantrawatpan C, U-Pratya Y, et al. Comparison of endothelial progenitor cell function in type 2 diabetes with good and poor glycemic control. *BMC Endocr Disord.* 2010;10:5.
 112. Stewart PA, Tuor UI. Blood-eye barriers in the rat: Correlation of ultrastructure with function. *J Comp Neurol.* 1994;340(4):566–76.
 113. Al Ahmad A, Gassmann M, Ogunshola OO. Maintaining blood-brain barrier integrity: Pericytes perform better than astrocytes during prolonged oxygen deprivation. *J Cell Physiol.* 2009;218(3):612–22.
 114. Wisniewska-Kruk J, Hoeben KA, Vogels IMC, Gaillard PJ, Van Noorden CJF, Schlingemann RO, et al. A novel co-culture model of the blood-retinal barrier based on primary retinal endothelial cells, pericytes and astrocytes. *Exp Eye Res.* 2012;96(1):181–90.
 115. Enge M, Bjarnega M, Gerhardt H, Gustafsson E, Asker N, Hammes H, et al. Endothelium-specific platelet-derived growth factor-B ablation mimics diabetic retinopathy. *EMBO J.* 2002;21(16):4307–16.
 116. Kuwabara T, Cogan DG. Retinal vascular patterns. VI. Mural cells of the retinal capillaries. *Arch Ophthalmol.* 1963;69:492-502.
 117. Geraldès P, Hiraoka-yamamoto J, Matsumoto M, Clermont A. Activation of PKC δ and SHP1 by hyperglycemia causes vascular cell apoptosis and diabetic retinopathy. *Nat Med.* 2009;15(11):1298–306.
 118. Patel JJ, Hykin PG, Gregor ZJ, Boulton M, Cree IA. Angiopoietin concentrations in diabetic retinopathy. *Br J Ophthalmol.* 2005;89(4):480–3.
 119. Rangasamy S, Srinivasan R, Maestas J, McGuire PG, Das A. A potential role for angiopoietin 2 in the regulation of the blood-retinal barrier in diabetic retinopathy. *Investig Ophthalmol Vis Sci.* 2011;52(6):3784–91.
 120. Beltramo E, Pomero F, Allione A, D’Alù F, Ponte E, Porta M. Pericyte adhesion is

- impaired on extracellular matrix produced by endothelial cells in high hexose concentrations. *Diabetologia*. 2002;45(3):416–9.
121. Kuiper EJ, Witmer AN, Klaassen I, Oliver N, Goldschmeding R, Schlingemann RO. Differential expression of connective tissue growth factor in microglia and pericytes in the human diabetic retina. *Br J Ophthalmol*. 2004;88(8):1082–7.
 122. Miyamoto K, Khosrof S, Bursell SE, Rohan R, Murata T, Clermont AC, et al. Prevention of leukostasis and vascular leakage in streptozotocin-induced diabetic retinopathy via intercellular adhesion molecule-1 inhibition. *Proc Natl Acad Sci U S A*. 1999;96(19):10836–41.
 123. McLeod DS, Lefer DJ, Merges C, Luttj G a. Enhanced expression of intracellular adhesion molecule-1 and P-selectin in the diabetic human retina and choroid. *Am J Pathol*. 1995;147(3):642–53.
 124. Barouch FC, Miyamoto K, Allport JR, Fujita K, Bursell SE, Aiello LP, et al. Integrin-mediated neutrophil adhesion and retinal leukostasis in diabetes. *Investig Ophthalmol Vis Sci*. 2000;41(5):1153–8.
 125. Jousseaume AM, Poulaki V, Le ML, Koizumi K, Esser C, Janicki H, et al. A central role for inflammation in the pathogenesis of diabetic retinopathy. *FASEB J*. 2004;18(12):1450–2.
 126. Lu M, Perez VL, Ma N, Miyamoto K, Peng H, Liao JK, Adamis AP. VEGF Increases Retinal Vascular ICAM-1 Expression In Vivo. *IOVS*. 1999;40(8):1808-12
 127. Jousseaume AM, Poulaki V, Qin W, Kirchhof B, Mitsiades N, Wiegand SJ, et al. Retinal vascular endothelial growth factor induces intercellular adhesion molecule-1 and endothelial nitric oxide synthase expression and initiates early diabetic retinal leukocyte adhesion in vivo. *Am J Pathol*. 2002;160(2):501–9.
 128. Nonaka A, Kiryu J, Tsujikawa A, Yamashiro K, Miyamoto K, Nishiwaki H, et al. PKC- β inhibitor (LY333531) attenuates leukocyte entrapment in retinal microcirculation of diabetic rats. *Investig Ophthalmol Vis Sci*. 2000;41(9):2702–6.
 129. Bolton SJ, Anthony DC, Perry VH. Loss of the tight junction proteins occludin and zonula occludens-1 from cerebral vascular endothelium during neutrophil - induced blood – brain barrier breakdown in vivo. *Neuroscience*. 1998;86(4):1245–57.
 130. Reese TS, Karnovsky MJ. Fine structural localization of blood-brain barrier to exogenous peroxidase. *J Cell Biol*. 1967;34(1):207–17.
 131. Schnitzer J. Retinal astrocytes: their restriction to vascularized parts of the mammalian retina. *Neurosci Lett*. 1987;78(1):29–34.
 132. Schnitzer J. Astrocytes in the guinea pig, horse, and monkey retina: Their occurrence coincides with the presence of blood vessels. *Glia*. 1988;1(1):74–89.

133. Tout S, Chan-Ling T, Hollander H, Stone J. The role of Muller cells in the formation of the blood-retinal barrier. *Neuroscience*. 1993;55(1):291–301.
134. Gardner TW, Lieth E, Khin SA, Barber AJ, Bonsall DJ, Leshner T, et al. Astrocytes increase barrier properties and ZO-1 expression in retinal vascular endothelial cells. *Investig Ophthalmol Vis Sci*. 1997;38(11):2423–7.
135. Willis CL, Leach L, Clarke GJ, Nolan CC, Ray DE. Reversible disruption of tight junction complexes in the rat blood-brain barrier, following transitory focal astrocyte loss. *Glia*. 2004;48(1):1–13.
136. Tretiach M, Madigan MC, Wen L, Gillies MC. Effect of Muller cell co-culture on in vitro permeability of bovine retinal vascular endothelium in normoxic and hypoxic conditions. *Neurosci Lett*. 2005;378(3):160–5.
137. Shen W, Li S, Chung SH, Gillies MC. Retinal vascular changes after glial disruption in rats. *J Neurosci Res*. 2010;88(7):1485–99.
138. Behzadian M a, Wang XL, Windsor LJ, Ghaly N, Caldwell RB. TGF-beta increases retinal endothelial cell permeability by increasing MMP-9: possible role of glial cells in endothelial barrier function. *Invest Ophthalmol Vis Sci*. 2001;42(3):853–9.
139. Giebel SJ, Menicucci G, McGuire PG, Das A. Matrix metalloproteinases in early diabetic retinopathy and their role in alteration of the blood-retinal barrier. *Lab Invest*. 2005;85(5):597–607.
140. Barber AJ, Antonetti DA, Gardner TW. Altered expression of retinal occludin and glial fibrillary acidic protein in experimental diabetes. *Penn State Retin Res Group Invest Ophthalmol Vis Sci*. 2000;41(11):3561–8.
141. Krady JK, Basu A, Allen CM, Xu Y, LaNoue KF, Gardner TW, et al. Minocycline reduces proinflammatory cytokine expression, microglial activation, and caspase-3 activation in a rodent model of diabetic retinopathy. *Diabetes*. 2005;54(5):1559–65.
142. Martiney JA, Litwak M, Berman JW, Arezzo JC, Brosnan CF. Pathophysiologic effect of interleukin-1b in the rabbit retina. *Am J Pathol [Internet]*. 1990;137(6):1411–23.
143. Vinores SA, Xiao WH, Shen J, Campochiaro. TNF-alpha is critical for ischemia-induced leukostasis, but not retinal neovascularization nor VEGF- induced leakage. *J Neuroimmunol*. 2007;182(1-2):73-9.
144. Coppack SW, Evans RD, Fisher RM, Fryan KN, Gibbons GF, et al. Adipose tissue metabolism in obesity Lipase action in vivo before and after a mixed meal. *Metabolism*. 1992; 41(3):264-72.
145. Dimitriadis G, Mitrou P, Lambadiari V, Maratou E, Raptis SA. Insulin effects in muscle and adipose tissue. *Diabets Res Clin Pract*. 2011;93:S52-9.

146. Frayn K. Adipose tissue as a buffer for daily lipid flux. *Diabetologia*. 2002;45(9):1201–10.
147. Leavens KF, Birnbaum MJ. Insulin signaling to hepatic lipid metabolism in health and disease. *Crit Rev Biochem Mol Biol*. 2011;46(3):200–15.
148. Goldberg IJ. Clinical review 124: Diabetic dyslipidemia - Causes and consequences. *J Clin Endocrinol Metab*. 2001;86(3):965–71.
149. Guy J, Ogden L, Wadwa RP, Hamman RF, Mayer-Davis EJ, et al. Lipid and Lipoprotein Profiles in Youth With and Without Type 1 Diabetes: The SEARCH for Diabetes in Youth Case-Control Study. *Diabetes Care*. 2009;32(3):416–20.
150. Petitti DB, Imperatore G, Palla SL, Daniels SR, Dolan LM, et al. Serum Lipids and Glucose Control. The search for diabetes in youth study. *Arch Pediatr Adolesc Med* [Internet]. 2007;161:159–65.
151. Ginsberg HN. Diabetic dyslipidemia: Basic mechanisms underlying the common hypertriglyceridemia and low HDL cholesterol levels. *Diabetes*. 1996;45(3 SUPPL.):27–30.
152. Krauss RM. Heterogeneity of plasma low-density lipoprotein and atherosclerosis risk. *curr opin lipidol*. 1994;5(5):339–49.
153. Rader DJ. Effect of Insulin Resistance, Dyslipidemia, and Intra-abdominal Adiposity on the Development of Cardiovascular Disease and Diabetes Mellitus. *Am J Med*. 2007;120(3 SUPPL. 1):S12–8.
154. Adams TH, Walzem RL, Smith DR, Tseng S, Smith SB. Hamburger high in total, saturated and trans-fatty acids decreases HDL cholesterol and LDL particle diameter, and increases TAG, in mildly hypercholesterolaemic men. *Br J Nutr*. 2010;103(1):91–8.
155. Kelley DS, Siegel D, Vemuri M, Mackey BE. Docosahexaenoic acid supplementation improves fasting and postprandial lipid profiles in hypertriglyceridemic men. *Am J Clin Nutr*. 2007;86:324–33.
156. Tilvis RS, Taskinen MR, Miettinen TA. Effect of insulin treatment on fatty acids of plasma and erythrocyte membrane lipids in type 2 diabetes. *Clin Chim Acta*. 1988;171(2–3):293–303.
157. Seigneur M, Freyburger G, Gin H, Claverie M. Serum fatty acid profiles in type I and type II diabetes: metabolic alterations of fatty acids of the main serum lipids. *Diabetes Res*. 1994;23:169–77.
158. Jakobsson A, Westerberg R, Jacobsson A. Fatty acid elongases in mammals: Their regulation and roles in metabolism. *Prog Lipid Res*. 2006;45(3):237–49.
159. Uchida Y. The role of fatty acid elongation in epidermal structure and

- function. *Dermatoendocrinol.* 2011;3(2):65–9.
160. Kihara A. Very long-chain fatty acids: Elongation, physiology and related disorders. *J Biochem.* 2012;152(5):387–95.
 161. Guillou H, Zadavec D, Martin PGP, Jacobsson A. The key roles of elongases and desaturases in mammalian fatty acid metabolism: Insights from transgenic mice. *Prog Lipid Res.* 2010;49(2):186–99.
 162. Brenner RR. Hormonal modulation of $\Delta 6$ and $\Delta 5$ desaturases: Case of diabetes. *Prostaglandins Leukot Essent Fat Acids.* 2003;68(2):151–62.
 163. Rimoldi OJ, Finarelli GS, Brenner R. Effects of Diabetes and Insulin on Hepatic $\Delta 6$ Desaturase Gene Expression. *Biochem Biophys Res Commun.* 2001;283(2):323–6.
 164. Waters K, Ntambi JM. Insulin and dietary fructose induce stearoyl-coA desaturase 1 gene expression in liver of diabetic mice. *J Biol Chem.* 1994;269(44):27773-7
 165. Wang Y, Botolin D, Xu J, Christian B, Mitchell E, Jayaprakasam B, et al. Regulation of hepatic fatty acid elongase and desaturase expression in diabetes and obesity. *J Lipid Res.* 2006;47(9):2028–41.
 166. Ohno Y, Suto S, Yamanaka M, Mizutani Y, Mitsutake S, Igarashi Y, et al. ELOVL1 production of C24 acyl-CoAs is linked to C24 sphingolipid synthesis. *Proc Natl Acad Sci U S A.* 2010;107(43):18439–44.
 167. Vasireddy V, Uchida Y, Salem N, Kim SY, Mandal NA, et al. Loss of functional ELOVL4 depletes very long-chain fatty acids (≥ 28) and the unique ω -o-acylceramides in skin leading to neonatal death. *Hum Mol Genet.* 2007;16(5):471-82.
 168. Zhang K, Kniazeva M, Han M, Li W, Yu Z, yang Z, et al. A 5-bp deletion in ELOVL4 is associated with two related forms of autosomal dominant macular dystrophy. *Nat Genet.* 2001;27(1):89–93.
 169. Mandal MNA, Ambasudhan R, Wong PW, Gage PJ, Sieving PA, Ayyagari R. Characterization of mouse orthologue of ELOVL4: Genomic organization and spatial and temporal expression. *Genomics.* 2004;83(4):626–35.
 170. Jakobsson A, Jørgensen JA, Jacobsson A. Differential regulation of fatty acid elongation enzymes in brown adipocytes implies a unique role for Elov13 during increased fatty acid oxidation. *Am J Physiol Endocrinol Metab.* 2005;289(4):E517–26.
 171. Green CD, Olson LK. Modulation of palmitate-induced endoplasmic reticulum stress and apoptosis in pancreatic β -cells by stearoyl-CoA desaturase and Elov16. *Am J Physiol Endocrinol Metab.* 2011;300(4):E640–9.
 172. Van Eck WF. The effect of a low fat diet on the serum lipids in diabetes and its

- significance in diabetic retinopathy. *Am J Med* [Internet]. 1959;27:196–211.
173. Houtsmuller AJ, Zahn KJ, Henkes HE. Unsaturated fats and progression of diabetic retinopathy. *Doc Ophthalmol*. 1980;48(2):363–71.
 174. Augustin AJ, Breipohl W, Böker T, Lutz J, Spitznas M. Increased lipid peroxide levels and myeloperoxidase activity in the vitreous of patients suffering from proliferative diabetic retinopathy. *Graefes Arch Clin Exp Ophthalmol*. 1993;231(11):647–50.
 175. Chew EY, Klein ML, Iii FLF, Remaley N a, Murphy RP, Chantry K, et al. Association of elevated serum lipid levels with retinal hard exudate in diabetic retinopathy. *Arch Ophthalmol*. 1996;114:1079-84.
 176. Ferris FL, Chew EY, Hoogwerf B. Serum lipids and diabetic retinopathy. *Diabetes care*. 1996;19(11):1291-93.
 177. Davis MD, Fisher MR, Gangnon RE, Barton F, Aiello LM, Chew EY, et al. Risk factors for high-risk proliferative diabetic retinopathy and severe visual loss: Early Treatment Diabetic Retinopathy Study Report #18. *Invest Ophthalmol Vis Sci*. 1998;39(2):233–52.
 178. Lyons TJ, Jenkins AJ, Zheng D, Lackland DT, McGee D, Garvey WT, et al. Diabetic retinopathy and serum lipoprotein subclasses in the DCCT/EDIC cohort. *Investig Ophthalmol Vis Sci*. 2004;45(3):910–8.
 179. Miljanovic B, Glynn RJ, Nathan DM, Manson JE, Schaumberg DA. A prospective study of serum lipids and risk of diabetic macular edema in type 1 diabetes. *Diabetes*. 2004;53(11):2883–92.
 180. The Action of Control Cardiovascular Risk in Diabetes Study Group. Effects of Medical Therapies on Retinopathy Progression in Type 2 Diabetes. *N Engl J Med*. 2010;363:233-44.
 181. Sprecher H, Chen Q. Polyunsaturated fatty acid biosynthesis: a microsomal-peroxisomal process. *Prostaglandins Leukot Essent Fat Acids*. 1999;60:317-21.
 182. Lecomte M, Paget C, Ruggiero D, Wiernsperger N, Lagarde M. Docosahexaenoic acid is a major n-3 polyunsaturated fatty acid in bovine retinal microvessels. *J Neurochem*. 1996;66(5):2160–7.
 183. Fliesler SJ, Anderson RE. Chemistry and metabolism of lipids in the vertebrate retina. *prog. lipid. Res*. 1983;22:79-131.
 184. Aveldaño MI. Phospholipid species containing long and very long polyenoic fatty acids remain with rhodopsin after hexane extraction of photoreceptor membranes. *Biochemistry*. 1988;27(4):1229–39.
 185. Brush RS, Tran JTA, Henry KR, McClellan ME, Elliott MH, Mandal MNA. Retinal sphingolipids and their very-long-chain fatty acid-containing species. *Investig*

- Ophthalmol Vis Sci. 2010;51(9):4422–31.
186. Tikhonenko M, Lydic T a, Wang Y, Chen W, Opreanu M, Sochacki A, et al. , Remodeling of retinal fatty acids in animals model of diabetes: a decrease in long-chain polyunsaturated fatty acids is associated with a decrease in fatty acid elongases ELOVL2 and ELOVL4. *Diabetes* 2010;59(1):219–27.
 187. Tikhonenko M, Lydic TA, Opreanu M, Li Calzi S, Bozack S, McSorley KM, et al. N-3 Polyunsaturated Fatty Acids Prevent Diabetic Retinopathy by Inhibition of Retinal Vascular Damage and Enhanced Endothelial Progenitor Cell Reparative Function. *PLoS One*. 2013;8(1):1–10.
 188. Opreanu M, Lydic T a, Reid GE, McSorley KM, Esselman WJ, Busik J V. Inhibition of cytokine signaling in human retinal endothelial cells through downregulation of sphingomyelinases by docosahexaenoic acid. *Invest Ophthalmol Vis Sci*. 2010;51(6):3253–63.
 189. Opreanu M, Tikhonenko M, Bozack S, Lydic TA, Reid GE, McSorley KM, et al. The unconventional role of acid sphingomyelinase in regulation of retinal microangiopathy in diabetic human and animal models. *Diabetes*. 2011;60(9):2370–8.
 190. Zhang XM, Yang Z, Karan G, Hashimoto T, Baehr W, Yang XJ, et al. Elov14 mRNA distribution in the developing mouse retina and phylogenetic conservation of Elov14 genes. *Mol Vis* [Internet]. 2003;9(April):301–7.
 191. Lagali PS, Liu J, Ambasadhan R, Kakuk LE, Bernstein SL, Seigel GM, et al. Evolutionarily conserved ELOVL4 gene expression in the vertebrate retina. *Investig Ophthalmol Vis Sci*. 2003;44(7):2841–50.
 192. Grayson C, Molday RS. Dominant negative mechanism underlies autosomal dominant Stargardt-like macular dystrophy linked to mutations in ELOVL4. *J Biol Chem*. 2005;280(37):32521–30.
 193. Agbaga M-P, Brush RS, Mandal MNA, Henry K, Elliott MH, Anderson RE. Role of Stargardt-3 macular dystrophy protein (ELOVL4) in the biosynthesis of very long chain fatty acids. *Proc Natl Acad Sci U S A*. 2008;105(35):12843–8.
 194. McMahon A, Jackson SN, Woods AS, Kedzierski W. A stargardt disease-3 mutation in the mouse Elov14 gene causes retinal deficiency of C32-C36 acyl phosphatidylcholines. *FEBS Lett*. 2007;581(28):5459-63.
 195. Harkewicz R, Du H, Tong Z, Alkuraya H, Bedell M, Sun W, et al. Essential role of ELOVL4 protein in very long chain fatty acid synthesis and retinal function. *J Biol Chem*. 2012;287(14):11469–80.
 196. Karan G, Lillo C, Yang Z, Cameron DJ, Locke KG, Zhao Y, et al. Lipofuscin accumulation, abnormal electrophysiology, and photoreceptor degeneration in mutant ELOVL4 transgenic mice: a model for macular degeneration. *Proc Natl Acad Sci U*

- S A. 2005;102(11):4164–9.
197. McMahon A, Butovich IA, Mata NL, Klein M, Ritter R, Richardson J, et al. Retinal pathology and skin barrier defect in mice carrying a Stargardt disease-3 mutation in elongase of very long chain fatty acids-4. *Mol Vis.* 2007;13(October 2006):258–72.
 198. Li W, Sandhoff R, Kono M, Zerfas P, Hoffmann V, Ding BCH, et al. Depletion of ceramides with very long chain fatty acids causes defective skin permeability barrier function, and neonatal lethality in ELOVL4 deficient mice. *Int J Biol Sci.* 2007;3(2):120–8.
 199. McMahon A, Butovich I a, Kedzierski W. Epidermal expression of an Elov14 transgene rescues neonatal lethality of homozygous Stargardt disease-3 mice. *J Lipid Res.* 2011;52(6):1128–38.
 200. Abcouwer SF, Lin C, Wolpert EB, Shanmugam S, Schaefer EW, Freeman WM, et al. Effects of ischemic preconditioning and bevacizumab on apoptosis and vascular permeability following retinal ischemia-reperfusion injury. *Invest Ophthalmol Vis Sci.* 2010 Nov;51(11):5920–33.
 201. Grassmé H, Jekle A, Riehle A, Schwarz H, Berger J, Sandhoff K, et al. CD95 Signaling via Ceramide-rich Membrane Rafts. *J Biol Chem.* 2001;276(23):20589–96.
 202. Zeidan YH, Hannun YA. Activation of acid sphingomyelinase by protein kinase C ζ -mediated phosphorylation. *J Biol Chem.* 2007;282(15):11549–61.
 203. Grassmé H, Riethmüller J, Gulbins E. Biological aspects of ceramide-enriched membrane domains. *Prog Lipid Res.* 2007;46(3–4):161–70.
 204. Kolesnick RN, Goñi FM, Alonso A. Compartmentalization of Ceramide Signaling: Physical Foundations and Biological Effects. *J Cell Physiol.* 2000;184(3):285–300.
 205. Grant MB, May WS, Caballero S, Brown G a J, Guthrie SM, Mames RN, et al. Adult hematopoietic stem cells provide functional hemangioblast activity during retinal neovascularization. *Nat Med.* 2002;8(6):607–12.
 206. Kocher AA, Schuster MD, Szabolcs MJ, Takuma S, Burkhoff D, et al. Neovascularization of ischemic myocardium by human bone - marrow – derived angioblasts prevents cardiomyocyte apoptosis, reduces remodeling and improves cardiac function. *Nat Med.* 2001;7(4):430-6.
 207. Kalka C, Masuda H, Takahashi T, Kalka-Moll WM, Silver M, Kearney M, et al. Transplantation of ex vivo expanded endothelial progenitor cells for therapeutic neovascularization. *Proc Natl Acad Sci U S A.* 2000;97(7):3422–7.
 208. Hristov M, Erl W, Weber PC. Endothelial progenitor cells: Mobilization, differentiation, and homing. *Arterioscler Thromb Vasc Biol.* 2003;23(7):1185–9.

209. Hirschi KK, Ingram DA, Yoder MC. Assessing identity, phenotype, and fate of endothelial progenitor cells. *Arterioscler Thromb Vasc Biol.* 2008;28(9):1584–95.
210. Kamihata H, Matsubara H, Nishiue T, Fujiyama S, Tsutsumi Y, Ozono R, et al. Implantation of Bone Marrow Mononuclear Cells Into Ischemic Myocardium Enhances Collateral Perfusion and Regional Function via Side Supply of Angioblasts, Angiogenic ligands, and Cytokines. *Circulation.* 2001;104(9):1046–52.
211. Kinnaird T, Stabile E, Burnett ES, Shou M, Lee CW, Barr S, Fuchs S, et al. Local Delivery of Marrow-Derived Stromal Cells Augments Collateral Perfusion Through Paracrine Mechanisms. *Circulation.* 2004;109(12):1543–9.
212. Tongers J, Roncalli JG, Losordo DW. Role of endothelial progenitor cells during ischemia-induced vasculogenesis and collateral formation. *Microvasc Res.* 2010;79(3):200–6.
213. Méndez-Ferrer S, Lucas D, Battista M, Frenette PS. Haematopoietic stem cell release is regulated by circadian oscillations. *Nature.* 2008;452(7186):442–7.
214. Katayama Y, Battista M, Kao WM, Hidalgo A, Peired AJ, Thomas SA, et al. Signals from the sympathetic nervous system regulate hematopoietic stem cell egress from bone marrow. *Cell.* 2006;124(2):407–21.
215. Schatteman GC, Hanlon HD, Jiao C, Dodds SG, Christy BA. Blood-derived angioblasts accelerate blood-flow restoration in diabetic mice. *J Clin Invest.* 2000;106(4):571–8.
216. Tepper OM, Galiano RD, Capla JM, Kalka C, Gagne PJ, Jacobowitz GR, et al. Human endothelial progenitor cells from type II diabetics exhibit impaired proliferation, adhesion, and incorporation into vascular structures. *Circulation.* 2002;106(22):2781–6.
217. Busik J V, Tikhonenko M, Bhatwadekar A, Opreanu M, Yakubova N, Caballero S, et al. Diabetic retinopathy is associated with bone marrow neuropathy and a depressed peripheral clock. *J Exp Med.* 2009;206(13):2897–906.
218. Kusuyama T, Omura T, Nishiya D, Enomoto S, Matsumoto R, Takeuchi K, et al. Effects of treatment for diabetes mellitus on circulating vascular progenitor cells. *J Pharmacol Sci.* 2006;102:96–102.
219. Fadini GP, Pucci L, Vanacore R, Baesso I, Penno G, Balbarini A, et al. Glucose tolerance is negatively associated with circulating progenitor cell levels. *Diabetologia.* 2007;50(10):2156–63.
220. Loomans CJ, de Koning EJ, Staal FJ, Rookmaaker MB, Verseyden C, de Boer HC, et al. Endothelial progenitor cell dysfunction: a novel concept in the pathogenesis of vascular complications of type 1 diabetes. *Diabetes.* 2004;53(1):195–9.

221. Caballero S, Sengupta N, Afzal A, Chang KH, Li Calzi S, Guberski DL, et al. Ischemic vascular damage can be repaired by healthy, but not diabetic, endothelial progenitor cells. *Diabetes*. 2007;56(4):960–7.
222. Jarajapu YP, Thampi P, Caballero S, Boulton ME, Grant MB. Differential paracrine dysfunction and hypoxic desensitization in diabetic CD34+ and CD14+ bone marrow derived (BMDC). *Circulation*. 2009;120:S1124 .
223. Segal MS, Shah R, Afzal A, Perrault CM, Chang K, et al. Nitric oxide cytoskeletal-induced alterations reverse the endothelial progenitor cell migratory defect associated with diabetes. *Diabetes*. 2006;55(1):102-9.
224. Aicher A, Zeiher AM, Dimmeler S. Mobilizing endothelial progenitor cells. *Hypertension*. 2005;45(3):321–5.
225. Thum T, Fraccarollo D, Schultheiss M, Froese S, Galuppo P, Widder JD, et al. Endothelial nitric oxide synthase uncoupling impairs endothelial progenitor cell mobilization and function in diabetes. *Diabetes*. 2007;56(3):666–74.
226. Vasa M, Breitschopf K, Zeiher AM, Dimmeler S. Nitric oxide activates telomerase and delays endothelial cell senescence. *Circ Res*. 2000;87(7):540–2.
227. Chakravarthy H, Navitskaya S, O'Reilly S, Gallimore J, Mize H, et al. Role of Acid Sphingomyelinase in Shifting the Balance Between Proinflammatory and Reparative Bone Marrow Cells in Diabetic Retinopathy. *Stem cells*. 2016;34(4):972-83.

Chapter 2. Overexpression of ELOVL4 stabilizes tight junctions and prevents VEGF-induced vascular permeability in diabetic retina and retinal cells

Authors: Nermin Kady, Xuwen Liu, Todd Lydic, Meesum Syed, Svetlana Navitskaya, Qi Wang, Sandra Hammer, Sandra O'Reilly, Chao Huang, Sergey S. Seregin, Andrea Amalfitano, Vince A. Chiodo, Sanford L. Boye, William W. Hauswirth, David A. Antonetti and Julia V. Busik

2.1 Abstract

Tight junctions contribute to the control of permeability in the blood brain and blood retinal barrier and loss of the junctional complex contributes to the pathology of a host of diseases of these neural tissues including brain tumors and dementia and blinding eye diseases such as diabetic retinopathy. Tight junctions involve close apposition of transmembrane proteins between cells. While, tight junction proteins have been studied in detail, the role of lipids in tight junction structure and permeability has received much less attention. In this study, using diabetes induced loss of blood-retinal barrier as a model, we addressed the role of very long chain (VLC ≥ 26) ceramides in tight junction integrity and function. VLC fatty acids that incorporate into VLC ceramides are produced by elongation of very long chain fatty acids 4 (ELOVL4). ELOVL4 is significantly reduced in the diabetic retina leading to decreased levels of VLC fatty acids. Overexpression of ELOVL4 in bovine retinal endothelial cells (BRECs) significantly decreased basal permeability, inhibited VEGF and IL-1 β induced permeability and simultaneously prevented VEGF-induced decrease in occludin expression and border staining of tight junction proteins; ZO-1 and claudin-5. Knockdown of ELOVL4 was associated with increased paracellular permeability. Moreover, intravitreal delivery of hELOVL4-AAV2 reduced diabetes-induced increase in vascular permeability in mice. Importantly, ultrastructure analysis

reveals that ceramides co-localize with tight junction complexes. Lipidomic analysis of tight junction isolates revealed the presence of omega-linked acyl-VLC ceramides. These very unusual structures are known to be important for the maintenance of skin water permeability barrier, but they have never been shown in tight junctions. The data presented here demonstrate that ELOVL4 is required for maintaining healthy blood retinal barrier and normalization of retinal ELOVL4 expression could prevent blood-retinal barrier dysregulation in DR through increase in VLC ceramides and stabilization of tight junctions.

2.2 Introduction

Diabetic Retinopathy (DR) remains a major cause of loss of vision despite recent advances in therapeutic options. Loss of the blood-retinal barrier (BRB) and increased vascular permeability marks early stages of DR and contributes to disease progression. Several factors have been shown to contribute to increased vascular permeability. Prominent among them are diabetes-induced increase in the level of vascular endothelial growth factor (VEGF) (1–3), interleukin-1 beta (IL-1 β) (4,5), tumor necrosis factor α (TNF α) (5), extracellular proteases; matrix metalloproteases 2 and 9 (6–8), and pericyte loss (9–11). Importantly, antibodies targeting VEGF demonstrate prevention of visual loss and even restoration of vision in many patients with diabetic macular edema (12). Hyperglycemia contributes an important role in the expression of these pro-inflammatory and pro-angiogenic factors (11,13–16). However, the etiology of DR progression remain incompletely understood and recent assessment of the Diabetes Complications and Control Trial suggest that only 11% of blindness may be accounted for by hyperglycemia (17).

Several recent clinical trials, including the ACCORD Eye Trial, have demonstrated that in addition to hyperglycemia, diabetic dyslipidemia may contribute a critical role in the development of DR (18). In agreement with the results of clinical trials, recent studies of diabetic animal models have demonstrated that altered retinal lipid metabolism and dyslipidemia leads to retinal inflammation and vascular degeneration (19–21). In particular, our laboratory identified a marked decrease in the expression of several retinal fatty acid elongases. Elongation is a complex reaction involving four enzymatic steps that result in addition of two carbons to the carboxyl end of fatty acids. Elongases perform the first rate-limiting condensation step in the

fatty acid elongation cycle in a substrate specific manner. Seven elongation of very long chain fatty acids (ELOVL) 1-7 have been identified in mammals with each elongase exhibiting a characteristic substrate specificity and tissue distribution (22,23). Elongases are highly expressed in normal retina where they actively participate in *de novo* lipogenesis, as well as mono and polyunsaturated fatty acid (PUFA) synthesis. Downregulation of elongases in diabetic retina results in decreased long-chain-to-short-chain fatty acids ratio. Moreover, synthesis of the major n3 PUFA that accumulate in the retina, docosahexaenoic acid (DHA; 22:6, n3), requires two extra elongation steps compared to the n6 PUFA, arachidonic acid (20:4,n6), thus decrease in elongation contributes to decreased n3-to-n6 PUFA ratio in the retina. This decrease in n3-to-n6 ratio was shown to be associated with increased expression of adhesion molecules, pro-inflammatory cytokines, and retinal vascular pathology (19).

ELOVL4 is the highest expressed elongase in the retina (24). ELOVL4 elongates extremely long fatty acids $\geq C24$ and its expression is restricted to the tissues with extremely long fatty acids such as the retina (24–27), thymus and skin (26), and at a lower level in the brain and testis(27). Fatty acids with $\geq C24$ chain are used as precursors by ELOVL4 for synthesis of $\geq C26$ very long chain PUFA (VLCPUFA) and saturated VLCFAs (23,28–30). Saturated VLCFAs are primarily incorporated into ceramides (Cer) and glucosylceramides (GlcCer) that are known to be highly expressed in epidermis (22,23). These ceramides with extremely long FA are major lipid components of stratum corneum and they have been shown to be essential in maintenance of the water permeability barrier in skin (22,31,32). Genetic studies with ELOVL4 mutant mice revealed that ELOVL4 plays an essential role in skin barrier function as these mice exhibit skin

barrier defect and neonatal death phenotype (33–35). Besides the role of ELOVL4 in the skin, ELOVL4 dysfunction has been associated with Stargardt-like macular dystrophy (STGD3) (36–38). Interestingly, ELOVL4 is one of the enzymes that was found to be downregulated in the retina by both diabetes (19) and retinal ischemia-reperfusion (39).

We hypothesized that VLC ceramides support BRB function in an ELOVL4 dependent manner. This study was designed to test the role of ELOVL4 and VLC ceramides in diabetes-induced increase in retinal vascular permeability and to identify if lipids, in particular VLC ceramides, localize in the tight junction and play a role in controlling the paracellular permeability of retinal endothelial cells.

2.3 Materials and methods

2.3.1 Cell culture

Bovine retinal endothelial cells (BREC) were isolated and grown in culture as previously described (2) and cultured on 1 $\mu\text{g}/\text{cm}^2$ fibronectin coated plates (Sigma-Aldrich) in MCDB-131 (Sigma-Aldrich) growth media supplemented with 10% FCS (Hyclone, Logan, UT), 10 ng/mL epidermal growth factor (Sigma-Aldrich), 0.2 mg/mL endothelial cell growth medium additive (EndoGro; Vec Technologies, Rensselaer, NY), 0.09 mg/mL heparin (Fisher Scientific, Pittsburgh, PA), 0.01 mL/mL antibiotic-antimycotic (GIBCO 100x, Invitrogen-Life Technologies, Carlsbad, CA), and 8 $\mu\text{g}/\text{mL}$ tylosin (Sigma-Aldrich), and maintained at 37°C in 95% air and 5% CO₂ in a humidified cell culture incubator. All experiments were performed with cells at passage 4-6. For biochemical purification of tight junction, Human retinal pigment epithelial cell line ARPE-19 (HRPE) cells were grown in Dulbecco's modified Eagle's medium/F12 (1:1 ratio, 5 mmol/l glucose) supplemented with 10% fetal calf serum, 1% penicillin/streptomycin, at 37°C in humidified 95% air and 5% CO₂.

2.3.2 Virus-mediated hELOVL4 overexpression

Human ELOVL4 was expressed using an E-1 and E-3 deleted adenoviral vector system containing the human ELOVL4 cDNA (AdhELOVL4) under control of the CMV promoter. Where subconfluent BRECs were transduced with either AdhELOVL4 or AdEmpty as a negative control at a multiplicity of infection (MOI) 20,000 overnight in MCDB media supplemented with 2 % serum. Successful overexpression was confirmed by quantitative real-time PCR (qPCR) and immunoblotting for hELOVL4 at the time of permeability studies (60 h post viral transduction).

For *in vivo* experiments, human ELOVL4 was engineered into adeno-associated virus

serotype 2 vectors containing four capsid tyrosine to phenylalanine (Y – F) mutations (AAV2 mut quad) (40) under control of the ubiquitous truncated chimeric CMV-chicken β -actin (smCBA) promoter. Empty AAV2 mut quad construct was used as a negative control. The virus was produced at the Department of Ophthalmology, University of Florida, Gainesville, FL.

2.3.3 siRNA transfection

BREC in culture were resuspended in nucleofector solution (Amaxa Biosystems, Gaithersburg, MD) to a final concentration 5×10^5 cells/100 μ l. Cell suspension was mixed with 100nM control or ELOVL4 StealthTM siRNA from Invitrogen Life Technologies (Carlsbad, CA, USA) into the electroporation cuvette, and were electroporated (Nucleofector program S-005; Amaxa Biosystems) and maintained in culture as above. After either 48h or 72 h, cells were collected for total mRNA and protein expression, respectively.

2.3.4 Permeability assay in vitro

Ad-Empty and Ad-hELOVL4 BRECs were grown to confluence on fibronectin-coated, 0.4- μ m pores transwell filters (Transwell; Corning Costar, Acton, MA, USA) at 75×10^3 cells/well, pretreated with 1% FCS, 0.01 ml/ml antibiotic/antimycotic and 100 nM hydrocortisone for 36 h. Apical and basolateral chambers were treated with recombinant human VEGF₁₆₅ (50 ng/ml for 30 min), or IL-1 β (10ng/ml for 15 min) where indicated. After treatments, 10 μ M of 70 kDa RITC-dextran was added to the apical chamber. BREC paracellular permeability to 70 KDa rhodamine isothiocyanate dextran (Sigma-Aldrich) was measured as previously described (2,3). Aliquots were collected from the basolateral chamber every 30 min for 4 h and placed in a 96-well black/clear bottom plate. At the last time point, aliquots were collected from the apical

chamber and placed in the 96-well plate. The RITC-dextran fluorescence was quantified with fluorescence imager (FluorImager 560/590; TECAN infinite 1000), and the rate of diffusive permeability (P_o) was calculated by the following formula:

$$P_o = [(F_A / \Delta t) V_A] / (F_L A)$$

Where, P_o = diffusive flux (cm / s); F_A is basolateral fluorescence; F_L is apical fluorescence; Δt is change in time; A is the surface area of the filter (in cm^2); and V_A is the volume of the basolateral chamber (in cm^3).

The average P_o for control conditions (AdEmpty) used in all experiments ranged from 2.5 to 2.8 $\times 10^{-6}$ cm/s.

2.3.5 Western blotting

Protein extraction and Western blot was performed using NuPAGE system (Invitrogen) as described previously (3,21). Briefly, AdEmpty and AdhELOVL4 BRECs were lysed in Triton-X-100-deoxycolate-SDS-based lysis buffer. Protease inhibitor cocktail tablet (Roche, Indianapolis, IN, USA) and phosphatase inhibitor (1 mM Na_4PPi , 10 mM NaF , 100 μM glycerophosphate, 1 mM Na_3PO_4) were freshly added. Protein concentration was determined by the BioRad DC protein colorimetric assay (BioRad, Hercules, CA, USA). 30 μg of protein were loaded on 4-12 % NuPAGE Bis -Tris gradient gels (Life Technologies, Carlsbad, CA) and ran at 200 V for 1 h, followed by transfer to nitrocellulose membrane, and immunoblotting with the following primary antibodies; rabbit polyclonal anti-ELOVL4 (Sigma, Cat. No. SAB4502884), rat monoclonal anti- ZO-1 (Millipore, Cat. No. MABT11), mouse monoclonal anti-occludin (Invitrogen, Cat. No. 33-1500) and rabbit polyclonal anti-claudin-5 (Invitrogen, Cat. No. 34-

1600), all used in dilution 1:1000. As control for protein loading, membranes were blotted with either mouse monoclonal anti- α tubulin (Sigma, Cat. No. T5168) or mouse monoclonal anti- β actin antibody (Cell Signaling, Cat. No. 4967) (1:4000). Primary antibodies were detected by horseradish peroxidase –conjugated or infrared secondary antibody (IRDye; LI-COR, USA). Immunoreactive bands were detected with either chemiluminescence with horseradish peroxidase substrate Lumigen TMA-6 (Lumigen, Southfield, MI) and FluorChem E system (Cell Biosciences, Santa Clara, CA) or Odyssey scanning system (LI-COR Odyssey Imaging System, USA).

2.3.6 Quantitative real-time PCR

Total RNA was extracted from BRECs or mouse retinas using Qiagen RNeasy (Qiagen Inc., Valencia, CA, USA) or mirVana isolation kit (Life Technologies, Carlsbad, CA) according to the manufacturer's instructions. NanoDrop 2000 (Thermo Scientific, IL, USA) was used to determine total RNA concentration. Total RNA was reverse transcribed into cDNA using superscript III first-strand synthesis system (Invitrogen, Carlsbad, CA). Human and mouse gene-specific primers for ELOVL4 were used. Expression levels were normalized to either bovine GAPDH or mouse cyclophilin. A no reverse transcriptase control was done as a negative control.

Human ELOVL4: GCACTCAACGACACGGTAGA and GGACCCAGCCACACAAAC

Bovine GAPDH: CATTGACCTTCACT CATGGT and ACCCTTCAAGTGAGCCCCAG

Mouse ELOVL4: CCATAGGCCACCACGATT and TCAAAGGCTACCTTCCTCATTAC

Mouse Cyclophilin: ATTCATGTGCCAGGGTGGTGA and CCGTTTGTGGGTCCAGCA

2.3.7 Immunocytochemistry

Cellular localization of the tight junction complexes in BRECs and mouse retina was evaluated by immunocytochemistry as described previously (5). Ad-Empty and Ad-hELOVL4 transduced cells were seeded on 12-mm diameter polystyrene coverslips (Nunc, Naperville, IL) in a 24 well tissue culture plate at density of 8×10^4 cells in 1 ml MCDB-131 complete media/ well for 1 day. For experiments the cells were pre-treated with 1% FBS, 0.01 ml/ml antibiotic/antimycotic and 100 nM hydrocortisone for 36 h and then treated with VEGF (50 ng/ml) for 30 min. After treatment cells were washed twice with DPBS (with Ca^{2+} , Invitrogen), fixed with 1% paraformaldehyde for 10 min at room temperature, washed with TBS, permeabilized with 0.2% TritonX-100/ TBS for 10 min at room temperature and blocked with 10 % goat serum in 0.1% triton X -100/TBS for 1 h at room temperature. Cells were incubated for 2 days at 4 °C with the following primary antibodies in the blocking solution (2% goat serum in 0.1% TritonX-100/TBS): rat monoclonal anti-ZO-1 (Millipore, Cat. No. MABT11), mouse monoclonal anti-ceramide (Sigma, Cat. No. C8104) or rabbit polyclonal anti-claudin-5 (Invitrogen, Cat. No. 34-1600) used in concentration 1:300. After 3 washes with TBS, primary antibodies were detected with Alexa Fluor 647 goat anti-rat IgG (650/668), Alexa Fluor 488 goat anti-mouse F (ab') 2 IgG (496/519) or Alexa Fluor 594 goat anti-rabbit IgG (590/617) (Molecular Probes, Invitrogen). The nuclei were stained with Hoechst (361/497) during secondary antibody incubation. Coverslips were mounted on slides using ProLong® Gold Antifade Mountan (Life Technologies, CARLSBAD, CA). XY images were sequentially scanned using confocal laser scanning microscope Nikon A1 Plus (Nikon Instruments, Inc., Melville, NY) with an Apo 60x/ NA 1.4, oil immersion objective. The near-IR, green, red and blue channels were acquired sequentially using 647-nm, 488.5-nm, 560.9-nm and 402.6- nm excitation, respectively. Near-IR channel

was acquired using 660-nm long pass emission filter while 500-550 band pass, 575-625 band pass and 428-463 band pass emission filters were used for green, red and blue channels, respectively.

Tight junction protein staining at the cell border was quantified by semi-quantitative ranking score system as previously described (5). With scale 1-5: 1 for 0% disruption of cell border staining where borders are straight and clear, 2 for 25% disruption with slight border disruption, 3 for 50% disruption with about 50% or more of cells border show disruption at many points, 4 for 75% disruption where cell shape is disrupted, 5 for 100% disruption where no clear cell shape and complete loss of staining between cell borders. Two observers examined ranking score in a blinded manner. For each condition, four images were examined. For each image four fields were analyzed and ranking scores were calculated. One-way ANOVA was used to determine the statistical difference between different conditions.

For co-localization, confocal images were analyzed using Nikon NIS Elements software to determine Pearson's coefficient of co-localization.

To evaluate TJ protein organization in retinal vasculature, whole retina flat mounts were immunolabeled for occludin using mouse monoclonal anti-occludin Alexa Fluor 488 conjugate (1:75) (Thermo Fisher Scientific, Cat. No. OC-3F10) for 3 days at 4 °C. Following incubation, retinas were washed and flat mounted on slides with Fluoromount mounting medium (Sigma Aldrich). Images were acquired using Nikon C2 (Nikon Instruments, Inc., Melville, NY).

2.3.8 Immunogold electron microscopy

Bovine retinas were fixed with 4% paraformaldehyde/0.5% glutaraldehyde for 24 h at 4 °C, cut into 5x5 mm pieces and analyzed using osmium tetroxide (41) or double immunogold labeling (42) as previously described. Retinal pieces were washed with PBS, dehydrated in a graded series of ethanol then infiltrated on LR-white resin and polymerized at 60 °C for 24 h in gelatin capsule. Ultrathin sections (70nm) were obtained by PowerTome Ultramicrotome (RMC Boeckeler Instruments, Tucson, AZ) and collected on formvar coated gold grids. Grids were incubated in blocking solution (0.01M PBS + 5 %BSA + 5 % normal goat serum) for 10-30 min., then rinsed 3 times. Simultaneous double immunogold labeling was done using the following primary antibodies; rabbit polyclonal anti-occludin (Invitrogen, Cat. No. 71-1500) and mouse monoclonal anti-ceramide (Sigma, Cat. No. C8104) used in dilution 1:1. Primary antibodies were detected with mixture of goat anti-rabbit IgG-15 nm gold conjugate and goat anti-mouse IgG-6 nm gold conjugate diluted (1:20). Finally, grids were stained with uranyl acetate and lead citrate and images were examined with JEOL 100 CX TEM (Japan Electron Optical laboratory, Tokyo, Japan) operated at 100 KV and equipped with Gatan ORIUS CCD camera.

2.3.9 TJ isolation and mass spectrometry

In order to determine molecular species of ceramides associated with the tight junction complexes, tight junctions were isolated as previously described (43). Briefly, ARPE-19 cells (15 x 150 mm culture plates) were lysed with hypo-osmotic buffer, collected, homogenized and centrifuged at 100,000 xg for 60 minutes at 4°C against a saturated sucrose cushion. The collected membrane was subsequently cryo- lysed using liquid nitrogen, then incubated

with either rabbit polyclonal anti-PKC zeta (Sigma, Cat. No. P 0713) or rat monoclonal anti-ZO-1 ((Millipore, Cat. No. MABT11) using protein A or G dynabeads, respectively according to manufacturer's instructions (Invitrogen, USA). Tight junction complexes bound to the beads were subjected to lipid extraction as previously described (44). Lipids obtained from tight junctions were analyzed by high resolution/accurate mass spectrometry and tandem mass spectrometry in positive and negative ionization modes, using an LTQ-Orbitrap Velos mass spectrometer (Thermo Scientific) operating at a resolving power of 100,000 defined at m/z 400. Sphingolipids were identified as previously described in both positive ion mode as $[M+H]^+$ and $[M-H_2O+H]^+$ molecular ions (45) and in negative ion mode as $[M+HCOO-H]^-$ ions (46). Ceramides of interest were further examined by higher-energy collisional dissociation MS/MS at 100,000 resolving power to confirm sphingolipid backbone and head group moieties. Mouse epidermal lipid extracts were similarly prepared and analyzed for optimization of analytical conditions used for detecting putative very long chain fatty acid-containing sphingolipids.

2.3.10 Animal model

All procedures involving animal models were performed according to the Association for Research in Vision and Ophthalmology (ARVO) Statement for the Use of Animals in Ophthalmic and Vision Research, and were approved and monitored by Institutional Animal Care and Use Committee at MSU. Streptozotocin (STZ)-induced male C57BL/6J mice were used as a model of type I of diabetes to access retinal vascular permeability and tight junction protein organization. 13-week-old Male C57BL/6J mice (Jackson Laboratory) were made diabetic by intraperitoneal injections of STZ (Sigma Aldrich) (65 mg/ kg) for five consecutive days. Age matched nondiabetic control mice received an equivalent amount of vehicle

(citrate buffer, pH 4.5). Diabetes was confirmed by blood glucose higher than 13.8 mmol/l (300 mg/dl) and decrease in the body weight gain. After two weeks of confirmed diabetes, animals received intravitreal injection of either AAV2-hELOVL4 quad mutant (right eye) or AAV2-Empty vector (left eye) as a control (2×10^9 viral genomes/eye in 1 μ l). Animals were sacrificed 6-8 weeks following viral injection (8-10 week of STZ induction) for retinal vascular permeability and retinal analysis.

2.3.11 Retinal vascular permeability

Two months after induction of diabetes, retinal vascular permeability was assessed as initial retinal vascular damage in DR. Briefly; Mice were injected with FITC-albumin (0.5 mg in 50 μ l PBS) (Sigma Aldrich). After 2 h, blood was collected, mice were perfused with 1% formaldehyde and fixed eyes were enucleated. Obtained retinas were flat mounted with 4 radial cuts and placed on glass slides with Fluoromount mounting medium (Sigma Aldrich). Images were obtained by using confocal laser scanning microscope Nikon C2 (Nikon Instruments, Inc., Melville, NY) with 20x / NA 0.75 objective. Green channel was acquired using 488 nm excitation wavelength and 500-550 band pass emission filters.

For each retina, at least 5 different fields were randomly acquired, measured using Angiogenesis tube formation application-MetaMorph imaging software (Molecular Devices, Downingtown, PA) by subtracting residual fluorescence inside the vessels from total fluorescence to determine leakage fluorescence intensity. The fluorescence intensity of the leakage was averaged between at least 5 fields for each retina and normalized to blood plasma fluorescence level.

2.3.12 Immunohistochemistry

Retinas were processed as previously described (47). Briefly, samples were fixed in zinc fixative, paraffin embedded and 4-5 micron sections were obtained with Reichert Jung 2030 rotary microtome. Sections were dried at a 56°C slide incubator for 2–24 h, deparaffinized and rinsed in several changes of distilled water followed by Tris buffered saline pH 7.4. Sections were blocked with 10% normal goat serum (Life Technologies, Carlsbad, CA) in 0.3%triton x-100 for 1 h at room temperature and immunolabeled with Isolectin GS-IB4 with Alexa Fluor 594 conjugate (1:50) (Molecular Probes, Invitrogen) and rabbit polyclonal anti-ELOVL4 (1:50) (Sigma) in blocking solution, overnight at 4°C. ELOVL4 primary antibody was detected by Alexa Fluor 488 goat anti-rabbit IgG (496/519) (Molecular Probes, Invitrogen). Images were captured using Nikon TE2000 fluorescence microscope equipped with Photometrics CoolSNAP HQ2 camera. For each slide, 3 different fields were collected. Co-localization of ELOVL4 (green) with retinal vasculature (red) was determined to evaluate transduction efficiency of AAV2 vector. Percentage of co-localization (yellow) was quantified using MetaMorph imaging software (Molecular Devices, Downingtown, PA).

2.3.13 Statistical analysis Data are expressed as mean \pm S.E.M. Results were analyzed for statistical significance by the Student's t-test or one-way analysis of variance (ANOVA) followed by post hoc Tukey test. (GraphPad Prism 7, GraphPad Software, San Diego, CA) was used for all statistical analysis. Significance was established at $P < 0.05$.

2.4 Results

2.4.1 Expression level of ELOVL4 controls retinal endothelial permeability

The effect of ELOVL4 on retinal vascular endothelial cell permeability was evaluated in monolayer of BRECs, a model of inner blood retinal barrier, after overexpression through the use of adenovirus (AdhELOVL4) or short interfering RNA (siRNA) to inhibit expression of ELOVL4. To ensure efficient overexpression and inhibition of hELOVL4, expression of ELOVL4 in BRECs was evaluated using qPCR and western blot. Human ELOVL4 was significantly expressed in adhELOVL4-transduced BRECs compared with AdEmpty-transduced cells (Fig. 9A and B), with human specific qPCR primers revealing expression only after transduction of the human exogenous gene (9A) while Western blot reveals a 50% increase in steady state ELOVL4 over endogenous protein (9B). To evaluate the effect of hELOVL4 on endothelial permeability under basal conditions, paracellular permeability to 70 kDa RITC-dextran was measured in AdhELOVL4 and AdEmpty transduced cells. Data from these experiments indicate that under basal conditions, overexpression of hELOVL4 results in a significant decrease in permeability to 70kDa RITC dextran (53.7 ± 5.7 % of control, $P=0.0016$; Fig. 9C). ELOVL4 was knocked down using siRNA. ELOVL4 mRNA and protein levels were significantly reduced in BRECs transfected with ELOVL4-siRNA in comparison to cells transfected with control siRNA (Fig 9D and E). Moreover, knockdown of ELOVL4 was associated with increased paracellular permeability (528.2 ± 242.2 % of control, $P= 0.0317$; Fig 9F).

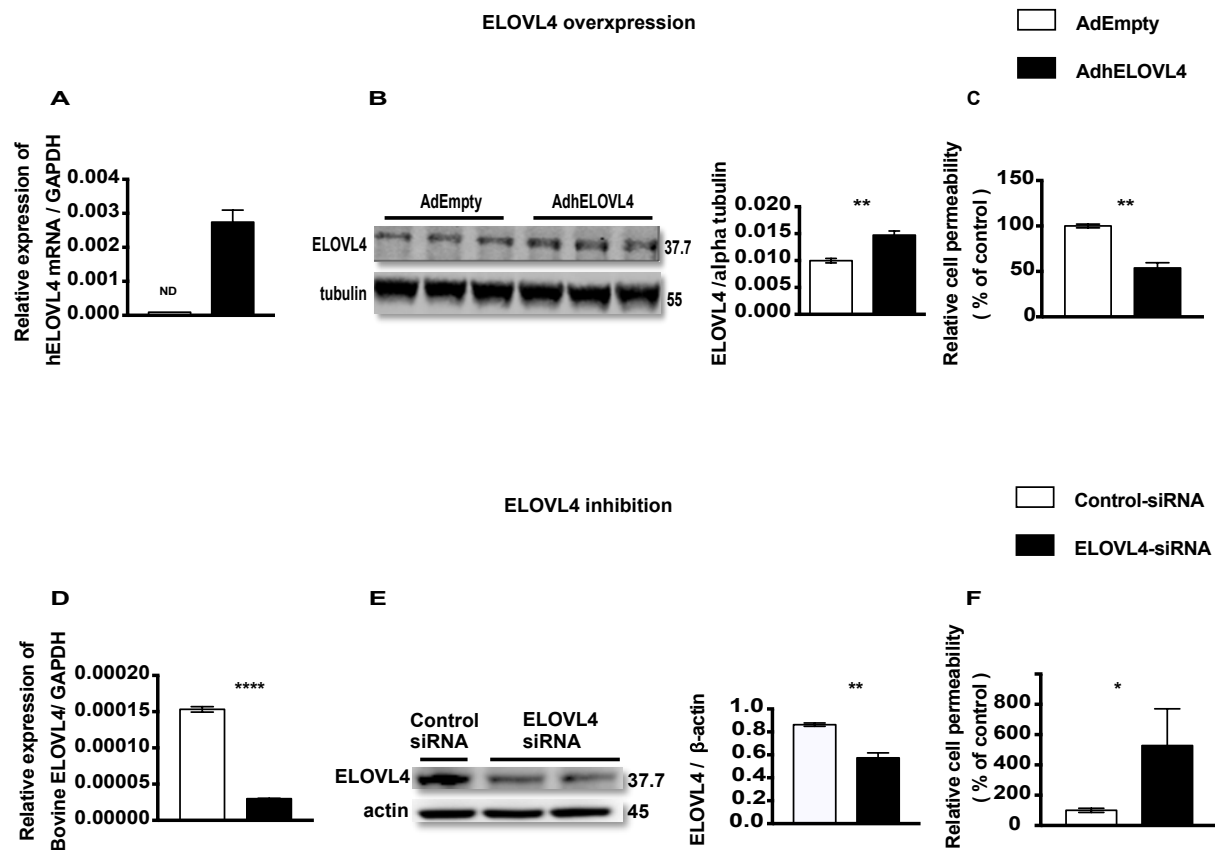


Figure 9. Expression level of ELOVL4 controls retinal endothelial permeability.

(A-B) BRECs were transduced with either AdEmpty (white bars) or AdhELOVL4 (black bars) and collected 60 h after adenovirus transduction for (A) RNA analysis by RT qPCR or (B) protein by Western blot to confirm adenovirus-mediated overexpression of hELOVL4. Human ELOVL4 mRNA expression was normalized to GAPDH (A) and protein expression was normalized to α -tubulin loading control (B).

Figure 9 (cont'd)

(C) Paracellular permeability to 70kDa RITC-dextran was determined in BRECs transduced with either AdEmpty (white bar) or AdhELOVL4 (black bar) in untreated cells. (D-F) BRECs were transfected with either control siRNA (white bars) or ELOVL4-siRNA (black bars) and collected for analysis. Expression profile of ELOVL4 was determined by either (D) RT qPCR, 48 h after transfection or (E) Western blot, 72 h after transfection to confirm silencing of ELOVL4. Bovine ELOVL4 mRNA expression was normalized to GAPDH (D) and protein expression was normalized to β -actin loading control (E). (F) Paracellular permeability to 70kDa RITC-dextran was determined in BRECs transfected with either control siRNA (white bars) or ELOVL4-siRNA (black bars). Results are shown as mean \pm SEM, n =3-6. *p< 0.05, **p<0.01, ***p<0.001, ****p<0.0001.

2.4.2 ELOVL4 overexpression prevents VEGF- and IL-1 β - induced increase in permeability

The effectiveness of anti-VEGF therapy for treating vision loss associated with diabetic macular edema (12, 48–52) and growing evidence for a contribution of chronic inflammation with elevated levels of pro-inflammatory factors, including interleukin-1 β (IL-1 β) (53–57) provide compelling evidence these cytokines lead to increased BRB permeability during early stages of DR. Our next goal was to evaluate the effect of overexpression of ELOVL4 on VEGF- and IL-1 β -induced endothelial cell permeability. AdhELOVL4 and AdEmpty transduced BRECs were grown to confluence as mentioned above and treated with VEGF (50 ng/ml, 30 min) or IL-1 β (10 ng/ml, 15 min). Paracellular permeability to 70 kDa FITC-dextran was measured. VEGF significantly increased cell permeability ($169.4 \pm 13.4\%$ of control; Fig. 10A). Similarly, IL-1 β increased cell permeability ($152.8 \pm 4.9\%$ of control, Fig. 10B). Human ELOVL4 overexpression prevented VEGF- and IL-1 β -induced increase in permeability ($88.5 \pm 8.6\%$ of control; Fig. 10A) and ($97.5 \pm 9.3\%$ of control; Fig. 10B), respectively.

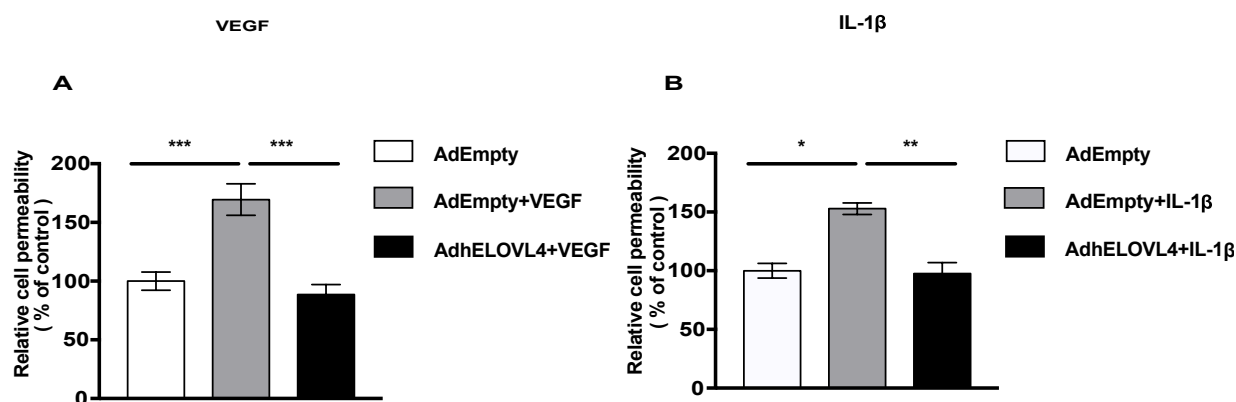


Figure 10. ELOVL4 overexpression block cytokine-induced retinal endothelial cell permeability.

(A-B) Paracellular permeability to 70kDa RITC-dextran was determined in BRECs transduced with either AdEmpty (white bar) or AdhELOVL4 (black bar), and either treated with VEGF (50 ng/ml) for 30 min (gray and black bars) (A); or treated with IL-1β (10 ng/ml) for 15 min (gray and black bars) (B). Results are shown as mean ± SEM, n =3-6. *p< 0.05, **p<0.01, ***p<0.001.

2.4.3 ELOVL4 overexpression increases the barrier properties of tight junction complex

To explore the mechanism by which overexpression of ELOVL4 reduces retinal vascular permeability, we examined the effect of ELOVL4 on TJ protein content and localization. Under basal condition, overexpression of hELOVL4 significantly increased occludin content in AdhELOVL4 transduced BRECs compared to AdEmpty transduced cells and prevented the VEGF – induced decrease in occludin (Fig. 11A). For ZO-1 and Claudin-5 no significant effects of hELOVL4 on total protein expression were observed (Fig. 11 B and C). Although hELOVL4 had no effect on ZO-1 and Claudin-5 total protein levels, immunostaining revealed that overexpression of hELOVL4 both increased protein staining at cell border, and prevented VEGF-induced disruption of continuous immunostaining of ZO-1 and claudin-5 at cell border (Fig. 11 D and E). These data suggest that overexpression of ELOVL4 may stabilize the TJ complex and suppress the VEGF-induced disruption of the complex.

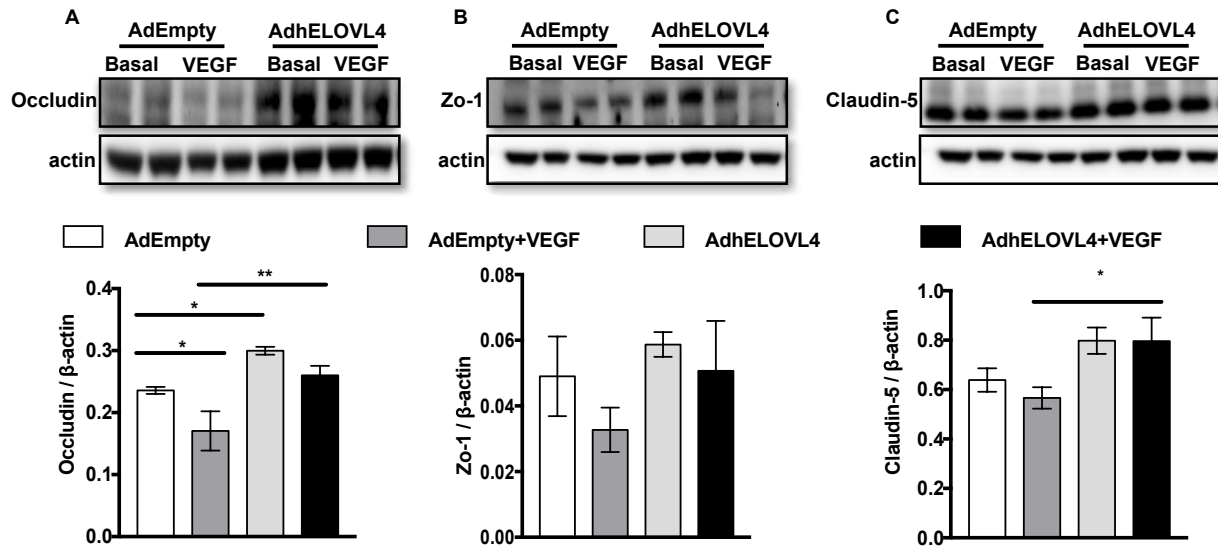
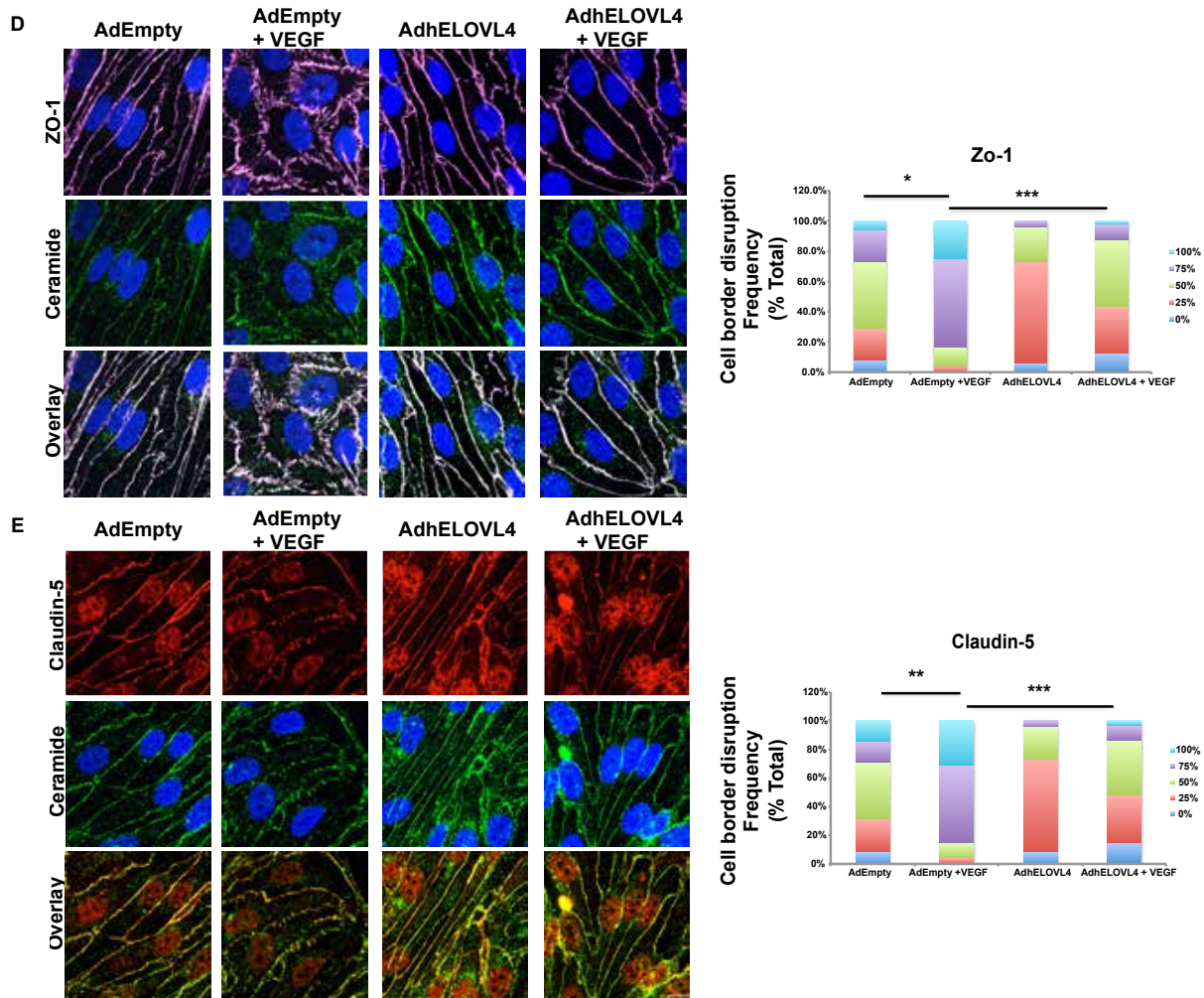


Figure 11. ELOVL4 overexpression increases the barrier properties of the tight junction complex.

(A-C) Confluent AdEmpty (white bars) and AdhELOVL4 (light gray bars) transduced BRECs were treated with VEGF (dark gray and black bars) (50 ng/ml) for 30 min. Total cell lysates were immunoblotted for (A) Occludin, (B) ZO-1, and (C) Claudin-5. β -actin served as loading control. Representative Western blots from three independent experiments are shown on top, with densitometry quantification below. Results are shown as mean \pm SEM (n=3). *p < 0.05, **p < 0.01, ***p < 0.001.

Figure 11 (cont'd)



(D-E) Confluent monolayers of BRECs treated as in A-C were immunolabeled for **(D)** ZO-1 (Far red) and Ceramide (green), or **(E)** Claudin-5 (red) and ceramide (green) and confocal images were taken. The results are from 2 independent experiments, for each condition, four images were examined. For each image four fields were analyzed. Scale bar, 10 μ m. Quantification of each protein staining at the cell border, is shown on the far right, the results represent frequency of each score as described in methodology. * $p < 0.05$, ** $p < 0.01$, *** $p < 0.001$.

2.4.4 Ceramide co-localizes with tight junction complex

Changes in tight junction protein content and localization after ELOVL4 overexpression prompted us to determine if hELOVL4-produced lipids co-localize with TJ complexes. As mentioned above ELOVL4 is responsible for production of VLC poly, mono unsaturated and saturated fatty acids. In the skin VLC fatty acids incorporated into VLC ceramides play an important role in the maintenance of barrier function (22,31). We tested the hypothesis that VLC ceramides incorporated into TJ complexes in the retinal endothelial cells. Immunocytochemistry for TJ proteins and ceramide was performed in BRECs. Interestingly, ceramide (green) was found to co-localize with the tight junction complexes and follow the same distribution as ZO-1 and claudin-5 at the cell border (Fig. 11 D and E). Quantification of co-localization of ceramide with either ZO-1 or claudin-5 in confocal images reveals an average Pearson coefficient of co-localization of 0.77 and 0.65, respectively. In addition to cell border distribution, typical punctate green cytoplasmic staining of ceramides was observed. To further verify the specificity of the immunofluorescence co-localization, we performed immunogold labeling and transmission electron microscopy using retinal vasculature in bovine retina. The tight junctions were first visualized by Osmium tetroxide (OsO₄) Staining (Fig. 12A). Neighboring sections were then used for immunogold labeling of occludin and ceramide. As shown in Fig. 12B, ceramide (smaller, 6 nm gold particles) is localized along the tight junction in close proximity with occludin protein (larger, 15 nm gold particles), as well as in the intercellular space between two neighboring endothelial cells (Fig. 12B, right, upper panel).

A Osmium tetroxide staining

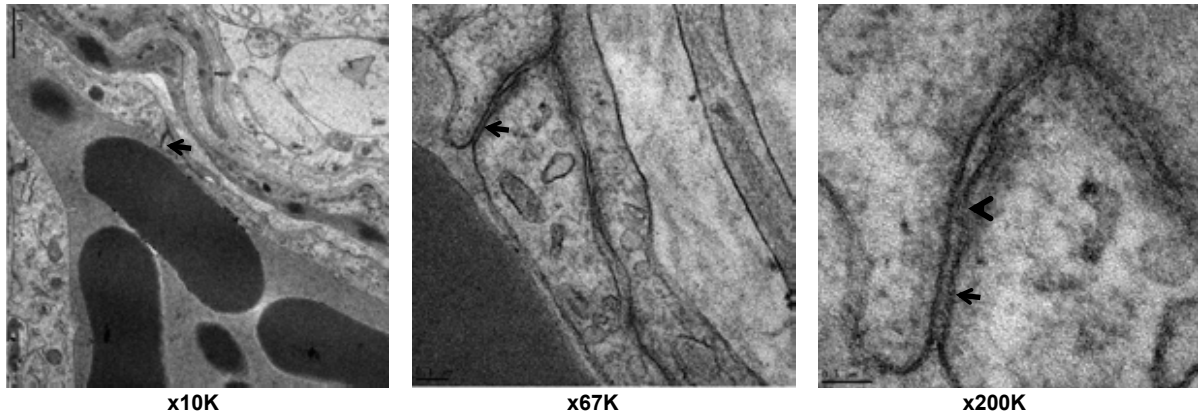
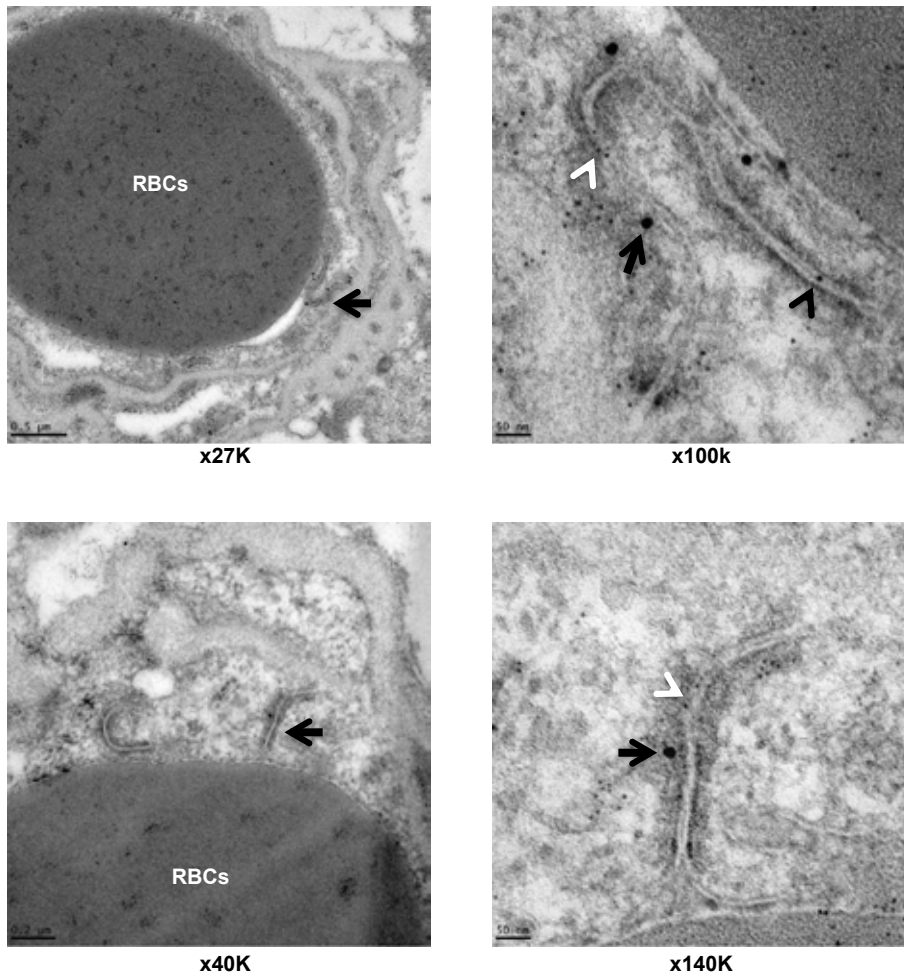


Figure 12. Ceramide co-localizes with tight junction complex.

(A) Tight junctions stained by Osmium tetroxide (OsO₄) staining (black arrows). (left) Lower magnification x10K, red blood cells (RBCs) in the intravascular compartment and the tight junction between two neighboring retinal endothelial cells (black arrow). Bar 1 μ m. (middle) Tight junction is enlarged for better visualization x67K (black arrow). Bar 0.1 μ m. (right) Kissing point, hallmark of tight junction (black arrowhead). Bar 0.5 μ m.

Figure 12 (cont'd)

B Immunogold labeling



(B) Immunogold localization of ceramide and TJ protein occludin in ultrathin sections of bovine retina. (B, left panel) Lower magnification x27K (upper) and x40K (lower), of the tight junction (black arrow), with RBC in the intravascular compartment. Bar 0.5 μm and 0.2 μm, respectively. (B, right panel) higher magnification x100k (upper), x140k (lower), Ceramide (smaller, 6 nm gold particles) (white arrowhead) localized along the tight junction in juxtaposition to the tight junction protein, occludin (larger, 15 nm gold particles) (black arrow). Bar 50 nm.

Figure 12 (cont'd)

Although most of ceramide labeling localized along the cytoplasmic side of the plasma membrane, it can also be visualized in the intercellular space between two neighboring endothelial cells (black arrowhead).

2.4.5 Identification of VLC omega-linked acyl-ceramide species in the tight junction complex

In order to determine which ceramide species interact with the tight junction complex, tight junction was isolated as previously described (43). ARPE-19 cells were lysed with hypo-osmotic buffer, collected, homogenized and centrifuged at 100,000xg for 60 minutes at 4°C against a saturated sucrose cushion. The collected membrane was subsequently cryo-lysed using liquid nitrogen, and tight junctions were immuno-isolated using either anti-PKC zeta or anti-ZO-1. Lipid extracts of three independent tight junction preparations were subjected to high resolution/accurate mass direct infusion-based lipidomic analysis. In order to guide detection and analysis of sphingolipids containing very long chain fatty acids, we concurrently analyzed lipid extracts of mouse epidermis, which is known to contain high levels of ceramides and omega-linked acyl ceramides containing very long chain fatty acids.

Interestingly, lipidomic analysis revealed that several ceramide molecular species co-localized with isolated tight junction complexes (Fig. 13A). While the majority of observed ceramide (Cer) species were detected between m/z 500- m/z 650 in both positive and negative ionization modes, corresponding to ceramides containing N-linked fatty acids ranging from C16-C24 in length, a small number of Cer species were detected at higher m/z values which coincided with C26:4 and C26:3 very long chain fatty acid-containing ceramides, which were observed above m/z 650 (Fig. 13A, Inset). Moreover, several ions were observed in the mass range of 900-1100 m/z , which were initially identified as putative omega-linked acyl-ceramide species based on agreement of the observed accurate mass measurements and isotope distributions with the theoretical values for each putative Cer species. The assignment of these ions was further supported by Orbitrap high resolution/accurate mass higher-energy collisional dissociation

MS/MS to evaluate the presence of the sphingosine backbone, with identical analysis also performed on mouse epidermal lipid extracts. . The top panel of Fig. 13B shows the epidermis tandem mass spectrum from HCD-MS/MS of m/z 943.8562, initially identified as a putative acyl-ceramide h42:1 (total acyl carbons: total double bonds). The product ion at m/z 264.2682 in this spectrum is indicative of a d18:1 sphingosine backbone. The bottom panel of Fig. 13B shows the HCD-MS/MS analysis of ARPE19 tight junctions purified by anti-PKC zeta IP with a lipid of m/z 943.8562. A product ion at m/z 264.2682 was also observed in the tight junction MS/MS spectrum, although at lower abundance than that observed for the epidermis lipid extract. The tight junction isolation was repeated in ARPE-19 homogenates using anti ZO-1 antibody for immunoprecipitation of tight junctions, to assess the potential antibody-specific dependence of the obtained tight junction lipid profiles. Mass spectrometry analysis of lipid extracts from anti ZO-1 precipitated tight junctions was performed as described above. The detected ceramide molecular species were comparable to those from tight junctions obtained from anti-PKZ immunoprecipitation, including the presence of the acyl-ceramide (d18:1/h24:0) at m/z 943.8562. These data combined with accurate mass-based formula prediction and available published data suggest an assignment of acyl-cer d18:1/h24:0, with an omega O-linked linoleic acid (33–35). Additional criteria used for assignment of putative acyl-ceramide species included absence of these ions in sample blanks and Protein-A bead negative controls, and a lack of other detected known sphingolipids which could theoretically be co-isolated during MS/MS analysis in the mass range in which these ions were observed in the isolated tight junction complexes. Relative quantitation of all epidermal ceramide species obtained by the same analytical methods, including Cer and acyl-cer species containing very long chain fatty acids, is shown for comparison in Fig. 13C.

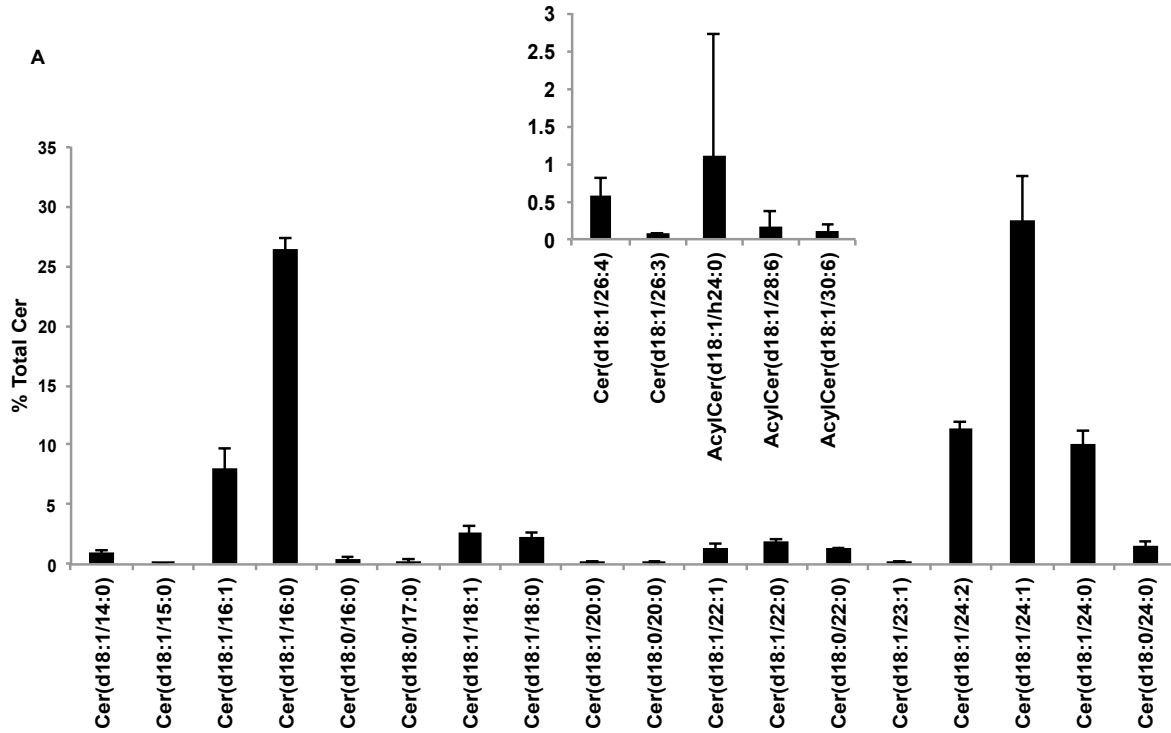
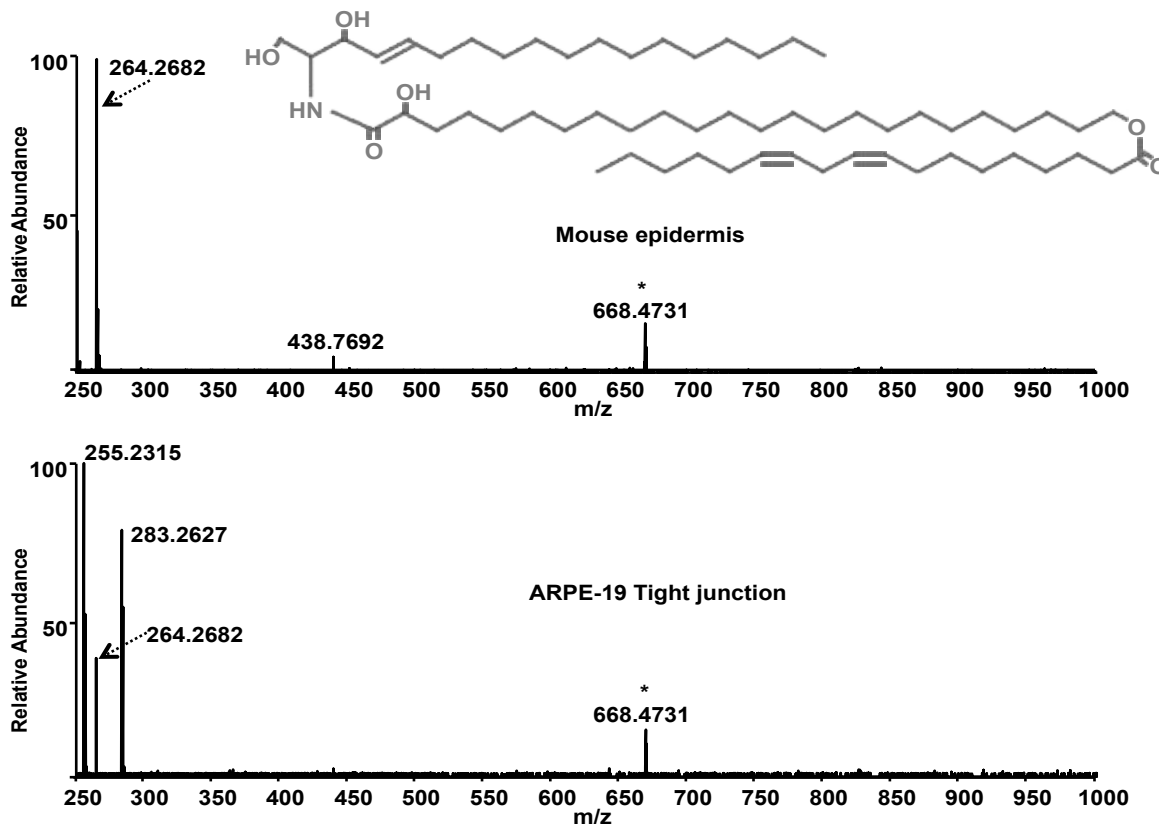


Figure 13. Tight junction ceramide content.

Lipid extracts of isolated tight junction complexes were subjected to high resolution/accurate mass spectrometry and tandem mass spectrometry to determine sphingolipid content. (A) Data are expressed as the average \pm standard deviation of $n=3$ independent tight junction preparations. Individual ceramide molecular species are presented as the percent of total ceramide abundance. Ceramide species were quantitated in negative ion MS mode as $[M+HCOO-H]^-$ ions. The sphingosine backbone and amide-linked fatty acid for the most abundant isomer at each m/z are given. Inset: Ceramide species containing $>C_{24}$ fatty acids.

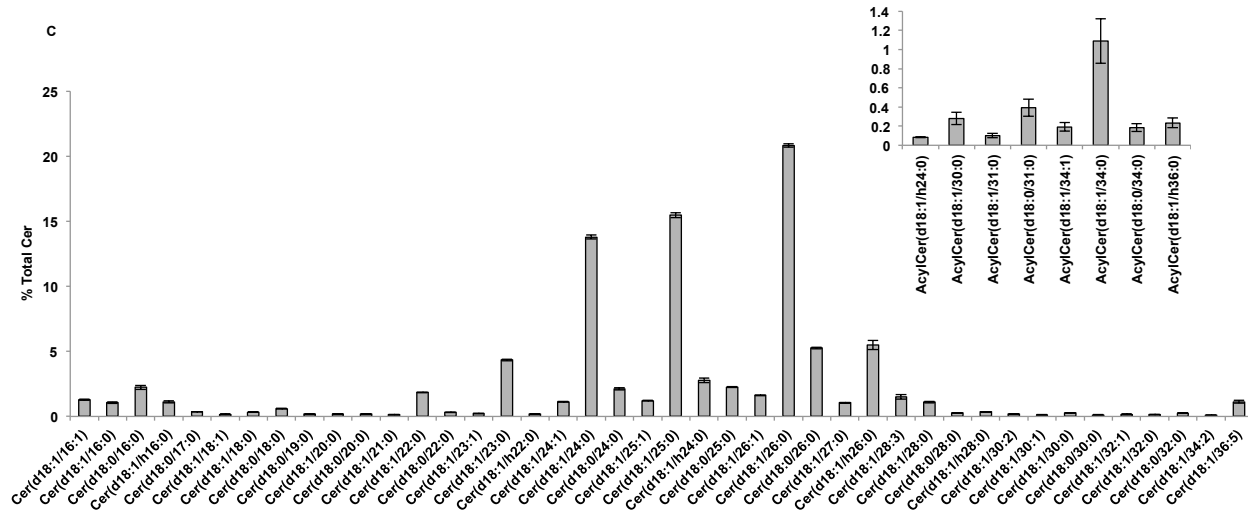
Figure 13 (cont'd)

B



(B) High resolution tandem mass spectrometry of epidermal and tight junction putative acyl ceramide. Positive ion mode Orbitrap Higher Energy Collisional Dissociation (HCD) MS/MS at 100,000 resolving power of m/z 943.8562, corresponding to putative protonated acyl-ceramide (d18:1/h24:0) in mouse epidermis (top panel) and ARPE-19 tight junctions (bottom panel) lipid extracts. * Matrix ion.

Figure 13 (cont'd)



(C) Mouse epidermis ceramide content. Lipid extracts of mouse epidermis were subjected to high resolution/accurate mass spectrometry and tandem mass spectrometry to determine sphingolipid content. Data are expressed as the average \pm standard deviation of $n=3$ replicate analyses. Individual ceramide molecular species are presented as the percent of total ceramide abundance. Ceramide species were quantitated in negative ion MS mode as $[M+HCOO-H]^-$ ions. The sphingosine backbone and amide-linked fatty acid for the most abundant isomer at each m/z are given. Inset: Epidermal acyl-ceramide species.

2.4.6 Verification of AAV2 mediated expression of hELOVL4 in mouse retina

In order to determine the effect of ELOVL4 on diabetes-induced blood retinal barrier dysfunction in vivo, 16 week old diabetic and non-diabetic mice received single intravitreal injection of 2×10^9 viral genomes of either AAV2-hELOVL4 mut quad (Rt eye) or AAV2-Empty vector (left eye) as a control two weeks after STZ induction. Animals were sacrificed 6-8 weeks following viral injection (8-10 week of STZ induction). Body weight gain and blood glucose concentration of diabetic mice and their age matched non-diabetic controls used in this study are described in Table 1.

In agreement with our previous study (19), ELOVL4 mRNA expression was reduced in diabetic retinas as compared to control (Fig. 14A). Transduction with AAV2- hELOVL4 led to hELOVL4 overexpression in both diabetic and non-diabetic retina as determined using human transgene-specific primers. As expected, hELOVL4 transcript was undetectable in AAV2-Empty injected contralateral retinas (Fig. 14B).

To determine the effect of diabetes with and without AAV2-hELOVL4 overexpression on vascular levels of ELOVL4, retinal cross sections were immunolabeled for ELOVL4 (green). Isolectin-B4 (red) was used to counterstain retinal vasculature. AAV2-Empty injected retinas were used as control. Diabetes induced downregulation of endothelial expression of ELOVL4, which was reversed by AAV2-hELOVL4 treatment (Fig. 14C).

Table 1. Average body weights and non-fasting blood glucose level of control and diabetic mice.

Group	Weight (g)	P value	Blood Glucose (mg/dL)	P value
Control (n=17)	29.6 ± 0.95	<0.0001	181.6 ± 4.62	<0.0001
Diabetic (n=25)	24.6 ± 0.33		479.4 ± 21.26	

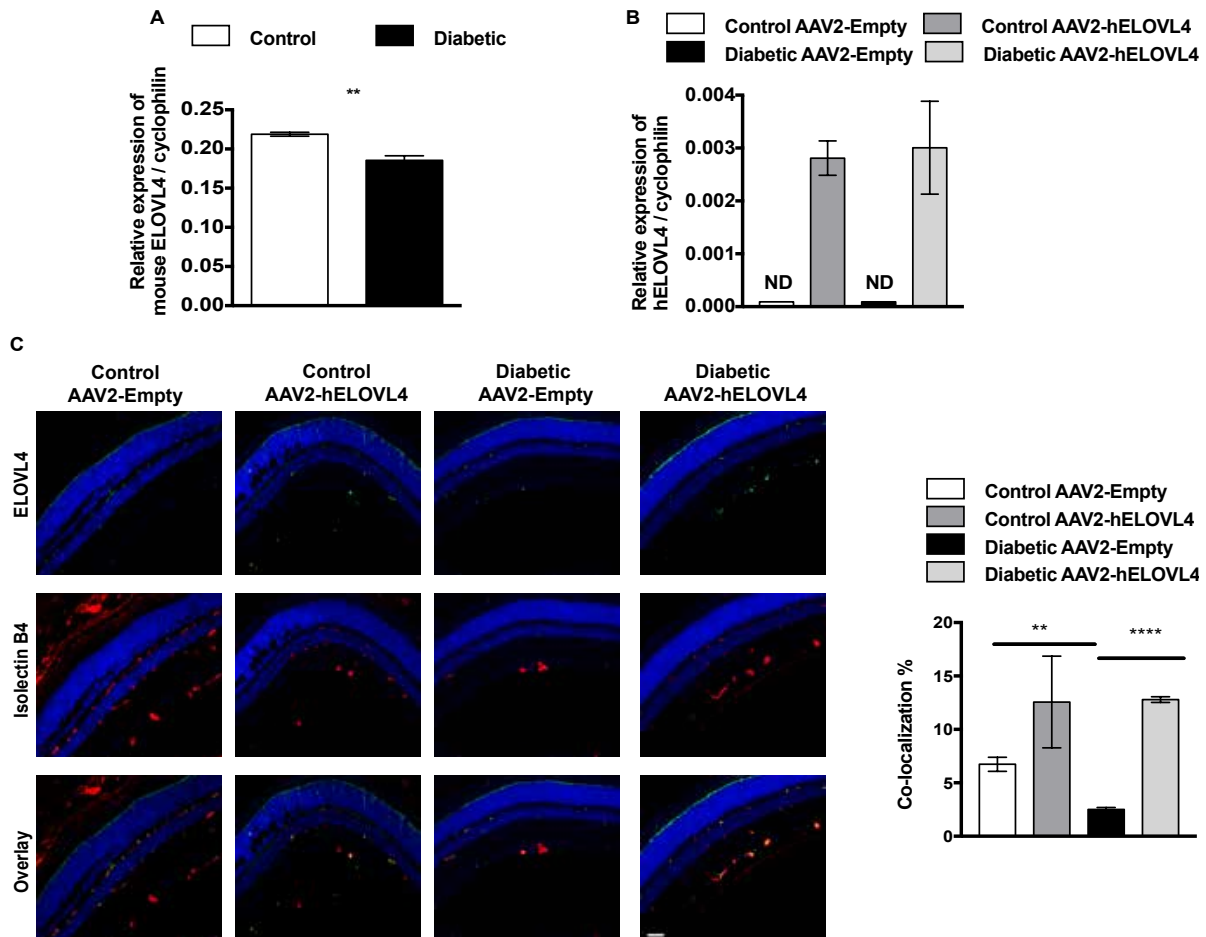


Figure 14. Verification of AAV2 mediated expression of hELOVL4 in mouse retina.

STZ-induced diabetic mice were intravitreally injected with either AAV2-hELOVL4 mut quad (right eye) or control AAV2-Empty vector (left eye) 2 weeks after diabetes induction. Retinal tissue was analyzed 6-8 weeks after viral injection. **(A)** qRT-PCR quantification of endogenous mouse ELOVL4 mRNA levels in control (white bar) and diabetic (black bar) retinas (n=3-4 per group). **(B)** qRT-PCR quantification of exogenous human ELOVL4 mRNA levels in control (white and dark gray bars) and diabetic (black and light gray bars) retinas (n= 4-6 per group).

Figure 14 (cont'd)

(C) Immunohistochemical detection of ELOVL4 (green, upper panel) co-localization with retinal vasculature (red, middle panel) with yellow color (lower panel) indicating vascular expression in retinal cross sections. Quantification of co-localization (yellow) is shown on the far right (n=3 per group). Scale bar, 20 μ m. *p< 0.05, **p<0.01, ***p<0.001, ****p<0.0001.

2.4.7 AAV2-hELOVL4 overexpression prevents diabetes-induced increase in retinal vascular permeability in vivo

We next determined whether ELOVL4 overexpression in retinal vasculature could prevent retinal vascular permeability at early stages of diabetes. Retinal vascular permeability was assessed 6 weeks after vector administration (8 weeks of diabetes) by measuring leakage of FITC-albumin. As expected, diabetes induced significant increase in vascular permeability (6.7 fold of control, $P=0.0051$; Fig. 15A) in retinas receiving AAV2-Empty vector (left eye) relative to non-diabetic controls (left eye). Notably, treatment with AAV2-hELOVL4 (right eye) prevented the diabetes-induced increase in vascular permeability. FITC-albumin leakage was significantly lower in diabetic mouse retinas receiving AAV2-hELOVL4 (right eye) than AAV2-Empty diabetic mouse retina (left eye) (1.6 fold of control, $P=0.1202$; Fig. 15A). These findings are consistent with the results obtained in BRECs.

To confirm the beneficial effect of ELOVL4 overexpression on tight junction distribution at cell border, whole retina flat mounts were immunolabeled for occludin in AAV2-Empty and AAV2-hELOVL4 transduced retinas. In AAV2-Empty diabetic retinas (left eye), occludin immunoreactivity was evidently disrupted and intermittently lost in retinal blood vessels. These changes were prevented in AAV2-hELOVL4 diabetic retinas (right eye), where occludin distribution was similar to that in non-diabetic control mice (Fig. 15B)

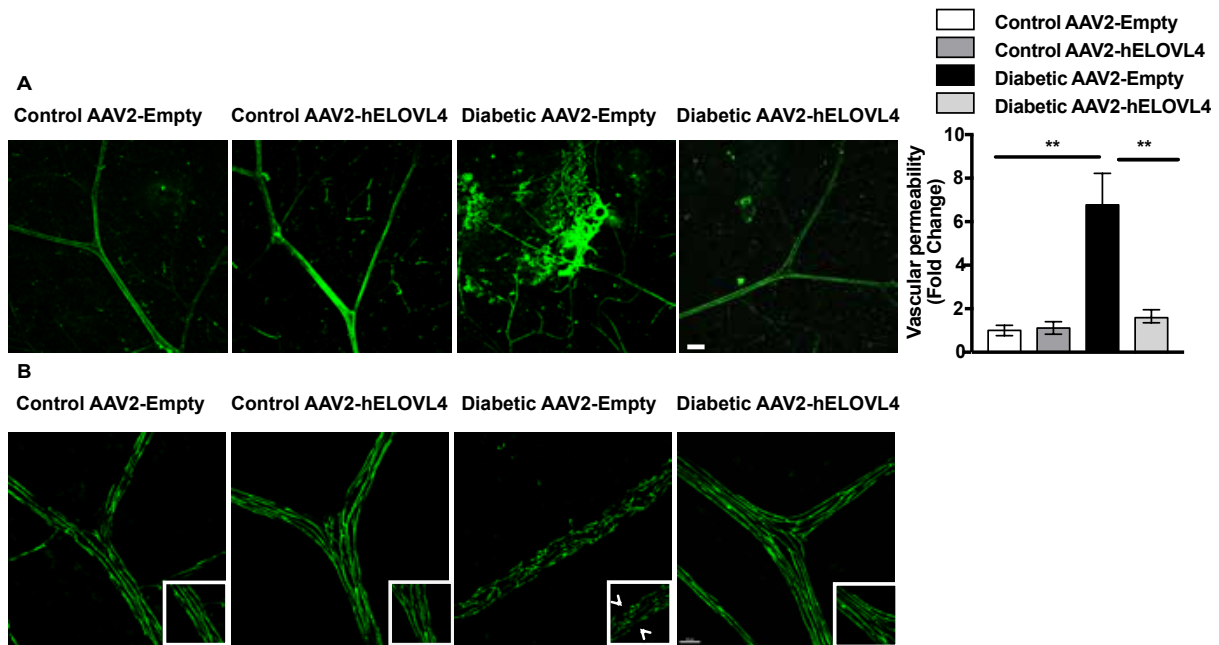


Figure 15. ELOVL4 overexpression prevents diabetes-induced vascular leakage in mice.

(A) Representative fluorescent images of retinal vascular permeability. Retina permeability was evaluated by measuring leakage fluorescence intensity as shown on the far right (n= 8-12 per group). Scale bar, 50 μ m. (B) Immunostaining of flat mounted whole retina for occludin. Arrowheads show disruption of continuous staining in diabetic retina. Scale bar, 20 μ m. *p< 0.05, **p<0.01, ***p<0.001.

2.5 Discussion

Hyperglycemia and dyslipidemia are the major metabolic abnormalities in diabetes, however historically diabetes was described as a problem of glucose metabolism and diabetic complications, including diabetic retinopathy, were generally considered as a result of hyperglycemia. The results of clinical trials, including DCCT, ACCORD and FIELD, however, do not support this one-sided view as they clearly demonstrate a large contribution of dyslipidemia to the pathogenesis of diabetic retinopathy (18,58–61). The mechanism(s) of dyslipidemia-induced retinal damage are not yet well elucidated, however it became clear that changes in retinal-specific lipid metabolism in diabetes play a major role in DR pathogenesis.

Elongases and desaturases are key enzymes in fatty acid metabolism; they regulate the length and degree of saturation of fatty acids and thereby their function and metabolic fate. As we and others have previously demonstrated, expression level of elongases and desaturases in the liver and retina is affected by diabetes with dramatic downregulation of elongases, including the most abundant retinal elongase ELOVL4 in the retina (19,62–64). ELOVL4 has substrate specificity profile for fatty acids of C24 or longer and it can elongate both poly, mono-unsaturated and saturated very long chain fatty acids (29). The role of ELOVL4 in the retina was mainly described for VLCPUFA (38,65,66). VLCPUFAs are mainly present in the rod outer-segment membrane, where they are suggested to contribute a role in photoreceptor function by stabilizing the rims of photoreceptor disks (38). Decrease in ELOVL4 in diabetic retina was associated with a decrease in VLCPUFA (i.e., 32:6n3) synthesis (19).

Although the highest retinal expression of ELOVL4 is found in photoreceptor inner segment (37), it is also expressed in other retinal layers (67,68). Herein, we demonstrated expression of ELOVL4 in retinal vasculature. The product of ELOVL4-mediated elongation will depend on the precursor fatty acids. As the photoreceptors are rich in n3 PUFA, the main products of ELOVL4 in photoreceptor cells are C32-36 PUFAs. Endothelial and epithelial cells have much lower n3 PUFA and higher saturated fatty acids content leading to higher level of VLC saturated fatty acid production that can be incorporated into ceramides. This is further supported by the studies demonstrating that ELOVL4 works in concert with ceramide synthases leading to VLC ceramide production (69). The role of VLC ceramides is best known in skin permeability barrier where they represent a major component of stratum corneum (33–35). Whether decrease in ELOVL4 and thus VLC ceramides production in the retina plays a role in BRB breakdown in diabetes was not known and represented a major focus of this study.

The studies here reveal that overexpression of ELOVL4 by recombinant adenoviral system normalized VEGF and IL-1 β induced retinal vascular permeability in BRECs and increased steady state content of tight junction protein occludin. Further, cell border organization was normalized for both ZO-1 and claudin 5. Importantly, intravitreal delivery of hELOVL4 in diabetic retina using AAV2 viral vector increased hELOVL4 expression in retinal endothelium and prevented diabetes-induced increase in vascular permeability in diabetic mice. These data strongly support the role of ELOVL4 in protective pro-barrier function.

Although this is the first study to demonstrate the role of ELOVL4 in retinal BRB, the essential role of ELOVL4 in skin barrier function is well known. Homozygous ELOVL4 mutant mice die within few hours after birth due defective skin barrier and severe dehydration (33–35), a

phenotype that can be rescued by skin specific expression of ELOVL4 to normalize skin permeability (70). This defective water insulation function of the skin was attributed to ELOVL4 loss of function and subsequent decrease in production of VLCFA ($C \geq 26$) and thereby VLC ceramides and acylceramides, critical lipid components of the skin barrier function, probably due its packing property within stratum corneum that resists water loss. The VLC ceramides and especially omega-linked acyl-ceramide species have never before been shown outside of stratum corneum.

The data presented in this study suggest that retinal pro-barrier effects of ELOVL4 are mediated by VLC ceramide production and incorporation into tight junction structures. Ceramide was found to co-localize with tight junction complexes and follow the same distribution as ZO-1 and claudin 5. Moreover, mass spectrometry analysis revealed very long chain ceramides in tight junction isolates. The presence of these VLC ceramides in BRB tight junctions suggests that similar to skin, they might serve pro-barrier function in the retinal microvasculature.

The role of plasma membrane lipid composition in the maintenance and organization of tight junction complexes has being postulated for a long time. In endothelial cells, gamma linolenic acid 18:3n6 and EPA 20:5n3 increased occludin content with subsequent decrease in paracellular permeability (71). Park et al. have demonstrated that gangliosides exert a protective effect on rat intestinal permeability, preventing lipopolysaccharide induced occludin degradation (72). TNF- α induced alteration in lipid composition of TJ microdomains causing occludin protein redistribution and increased paracellular permeability (73). Palmitoylation- covalent attachment of the palmitic fatty acid to cysteine residues of proteins- of tight junction protein claudin was found to be essential for protein localization and enhanced property of tight junctions (74).

In addition to structural role of lipids in surrounding plasma membrane, lipidic nature of tight junction itself was first proposed more than 30 years ago by Kachar et al. They suggested that tight junction strands are formed of inverted lipid cylinders where apposing cells contact each other through fusion points between exoplasmic leaflet of the two neighboring cells (75). This was further supported by freeze fracture preparations that demonstrate the presence of phospholipids and cholesterol particles in tight junction strands (76,77). Model of lipid bridges at tight junctions has been postulated as a route for lateral transfer of phospholipids and lipid-protein complexes between neighboring cells (78,79). Our study is the first to demonstrate that ceramides co-localize within tight junction proteins demonstrated by immunofluorescent staining, electron microscopy and tight junction purification followed by MS analysis. Specifically we demonstrated the presence of VLC ceramides and, importantly, omega-linked acyl-ceramide species by mass spectrometry analysis of tight junction structures. Until now VLC ceramides were only found in water permeability barrier of the skin.

The exact confirmation of omega-linked acyl-VLC ceramides in the tight junction structure is not known, and will require further investigation, however these very long highly saturated lipids may have a role in stabilizing tight junction proteins and protecting against degradation. Indeed, overexpression of hELOVL4 in BRECs, significantly increased occludin content and prevented the VEGF – induced decrease in occludin. This effect was due to translational or posttranslational regulation as occludin mRNA level was not increased after ELOVL4 overexpression (occludin mRNA/ GAPDH; in AdEmpty transduced cells = 0.005 ± 0.002 , while in hELOVL4 transduced cells = 0.004 ± 0.0002).

Based on the structure, omega-linked acyl-VLC ceramides could be incorporated in the plasma membranes and aid in organizing junctional domain. The long fatty acid tail of omega-linked acyl-ceramides could potentially allow for traversing the thickness of double layer, bridging the space between tight junction proteins of apposing cells and thereby regulating barrier function. More detailed structural studies would be required to assign the exact function to these lipids in the tight junctions. In summary, we have shown that ELOVL4-mediated production of VLC-ceramides is necessary for retinal endothelial barrier function. Overexpression of ELOVL4 prevented diabetes-induced retinal permeability and BRB breakdown. VLC ceramides may be necessary for tight junction stability and thereby enhancing barrier property. Normalization of retinal ELOVL4 expression may provide a potential therapeutic strategy for the prevention of diabetes-induced early breakdown of the blood-retina barrier by modulating retinal sphingolipid metabolism.

REFERENCES

REFERENCES

1. Antonetti DA, Barber AJ, Hollinger LA, Wolpert EB, Gardner TW. Vascular Endothelial Growth Factor Induces Rapid Phosphorylation of Tight Junction Proteins Occludin and Zonula Occluden 1. *J Biol Chem.* 1999;274(33):23463–7.
2. Murakami T, Felinski EA, Antonetti DA. Occludin phosphorylation and ubiquitination regulate tight junction trafficking and vascular endothelial growth factor-induced permeability. *J Biol Chem.* 2009;284(31):21036–46.
3. Harhaj NS, Felinski E a, Wolpert EB, Sundstrom JM, Gardner TW, Antonetti DA. VEGF activation of protein kinase C stimulates occludin phosphorylation and contributes to endothelial permeability. *Invest Ophthalmol Vis Sci.* 2006;47(11):5106–15.
4. Zhu W, London NR, Gibson CC, Davis CT, Tong Z, Sorensen LK, et al. Interleukin receptor activates a MYD88-ARNO-ARF6 cascade to disrupt vascular stability. *Nature.* 2012;492(7428):252–5.
5. Aveleira C a, Lin C-M, Abcouwer SF, Ambrósio AF, Antonetti D a. TNF- α signals through PKC ζ /NF- κ B to alter the tight junction complex and increase retinal endothelial cell permeability. *Diabetes.* 2010;59(11):2872–82.
6. Behzadian MA, Wang X, Windsor LJ, Ghaly N, Caldwell RB. TGF-beta Increases Retinal Endothelial Cell Permeability by Increasing MMP-9 : Possible Role of Glial Cells in AND. *Invest Ophthalmol Vis Sci.* 2001;42(3):853-9.
7. Navaratna D, Mcguire PG, Menicucci G, Das A. Proteolytic degradation of VE-cadherin alters the blood-retinal barrier in diabetes. *Diabetes.* 2007;56(9)2380-2387.
8. Kim J, Kim C-S, Lee YM, Jo K, Shin SD, Kim JS. Methylglyoxal induces hyperpermeability of the blood-retinal barrier via the loss of tight junction proteins and the activation of matrix metalloproteinases. *Graefes Arch Clin Exp Ophthalmol.* 2012;250(5):691–7.
9. Enge M, Bjarnega M, Gerhardt H, Gustafsson E, Asker N, Hammes H, et al. Endothelium-specific platelet-derived growth factor-B ablation mimics diabetic retinopathy. *EMBO J.* 2002;21(16):4307–16.
10. Gavard J, Patel V, Gutkind JS. Angiopoietin-1 prevents VEGF-induced endothelial permeability by sequestering Src through mDia. *Dev Cell.* 2008;14(1):25–36.
11. Gerald P, Hiraoka-yamamoto J, Matsumoto M, Clermont A. Activation of PKC δ 47and SHP1 by hyperglycemia causes vascular cell apoptosis and diabetic retinopathy. *Nat Med.* 2009;15(11): 1298-306.
12. Nguyen QD, Brown DM, Marcus DM, Boyer DS, Patel S, Feiner L, et al.

- Ranibizumab for diabetic macular edema: Results from 2 phase iii randomized trials: RISE and RIDE. *Ophthalmology*. 2012;119(4):789–801.
13. Cunha-Vaz J, Ribeiro L, Lobo C. Phenotypes and biomarkers of diabetic retinopathy. *Prog Retin Eye Res*. 2014;41:90-111.
 14. Klaassen I, Van Noorden CJ, Schlingemann RO. Molecular basis of the inner blood-retinal barrier and its breakdown in diabetic macular edema and other pathological conditions. *Prog Retin Eye Res*. 2013;34:19–48.
 15. Engerman RL, Kern TS. Experimental Galactosemia Produces Diabetic-like Retinopathy. *Diabetes*. 1984;33(1):97–100.
 16. Antonetti DA, Barber AJ, Khin S, Lieth E, Tarbell JM, Gardner TW. Vascular Permeability in Experimental Diabetes Is associated with Reduced Endothelial Occludin Content:vascular endothelial growth factor decreases occludin in retinal endothelial cells. *Diabetes*. 1998;47(12):1953-9.
 17. Giacco F, Brownlee M. Oxidative stress and diabetic complications. *Circ Res*. 2010;107(9):1058–70.
 18. The Action of Control Cardiovascular Risk in Diabetes Study Group. Effects of Medical Therapies on Retinopathy Progression in Type 2 Diabetes. *N Engl J Med*. 2010;363:233-44.
 19. Tikhonenko M, Lydic T a, Wang Y, Chen W, Opreanu M, Sochacki A, et al. , Remodeling of retinal fatty acids in animals model of diabetes: a decrease in long-chain polyunsaturated fatty acids is associated with a decrease in fatty acid elongases ELOVL2 and ELOVL4. *Diabetes*. 2010;59(1):219–27.
 20. Opreanu M, Tikhonenko M, Bozack S, Lydic T a, Reid GE, McSorley KM, et al. The unconventional role of acid sphingomyelinase in regulation of retinal microangiopathy in diabetic human and animal models. *Diabetes*. 2011;60(9):2370–8.
 21. Opreanu M, Lydic T a, Reid GE, McSorley KM, Esselman WJ, Busik J V. Inhibition of cytokine signaling in human retinal endothelial cells through downregulation of sphingomyelinases by docosahexaenoic acid. *Invest Ophthalmol Vis Sci*. 2010;51(6):3253–63.
 22. Uchida Y. The role of fatty acid elongation in epidermal structure and function. *Dermatoendocrinol*. 2011;3(2):65–9.
 23. Kihara A. Very long-chain fatty acids: Elongation, physiology and related disorders. *J Biochem*. 2012;152(5):387–95.
 24. Mandal MN a, Ambasadhan R, Wong PW, Gage PJ, Sieving P a, Ayyagari R. Characterization of mouse orthologue of ELOVL4: genomic organization and spatial and

- temporal expression. *Genomics*. 2004;83(4):626–35.
25. Lagali PS, Liu J, Ambasadhan R, Kakuk LE, Bernstein S, Seigel GM, et al. Evolutionarily Conserved ELOVL4 Gene Expression in the Vertebrate Retina. *Invest Ophthalmol Vis Sci*. 2003;44(7):2841–50.
 26. Umeda S, Ayyagari R, Suzuki MT, Ono F. Molecular Cloning of ELOVL4 Gene from Cynomolgus Monkey (*Macaca fascicularis*). *Exp. Anim.* 2003;52(2):129–35.
 27. Zhang X, Yang Z, Karan G, Hashimoto T, Baehr W, Yang X. Elov14 mRNA distribution in the developing mouse retina and phylogenetic conservation of Elov14 genes. *Molecular Vision*. 2003;9:301–7.
 28. Agbaga M-P, Mandal MN a, Anderson RE. Retinal very long-chain PUFAs: new insights from studies on ELOVL4 protein. *J Lipid Res*. 2010;51(7):1624–42.
 29. Agbaga M-P, Brush RS, Mandal MNA, Henry K, Elliott MH, Anderson RE. Role of Stargardt-3 macular dystrophy protein (ELOVL4) in the biosynthesis of very long chain fatty acids. *Proc Natl Acad Sci U S A*. 2008;105(35):12843–8.
 30. Busik JV, Esselman WJ, Reid GE. Examining the role of lipid mediators in diabetic retinopathy. *Clin Lipidol*. 2012;7(6):661–75.
 31. Wertz PW, Downing DT. Ceramides of pig epidermis: structure determination. *J lipid Res*. 1983;24(6):759–65.
 32. Imokawa g, Abe A, Jin K, Higaki Y, Kawashima M, Hidano A. Decreased level of ceramides in stratum corneum of atopic dermatitis: an etiologic factor in atopic dry skin. *J Invest Dermatol*. 1991;96(4):523–6.
 33. Vasireddy V, Uchida Y, Salem N, Kim SY, Mandal NA, et al. Loss of functional ELOVL4 depletes very long-chain fatty acids (≥ 28) and the unique ω -o-acylceramides in skin leading to neonatal death. *Hum Mol Genet*. 2007;16(5):471–82.
 34. McMahon A, Butovich IA, Mata NL, Klein M, Ritter R, Richardson J, et al. Retinal pathology and skin barrier defect in mice carrying a Stargardt disease-3 mutation in elongase of very long chain fatty acids-4. *Mol Vis*. 2007;13:258–72.
 35. Li W, Sandhoff R, Kono M, Zerfas P, Hoffmann V, Ding BCH, et al. Depletion of ceramides with very long chain fatty acids causes defective skin permeability barrier function, and neonatal lethality in ELOVL4 deficient mice. *Int J Biol Sci*. 2007;3(2):120–8.
 36. Okuda A, Naganuma T, Ohno Y, Abe K, Yamagata M, Igarashi Y, et al. Hetero-oligomeric interactions of an ELOVL4 mutant protein: implications in the molecular mechanism of Stargardt-3 macular dystrophy. *Mol Vis*. 2010;16:2438–45.
 37. Zhang K, Kniazeva M, Han M, Li W, Yu Z, Yang Z, et al. A 5-bp deletion in

- ELOVL4 is associated with two related forms of autosomal dominant macular dystrophy. *Nat Genet.* 2001;27(1):89–93.
38. Karan G, Lillo C, Yang Z, Cameron DJ, Locke KG, Zhao Y, et al. Lipofuscin accumulation, abnormal electrophysiology, and photoreceptor degeneration in mutant ELOVL4 transgenic mice: a model for macular degeneration. *Proc Natl Acad Sci U S A.* 2005;102(11):4164–9.
 39. Abcouwer SF, Lin C, Wolpert EB, Shanmugam S, Schaefer EW, Freeman WM, et al. Effects of ischemic preconditioning and bevacizumab on apoptosis and vascular permeability following retinal ischemia-reperfusion injury. *Invest Ophthalmol Vis Sci.* 2010;51(11):5920–33.
 40. Ryals RC, Boye SL, Dinculescu A, Hauswirth WW, Boye SE. Quantifying transduction efficiencies of unmodified and tyrosine capsid mutant AAV vectors in vitro using two ocular cell lines. *Mol Vis.* 2011;17:1090-102.
 41. Wigglesworth VB. Lipid staining for the electron microscope: a new method. *J Cell Sci.* 1975;19(3):425–37.
 42. Mahendrasingam S, Wallam CA, Hackney CM. Two approaches to double post-embedding immunogold labeling of freeze-substituted tissue embedded in low temperature Lowicryl HM20 resin. *Brain Res Brain Protoc.* 2003;11(2):134–41.
 43. Tang VW. Proteomic and bioinformatic analysis of epithelial tight junction reveals an unexpected cluster of synaptic molecules. *Biol Direct.* 2006;1:37.
 44. Busik J V, Reid GE, Lydic TA. Global analysis of retinal lipids by complementary precursor ion and neutral loss mode tandem mass spectrometry. *Methods Mol Biol.* 2009;579:33-70.
 45. Lydic T a, Busik J V, Reid GE. A monophasic extraction strategy for the simultaneous lipidome analysis of polar and nonpolar retina lipids. *J Lipid Res.* 2014;55(8):1797–809.
 46. Byeon SK, Lee JY, Lee J-S, Moon MH. Lipidomic profiling of plasma and urine from patients with Gaucher disease during enzyme replacement therapy by nanoflow liquid chromatography–tandem mass spectrometry. *J Chromatogr A.* 2015;1381:132–9.
 47. Chakravarthy H, Beli E, Navitskaya S, O’Reilly S, Wang Q, Kady N, et al. Imbalances in mobilization and activation of pro-inflammatory and vascular reparative bone marrow-derived cells in diabetic retinopathy. *PLoS One.* 2016;11(1):1–21.
 48. Aiello LP, Avery RL, Arrigg PG, Keyt BA, Jampel HD et al. Vascular endothelial growth factor in ocular fluid of patients with diabetic retinopathy and other retinal disorders. *N Engl J Med.* 1994;331:1480-7.
 49. Mathews MK, Merges C, Mcleod DS, Luty GA. Vascular Endothelial Growth Factor and Vascular Permeability Changes in Human Diabetic Retinopathy. *Invest Ophthalmol Vis*

- Sci.1997;38:2729-41.
50. Hammes HP, Lin J, Bretzel RG, Brownlee M, Breier G. Upregulation of the vascular endothelial growth factor/vascular endothelial growth factor receptor system in experimental background diabetic retinopathy of the rat. *Diabetes*. 1998;47(3):401–6.
 51. Qaum T, Xu Q, Jousen AM, Clemens MW, Qin W, Miyamoto K, et al. VEGF-initiated Blood – Retinal Barrier Breakdown in Early Diabetes. *Invest Ophthalmol Vis Sci*. 2001;42:2408–13.
 52. Caldwell RB, Bartoli M, Behzadian MA, El-Remessy AEB, Al-Shabrawey M, Platt DH, et al. Vascular endothelial growth factor and diabetic retinopathy: pathophysiological mechanisms and treatment perspectives. *Diabetes Metab Res Rev*. 2003;19(6):442–55.
 53. Koleva-Georgieva DN, Sivkova NP, Terzieva D. Serum inflammatory cytokines IL-1 β , IL-6, TNF- α and VEGF have influence on the development of diabetic retinopathy. *Folia Med*. 2011;53(2):44–50.
 54. Martiney J a., Berman JW, Brosnan CF. Chronic inflammatory effects of interleukin-1 on the blood-retina barrier. *J Neuroimmunol*. 1992;41(2):167–76.
 55. Claudio L, Martiney JA, Brosnan CF. Ultrastructural studies of the blood-retina barrier after exposure to interleukin-1 beta or tumor necrosis factor-alpha . *Lab Invest*.1994;70(6):850-61.
 56. Demircan N, Safran BG, Soylu M, Ozcan a a, Sizmaz S. Determination of vitreous interleukin-1 (IL-1) and tumour necrosis factor (TNF) levels in proliferative diabetic retinopathy. *Eye (Lond)*. 2006 ;20(12):1366–9.
 57. Kowluru R a, Odenbach S. Role of interleukin-1beta in the development of retinopathy in rats: effect of antioxidants. *Invest Ophthalmol Vis Sci*. 2004;45(11):4161–6.
 58. Lyons TJ, Jenkins AJ, Zheng D, Lackland DT, McGee D, Garvey WT, et al. Diabetic retinopathy and serum lipoprotein subclasses in the DCCT/EDIC cohort. *Investig Ophthalmol Vis Sci*. 2004;45(3):910–8.
 59. Klein RL, McHenry MB, Lok KH, Hunter SJ, Le N-A, Jenkins AJ, et al. Apolipoprotein C-III protein concentrations and gene polymorphisms in Type 1 diabetes: associations with microvascular disease complications in the DCCT/EDIC cohort. *J Diabetes Complications*. 2005;19(1):18–25.
 60. Scott R, Best J, Forder P, Taskinen MR, Simes J, et al. Fenofibrate Intervention and Event Lowering in Diabetes (FIELD) study: baseline characteristics and short-term effects of fenofibrate. *Cardiovasc Diabetol*. 2005;4:13.
 61. Ferris FL, Chew EY, Hoogwerf BJ. Serum Lipids and Diabetic Retinopathy. *Diabetes care*.1996;19(11):1291–3.

62. Wang Y, Botolin D, Xu J, Christian B, Mitchell E, Jayaprakasam B, et al. Regulation of hepatic fatty acid elongase and desaturase expression in diabetes and obesity. *J Lipid Res.* 2006;47(9):2028–41.
63. Wang Q, Tikhonenko M, Bozack SN, Lydic TA, Yan L, Panchy NL, et al. Changes in the Daily Rhythm of Lipid Metabolism in the Diabetic Retina. *PLoS One.* 2014;9(4):1-13.
64. Green CD, Olson LK. Modulation of palmitate-induced endoplasmic reticulum stress and apoptosis in pancreatic β -cells by stearoyl-CoA desaturase and Elovl6. *Am J Physiol Endocrinol Metab.* 2011;300(4):E640-9.
65. McMahon A, Jackson SN, Woods AS, Kedzierski W. A stargardt disease-3 mutation in the mouse Elovl4 gene causes retinal deficiency of C32-C36 acyl phosphatidylcholines. *FEBS Lett.* 2007;581(28):5459-63.
66. Harkewicz R, Du H, Tong Z, Alkuraya H, Bedell M, Sun W, et al. Essential role of ELOVL4 protein in very long chain fatty acid synthesis and retinal function. *J Biol Chem.* 2012;287(14):11469–80.
67. Grayson C, Molday RS. Dominant negative mechanism underlies autosomal dominant Stargardt-like macular dystrophy linked to mutations in ELOVL4. *J Biol Chem.* 2005;280(37):32521–30.
68. Sommer JR, Estrada JL, Collins EB, Bedell M, Alexander C a, Yang Z, et al. Production of ELOVL4 transgenic pigs: a large animal model for Stargardt-like macular degeneration. *Br J Ophthalmol.* 2011;95(12):1749–54.
69. Sandhoff R. Very long chain sphingolipids : Tissue expression , function and synthesis. *FEBS Lett.* 2010;584:1907–13.
70. McMahon A, Butovich I a, Kedzierski W. Epidermal expression of an Elovl4 transgene rescues neonatal lethality of homozygous Stargardt disease-3 mice. *J Lipid Res.* 2011;52(6):1128–38.
71. Jiang WG, Bryce RP, Horrobin DF, Mansel RE. Regulation of Tight Junction Permeability and Occludin Expression by Polyunsaturated Fatty Acids. *Biochem Biophys Res Commun.* 1998;244(2):414–20.
72. Park EJ, Thomson ABR, Clandinin MT. Protection of intestinal occludin tight junction protein by dietary gangliosides in lipopolysaccharide-induced acute inflammation. *J Pediatr Gastroenterol Nutr.* 2010;50(3):321–8.
73. Li Q, Zhang Q, Wang M, Zhao S, Ma J, Luo N, et al. Interferon-gamma and tumor necrosis factor-alpha disrupt epithelial barrier function by altering lipid composition in membrane microdomains of tight junction. *Clin Immunol.* 2008 126(1):67–80.
74. Van Itallie CM, Gambling TM, Carson JL, Anderson JM. Palmitoylation of claudins is required for efficient tight-junction localization. *J Cell Sci.* 2005;118(7):1427–

- 36.
75. Kachar B, Reese TS. Evidence for the lipidic nature of tight junction strands. *Nature*.1982;296:464-6.
 76. Kan FW. Cytochemical Evidence for the Presence of Phospholipids in Epithelial Tight Junction Strands. *J Histochem Cytochem*.1993;41(5):649-56.
 77. Feltkamp CA, Van der waerden AW. Junction formation between cultured normal rat hepatocytes. An ultrastructural study on the presence of cholesterol and the structure of developing tight- junction strands. *J Cell Sci*.1983;63:271–86.
 78. Laffafian I, Hallett MB. Lipid-Protein Cargo Transfer : A Mode of Direct Cell-to-Cell Communication for Lipids and Their Associated Proteins. *J cell Physiol*. 2007;210(2):336–42.
 79. Grebenkfimper K. Translational diffusion measurements of a fluorescent phospholipid between MDCK-I cells support the lipid model of the tight junctions. *Chem Phys Lipids*. 1994;71(94):133–43.

Chapter 3. Increase in acid sphingomyelinase level in human retinal endothelial cells and CD34⁺ circulating angiogenic cells isolated from diabetic individuals is associated with dysfunctional retinal vasculature and vascular repair process in diabetes

This chapter is a modified version of an article accepted in Clinical Lipidology.

Authors: Nermin Kady, Yuanqing Yan, Tatiana Salazar, Qi Wang, Harshini Chakravarthy, Chao Huang, Eleni Beli, Svetlana Navitskaya, Maria Grant, Julia Busik.

3.1 Abstract

Diabetic retinopathy (DR) is a microvascular disease that results from retinal vascular degeneration and its defective repair due to diabetes induced endothelial progenitor dysfunction. Understanding the key molecular factors involved in vascular degeneration and repair is paramount for developing effective DR treatment strategies. We propose that diabetes-induced activation of acid sphingomyelinase (ASM) plays essential role in retinal endothelial and CD34⁺ circulating angiogenic cell (CAC) dysfunction in diabetes.

Primary cultures of human retinal endothelial cells (HRECs) isolated from control and diabetic donor tissue and human CD34⁺ CACs from control and diabetic patients were used in this study. ASM mRNA expression was assessed by quantitative PCR, ASM concentration was determined by ELISA assay. To evaluate the effect of diabetes-induced ASM on HRECs and CD34⁺ CACs function, tube formation, CAC incorporation into endothelial tubes, and diurnal release of CD34⁺ CACs in diabetic individuals was determined.

ASM expression level was significantly increased in HRECs isolated from diabetic compared to control donor tissue, as well as CD34⁺CACs and plasma of diabetic patients. A significant decrease in tube area was observed in HRECs from donors with signs of NPDR as compared to control HRECs. The tube formation deficiency was associated with increased expression of

ASM in diabetic HRECs. Moreover, diabetic CD34⁺ CACs with high ASM showed defective incorporation into endothelial tubes. Diurnal release of CD34⁺ CACs was disrupted with the rhythmicity lost in diabetic patients.

Collectively, these findings support that diabetes-induced ASM upregulation has a marked detrimental effect on both retinal endothelial cells and CACs. ASM may provide novel therapeutic target for treating DR.

3.2 Introduction

Diabetic retinopathy (DR) is a microvascular disease that results from diabetes-induced retinal damage that is further exacerbated by bone marrow dysfunction. Bone marrow dysfunction leads to decreased release of cells into the circulation and changes in hematopoiesis resulting in increased circulating pro-inflammatory monocytes and diminished repair due to defective progenitor cells. Although DR influence all retinal cells, clinical manifestations of DR are mainly due to changes in retinal vessels, where early histological alterations include pericyte loss, thickening of basement membrane, capillary occlusion and endothelial cell degeneration (1,2) . These are followed by break down of blood retinal barrier (BRB) and leaky vasculature leading to hemorrhages, hard exudates, and retinal edema; structural changes involving the vascular wall leading to microaneurysms; and finally neovascularization, vitreous hemorrhage and fibrous tissue formation (3). Impaired vision due to macular edema, or vision loss due to neovascularization-induced vitreous hemorrhage or tractional retinal detachment usually takes place in the later stages of the disease.

Circulating angiogenic cells (CACs), a population of vascular progenitors originated from HSC (4), are considered as key regulators for healthy maintenance of retinal vasculature. Diabetic metabolic abnormalities lead to defective vascular maintenance due, in part, to failed attempts by dysfunctional CACs to repair damaged endothelium.

HSCs isolated from bone marrow or CACs from peripheral blood of control (healthy) animals have been shown to repair ischemic damage and aid in reperfusion of ischemic tissues (4–6). Several studies have shown an association between DR risk and both reduced number (7–10) and function of CACs (11–16).

Several key hyperglycemia- and dyslipidemia-activated pathways leading to retinal endothelial cell and CAC dysfunction have been identified. Prominent among these are pathways that promote an increase of pro-inflammatory cytokines, pro-inflammatory lipids and pro-angiogenic factors (17–26). We have previously demonstrated activation of the central enzyme of sphingolipid metabolism, acid sphingomyelinase (ASM), as a key metabolic abnormality in diabetic retinal vasculature and CACs. ASM hydrolyzes sphingomyelin (SM) into pro-inflammatory and pro-apoptotic ceramide. Activation of ASM plays an important role in signal transduction in response to various stimuli including IL-1 β (27,28) and TNF- α (29). Endothelial cells represent a major source of ASM (30–33). Inhibition of ASM exhibits protective effect in diabetes preventing diabetes-induced retinal inflammation and vascular degeneration (15,33,34).

Previously, we have identified key defects in circadian regulation of CACs. We showed that bone marrow denervation results in loss of circadian release of vascular reparative cells from the bone marrow and generation of increased numbers of proinflammatory cells. Using a rat model of T2D, we showed that the decrease in CACs release from diabetic bone marrow is caused by bone marrow neuropathy and that these changes precede the development of diabetic retinopathy. We observed a marked reduction in clock gene expression in the retina and in CACs. Denervation of the bone marrow resulted in progenitors being “trapped” within the

bone marrow and in loss of the circadian release of these cells into the circulation. This reduction in the circadian peak of CAC release into the circulation led to diminished reparative capacity and resulted in development of acellular retinal capillaries (7). We also showed that Per2 mutant mice recapitulate key aspects of diabetes without the associated metabolic abnormalities. In Per2 mutant mice, we observed a threefold decrease in proliferation and 50% reduction in nitric oxide levels in CACs. Tyrosine hydroxylase-positive nerve processes and neurofilament-200 staining were reduced in Per2 mutant mice (suggestive of diabetic neuropathy) and increased acellular capillaries were identified (35). We also showed that as CD34⁺ CACs acquired differentiation markers (towards the endothelial lineage), robust oscillations of clock genes are observed (36).

It is well accepted in diabetic complications field that cells isolated from diabetic tissue keep diabetic phenotype for several passages even when cultured in normal glucose. This is due to “metabolic memory”, or "legacy effect" for vascular disease in diabetes - the prolonged benefits of good glycemic control, as well as the prolonged harm poor control in diabetic patients(11,37–39). In this study we used HREC cells isolated from control and diabetic donor tissue as a model.

In the current study, we have focused exclusively on human CACs. We asked if the defect in circadian release observed in rodents with diabetes occurred in humans. We examined the effect of diabetes-induced ASM activity on the function of human CACs and retinal endothelial cells comparing the angiogenic ability of control (low ASM) and diabetic (high ASM) HRECs to form tube-like structures in vitro and determining the capacity of control (with low ASM) and diabetic (with high ASM) CACs to support endothelial tube formation.

3.3 Materials and methods

3.3.1 Circadian study of human CD34⁺ CACs

The study was approved by the University of Florida IRB #411-2010. All study subjects provided informed consent. Individuals were brought into the Clinical Research Center at the University of Florida for 48 h. During the first 24 h, individuals were evaluated and on the evening of the first day, a heparin lock was inserted into their forearm. During the second 24-h period, the individuals had 1 mL of blood removed every 2 h for a total of 24 h and analyzed for the number of CD34⁺ cells by flow cytometry. Clinical characteristics of the patients are presented in Table 2.

3.3.2 Postmortem imaging of human retina and cell culture

Primary cultures of HRECs were prepared from postmortem tissue obtained from National Disease Research Interchange, Philadelphia, PA and Midwest Eye-Banks, Ann Arbor, MI. The tissue was received within 36 h after death. The donor characteristics are provided in Table 3. Primary HRECs were isolated as previously described (40). As previously demonstrated the cells isolated from control and diabetic donors keep their phenotypes for 4-6 passages due to metabolic memory phenomenon (11,37–39). On arriving in the laboratory, the eyes were placed on sterile gauze, and they were washed with povidone- iodine solution (Purdue Pharma L.P. Stamford, CT). After 10 minutes, the globe was punctured approximately 2 mm from the limbus, a circumferential incision was made and the anterior chamber was removed. A vitreous spatula was used to loosen the vitreous adherent to the anterior retina. When all the vitreous was removed, the retina was gently removed from the layer of retinal pigment epithelium and cut at the optic nerve. Before proceeding into the isolation of HRECs, retinas were rinsed,

flatmounted and retinal imaging was taken using a Nikon SMZ-800 Stereo Microscope with Prior Proscan 3 Motorized XY System with Z Drive and MetaMorph Modules to perform image stitching, to properly determine the stage of retinopathy of the donors used for isolation of HRECs. Retinas included in this study have at least three signs of non-proliferative diabetic retinopathy (NPDR) such as microaneurysms, intraretinal haemorrhages and intraretinal microvascular abnormalities (IRMA). Retina was then placed on a 53- μ m Nylon mesh filter (Sefar America, Buffalo, NY.), washed with a solution containing Glucose (5.5 mM), L-Glutamine (2 mM) and 1x MEM Non-Essential Amino Acids Solution (GIBCO, Life Technologies, Carlsbad, CA). The retinas were then placed into a 25-ml flask containing 100 U/ml of collagenase, Type 1 (Worthington Biochemical Co., Lakewood, NJ) in the above-mentioned solution containing 22% Bovine serum albumin (Sigma) and 0.01% Soybean Trypsin Inhibitor (Sigma). Retinas were then mechanically agitated using a shaker and allowed to digest at 37°C for approximately 60 minutes or until no tissue fragments could be seen. After digestion, cells were centrifuged at 1000 rpm for 5 minutes. The supernatant was removed and pellet was suspended in fresh media; 1:1 mix of low glucose Dulbecco's modified Eagle's medium (DMEM 1g/L) / F-12 nutrient mix (GIBCO, Life Technologies, Carlsbad, CA) supplemented with 10 % fetal calf serum (Hyclone, Logan, UT), 1% endothelial cell growth supplement (Millipore, MA), 1% insulin-transferrin- sodium selenite media supplement (Sigma) and 1% penicillin-streptomycin antimycotic (GIBCO, Invitrogen-Life Technologies, Carlsbad, CA). Glucose concentration in the final media was adjusted to 5.5 mM. The cells were maintained at 37°C in 95% air and 5% CO₂ in a humidified cell culture incubator. Passages 3 to 5 were used in the experiments.

3.3.3 Human CD34⁺ CACs isolation

Human peripheral blood samples (150 ml) were collected into Sodium Citrate-containing CPTTM glass vacuum tubes (BD, Franklin Lakes, NJ). Written informed consent was obtained from each patient, and all procedures were approved by the Institutional Review Board at the University of Florida (IRB # 408-2010). Peripheral blood mononuclear cells (MNCs) were isolated from the blood by density gradient centrifugation using Lympholyte (Cedarlane Laboratories Ltd., Ontario, Canada). The CD34⁺ cell fraction was then isolated from the MNCs using the EasySepTM CD34⁺ positive selection system according to the manufacturer's instructions (Stem Cell Technologies, Vancouver, BC, Canada). Clinical characteristics of the patients are presented in Table 3.

3.3.4 Tube formation assay

Tube formation assay was performed using BD BioCoat Angiogenesis System-Endothelial Cells Tube Formation Matrigel Matrix 96-well plate (BD Biosciences Discovery Labware, Bedford, MA) according to the manufacturer's instructions. Briefly, isolated CD34⁺ CACs and HRECs were labeled with Qtracker 655 and Qtracker 525 (Invitrogen); respectively. Control or diabetic HRECs were mixed in a 4:1 ratio with either control or diabetic CD34⁺ cells, seeded into Matrigel Matrix 96-well plate) and incubated for 16 to 18 h at 37°C (5% CO₂). After incubation, wells were assessed for the presence of tube-like structures and images were taken in 10x magnifications using a Nikon TE2000 fluorescence microscope equipped with Photometrics CoolSNAP HQ2 camera. At least three different fields were randomly selected and captured to collect images for each well. Tube area and percentage of CD34⁺ incorporated into tubules were calculated using MetaMorph software system (Molecular Devices, Downingtown, PA). Statistics

were performed on 3 independent wells per condition with minimum three images taken from each well.

3.3.5 Quantitative real-time PCR

Total RNA was extracted from HRECs, human CD34⁺ cells using QuickGene RNA (Fujifilm, Minato-Ku, Tokyo, Japan) or Qiagen RNeasy (Qiagen Inc., Valencia, CA, USA) according to the manufacturer's instructions. NanoDrop 2000 (Thermo Scientific, IL, USA) was used to determine total RNA concentration. Total RNA was reverse transcribed into cDNA using superscript III first-strand synthesis system (Invitrogen, Carlsbad, CA). Human gene-specific primers for ASM were used. Expression levels were normalized to human cyclophilin. Sequence of specific primers used is given below:

Human ASM: caacctcgcgctgaagaa and tccaccatgtcatcctcaaa

Human Cyclophilin: aaggtcccaaagacagcaga and cttgccaccagtgcattat

3.3.6 ELISA assay

Blood samples were collected, centrifuged and plasma was stored at -80 °C. Samples were assayed for human ASM concentration using ELISA kit (Cloud –Clone Corp., Houston, TX, USA) according to the manufacturer's protocol.

3.3.7 Statistical analysis

Data are presented as mean ± S.E.M. Results were analyzed for statistical significance by the Student's t-test (GraphPad Prism 7, GraphPad Software, San Diego, CA). Significance was established at $P < 0.05$.

Table 2. Clinical characteristics of control and diabetic subjects involved in the circadian study.

Subject #	Gender	Age	Diabetes duration	HbA1C	CVD	Retinopathy	Medications
Diabetic 1	Female	67	T2D 4 months	7.5	No	No	Glucophage
Diabetic 2	Female	65	T2D 20 years	8.8	No	No	Lantus
Diabetic 3	Male	76	T2D	7.4	No	No	Glucophage
Diabetic 4	Female	64	T2D	6.3	No	No	Actos
Diabetic 5	Female	67	T2D	6.4	No	No	Glucophage
Diabetic 6	Female	68	T2D 9 years	6.8	No	No	Diabeta
Diabetic 7	Female	48	T2D years	6.0	No	No	Metformin
Diabetic 8	Female	59	T2D 10 years	7.7	No	No	Humulin
Control 1	Female	43			No	No	
Control 2	Female	57			No	No	
Control 3	Female	68			No	No	
Control 4	Male	43			No	No	

Table 2. (cont'd)

Inclusion criteria: Individuals between the ages of 21 and 65 years were eligible to participate.

Exclusion criteria: Subjects were excluded for the following reasons: a) evidence of ongoing acute or chronic infection (HIV, Hepatitis B or C, or tuberculosis); b) ongoing malignancy; c) cerebral vascular accident or cerebral vascular procedure; d) current pregnancy; e) history of organ transplantation; f) presence of a graft; g) uremic symptoms, such as an estimated glomerular filtration rate of less than 20 cc/min (by Modification of Diet in Renal Disease equation), or an albumin of less than 3.6 (to avoid malnutrition as a confounding variable); h) a history of smoking; and i) anemia.

Table 3. Clinical characteristics of control and diabetic HRECs donors and CD34⁺ CACs subjects involved in the study.

HRECs donor #	Gender	Age	Diabetes duration	CVD	Retinopathy	Nephropathy	Neuropathy	Medications
Diabetic 1	Male	71	T2D 18 years	Yes	Moderate NPDR	Yes	No	Insulin
Diabetic 2	Male	66	T2D 16 years	Yes	Sever NPDR	Yes	No	Insulin Humalog and Humalin-N
Diabetic 3	Female	50	T2D 15 years	No	Sever NPDR	No	No	Insulin
Diabetic 4	Male	73	T2D 6 years	Yes	Mild NPDR	Yes	Yes	Insulin
Diabetic 5	Male	71	T2D 20 years	Yes	Moderate NPDR	Yes	No	Insulin
Diabetic 6	Male	62	T2D 22 years	Yes	Mild NPDR	Yes	No	Insulin
Diabetic 7	Male	70	T2D 15 years	Yes	Moderate NPDR	Yes	No	Insulin
Control 1	Female	58	No	No	No	No	No	
Control 2	Male	56	No	Yes	No	No	No	
Control 3	Male	71	No	No	No	No	No	
Control 4	Female	52	No	No	No	No	No	

Table 3. (cont'd)

CD34+ CACs subject #	Gender	Age	Diabetes duration	HbA1C	CVD	Retinopathy	Nephropathy	Neuropathy
Diabetic 1	Male	55	T2D 10 years	14	No	Sever NPDR	No	No
Diabetic 2	Female	58	T2D	6.5	No	Moderate NPDR	No	No
Diabetic 3	Female	59	T2D	7.1	No	Moderate NPDR	No	No
Diabetic 4	Male	41	T2D	14	No	PDR	No	No
Control 1	Female	57	No		No	No	No	No
Control 2	Male	49	No		No	No	No	No
Control 3	Female	39	No		No	No	No	No
Control 4	Female	58	No		No	No	No	No

3.4 Results

3.4.1 ASM expression level is increased in HREC, CD34⁺ CACs and blood plasma of diabetic donors

To determine whether human diabetic tissues exhibited the same increase in ASM as we observed in animal models (15,33), we measured ASM expression level in human RECs, CD34⁺ CACs and plasma samples in both diabetic and control donors. ASM expression level was significantly increased in all three tissue types in diabetic compared to control donors (Fig. 16A, B and C).

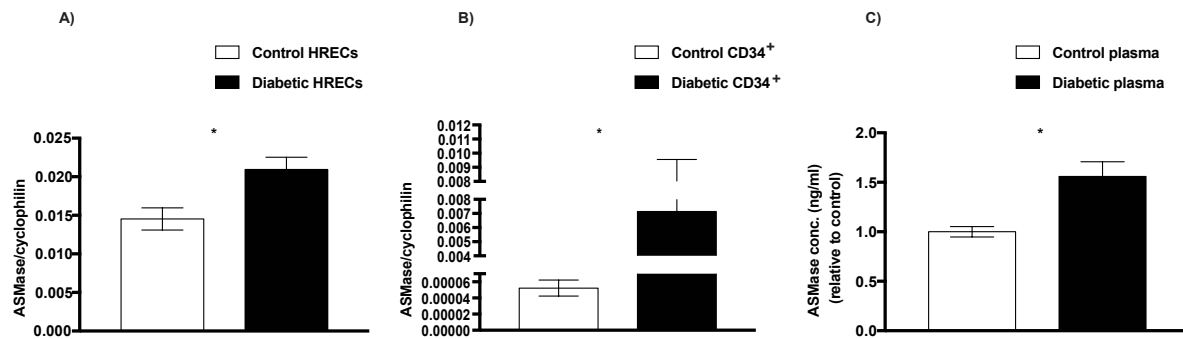


Figure 16. Diabetes induced increase in ASM expression.

Total RNA was isolated and the transcript level of ASM was analyzed by qRT-PCR in (A) HRECs, (B) CD34⁺ cells and (C) plasma from diabetic donors (n=4-7) compared with control donors (n=3-4). Data are means ± SEM. **P* < 0.05, significantly different as determined by Student's *t*-test. Abbreviations: ASM, acid sphingomyelinase; HRECs, human retinal endothelial cells.

3.4.2 Diabetes induces decrease in HREC tube formation

As shown above and previously demonstrated, HRECs isolated from diabetic donors have high ASM activity and expression level. To evaluate the effect of diabetes-induced increase in ASM on HRECs function, we performed tube formation assay to measure the ability of retinal endothelial cells to form blood-vessel-like tubular structure. Tube formation by HRECs isolated from healthy control retinas was compared to cells isolated from retinas with signs of NPDR as determined by post-mortem retinal imaging (Fig. 17A). A significant decrease in tube area was observed in HRECs from retinas with signs of NPDR as compared to control HRECs (Fig. 17B).

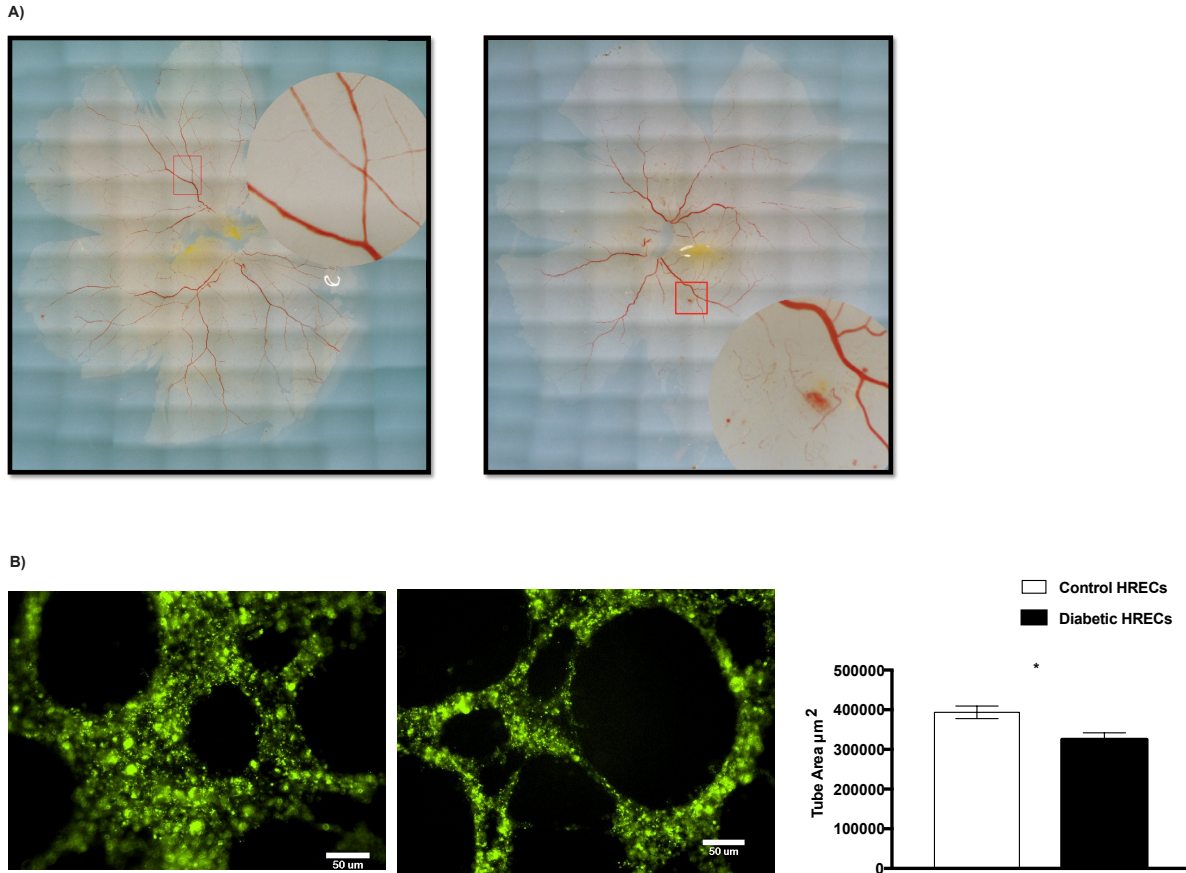


Figure 17. Diabetes impairs tube formation capacity of HRECs.

(A) Postmortem imaging of human retina. Control retina with well-organized blood vessels (left), Diabetic retina with signs of NPDR; intraretinal hemorrhages and microaneurysms (right).

(B) An in vitro tube formation assay was performed in control (n=4) and diabetic (n=7) HRECs using Matrigel Matrix 96-well plate. Representative images of tube-like structures are shown.

The cells were stained with Qtracker 525 (green), images were taken in 10x magnification and total tube areas were calculated using MetaMorph software system. Quantification of tube area is shown on far right. Data are means \pm SEM. * $P < 0.05$, significantly different as determined by Student's t-test. Scale bar = 50 μm .

3.4.3 Diabetes induced increase in ASM is associated with CD34⁺ CACs dysfunction

To determine the role of ASM expression in diabetes-induced defect in CD34⁺ CACs function, we seeded CD34⁺ CACs isolated from both control (low ASM) and diabetic (high ASM) subjects with HRECs and examined whether the level of ASM expression in CACs affect their ability to incorporate into the endothelial tubes formed by the HRECs. Interestingly, CD34⁺ CACs seeded alone did not form tube-like structures, but they did incorporate into tubes formed by HRECs when co-cultured with retinal endothelial cells (Fig. 18C). Increased incorporation into tubes formed by diabetic HRECs was observed for the control CD34⁺ CACs (low ASM) compared to diabetic CACs (high ASM; Fig. 18B). As expected, control HRECs exhibited robust tube formation. Incorporation of CACs into control HREC tubes was not affected by the level of ASM in CACs (Fig. 18A). These data demonstrate that high ASM expression levels in CD34⁺ CACs correlate with impaired incorporation ability, whereas CACs expressing lower levels of ASM display enhanced *in vitro* incorporation.

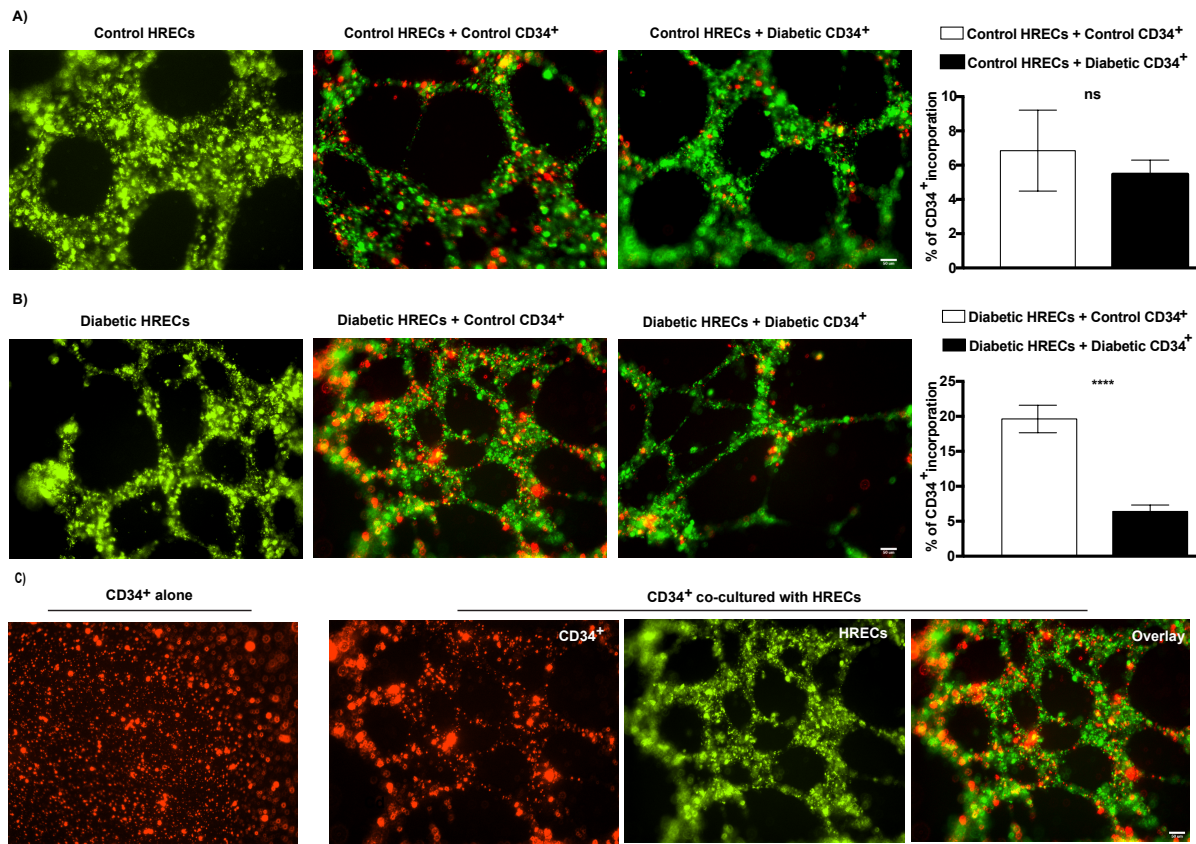


Figure 18. Reduced incorporation of diabetic CD34⁺ CACs into diabetic HRECs tubes.

Tube formation by HRECs (Qtracker 525, green) isolated from control (A) or diabetic (B) donors either without CACs (left panel), or co-incubated with control (middle panel) or diabetic (right panel) CACs (Qtracker 655, red) is shown. Quantification of % of CD34⁺ CACs incorporation into HRECs tubes is shown on far right. Data are means \pm SEM (n= 4-7). *** $P < 0.0001$, significantly different from control as determined by Student's t -test; not significant at $P > 0.05$. Scale bar = 50 μ m.

Figure 18 (cont'd)

(C) CD34⁺ CACs alone were not able to form tube-like structures (left panel), but incorporated into HREC tubes, forming tube-like structures, when co-cultured with HRECs (right three panels). Abbreviations: CACs, circulating angiogenic cells.

3.4.4 Diabetes induced increase in ASM is associated with loss of circadian release of CD34⁺ CACs

We have previously demonstrated that normal diurnal pattern of CACs release from the bone marrow is critical for efficient repair of retinal vasculature in rodents (7). Increase in ASM activity in CACs in diabetic animal models was associated with decreased membrane fluidity and impaired migration leading to increased CAC retention and loss of circadian release from the bone marrow (34). We next determined the effect of diabetes on circadian release of CD34⁺ CACs in diabetic patients. Peripheral blood of type 2 diabetic individuals was collected every 2 h for 24 h and analyzed for the number of CD34⁺ CACs by flow cytometry and compared with control subjects. The dash line is the model fitted curve for individual subjects and bold curve is the fitted curve for population (Fig. 19 A and B). In agreement with previous studies, healthy individuals had a peak of circulating CD34⁺ cells in the middle of the night, representing the rest phase for humans (Fig. 19A), however this peak of CD34⁺ release was lost in T2D subjects (Fig. 19B)

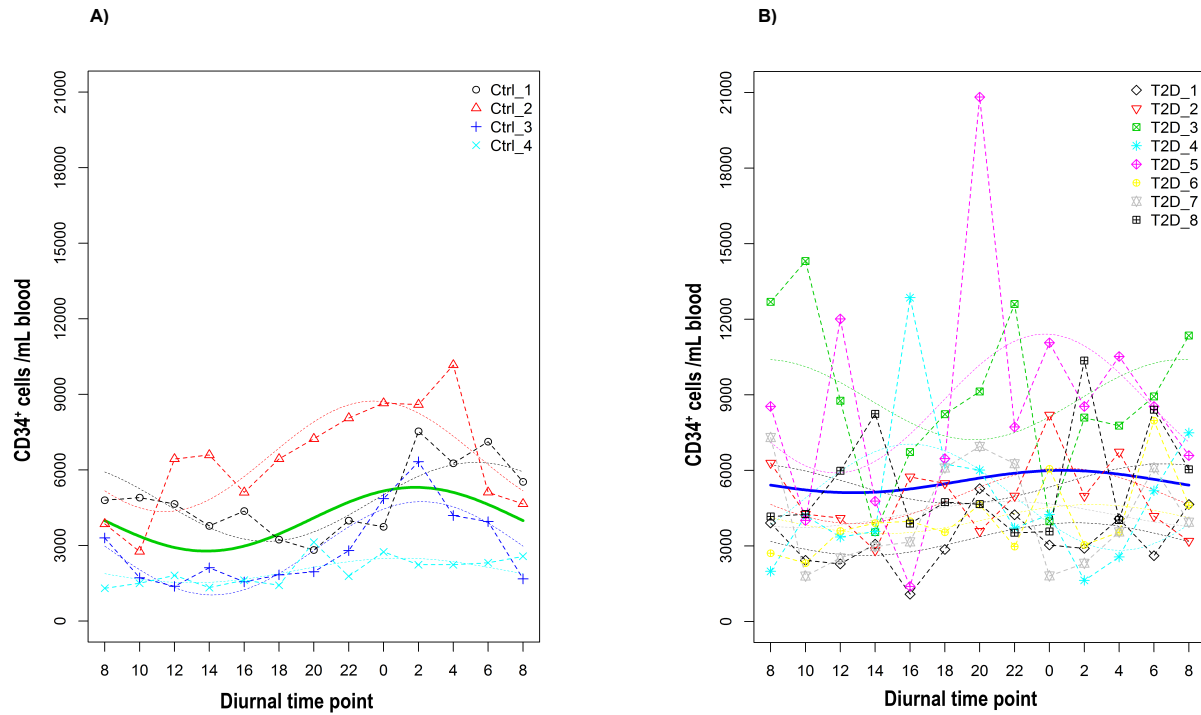


Figure 19. Loss of circadian release of diabetic CD34⁺ CACs.

Peripheral blood was collected every 2 h for a total of 24 h from (A) control (n=4) and (B) diabetic (n=8) subjects and was analyzed for the number of CD34⁺ CACs by flow cytometry. (A) In control subjects, there is a clear peak of circulating CD34⁺ CACs that occurred in the middle of the night. (B) Rhythmic CD34⁺ CACs release pattern was blunted in Type 2 diabetic patients. The dash line is the model fitted curve for individual patients and bold curve is the fitted curve for population.

3.5 Discussion

Diabetic retinopathy is a sight threatening complication of diabetes with limited treatment strategies. Understanding the key molecular factors involved in the disease is important for developing therapeutic targets to prevent progression into ocular neovascularization and blindness. ASM is shown to be a key element in inflammatory signaling through ceramide-mediated signal transduction (41,42). Diabetes-induced increase in ASM activity has been shown to modulate inflammatory response in mature retinal endothelial cells (43), however, there is no direct experimental evidence showing ASM effect on endothelial function. Here we demonstrated that HRECs isolated from type 2 diabetic subjects with signs of NPDR had altered retinal endothelial cell function with impaired capacity to form tube-like structures when compared with control HRECs. The deficiency in tube formation was associated with increased expression of ASM in diabetic HRECs. This is consistent with previous studies showing ASM-mediated endothelial cell apoptosis in various tissues including retina, lungs and gastrointestinal tract (30,31,33,44), and ASM antiangiogenic effect in tumor treatment (45). Endothelium is the major source of ASM production in the body with endothelial cells synthesizing 20 times as much ASM as any other cell type (32); thus, it is not surprising that ASM plays a major role in endothelial cells function. In agreement with previous studies (32), endothelial cells had very high ASM expression level, which was further increased in diabetes. Moreover, increased ASM level in plasma further reflects the increased production and secretion of ASM by activated endothelial cells.

Retinal vascular repair and revascularization is aided by CACs (4,13,16,46–49). We examined the effect of diabetes-induced increase in ASM on the ability of CD34⁺ CACs to incorporate and thus help in repair of defective vascular-like tube structures formed by

diabetic HRECs. We demonstrated that diabetic CD34⁺ CACs, with high ASM, showed minimal incorporation into the defective tubes formed by diabetic HRECs. Non-diabetic CD34⁺ CACs with low ASM showed robust incorporation. These results are in line with other studies showing that diabetic CACs are defective in proliferation, migration, adhesion, differentiation, and participation in vascular regeneration process (13,14,16,46,50,51). Interestingly, no significant difference was observed between non-diabetic and diabetic CD34⁺ CACs incorporation into control HRECs. This is consistent with our previous studies demonstrating lack of incorporation of control CACs into healthy vasculature that does not require repair in non-diabetic (13). We have previously demonstrated that high level of ASM inversely correlates with migration and reparative capacity of CACs, with the inhibition of diabetes-induced ASM resulting in improved migration and retinal vascular regeneration in diabetic mouse model (15,34).

In this study, we compared effect of ASM on functional capacity of healthy and diabetic CACs in human on control and diabetic HRECs. We revealed that the defective incorporation of diabetic CD34⁺ CACs was associated with high ASM. As previously shown, high ASM activity leads to accumulation of membrane ceramides. Accumulation of ceramide results in decreased membrane fluidity, cell rigidity and defective migration which can explain defective incorporation of diabetic CACs (15,34,52) and likely supports their defective release from the bone marrow into the systemic circulation.

Although several lines of evidence demonstrate that ASM expression is an important factor for progenitor cell release from the marrow, migration, proliferation and homing to the injured vasculature; other factors beyond ASM activation are also known to be involved in diabetes-induced CAC dysfunction. These include bone marrow neuropathy and low level of neurotransmitters production; increase in TGF beta leading to decreased NO bioavailability

and diminished expression of CXCR-4 (7,53). These factors affect chemoattraction to SDF1 and lead to increase in stem cell quiescence in the bone marrow niche. In health ASM works in concert with other factors to maintain optimal bone marrow stem cell production and release, however activation of ASM along with other factors disrupts this balance in diabetes (7,34,54,55).

The physiological release of bone marrow progenitor cells including CD34⁺ CACs into the circulation is not constant, but follows circadian oscillations. These oscillations are regulated by sympathetic signaling to bone marrow stromal cells, which results in CXCL12 (SDF-1) down regulation and progenitor egress from the bone marrow; all of these processes occur in circadian pattern under control of clock genes (56). Diabetic bone marrow neuropathy with disruption of circadian rhythm may contribute to endothelial progenitor cell dysfunction. Wang et al. have demonstrated that mutation in circadian gene *Per2* leads to reduced endothelial cell progenitor mobilization and revascularization (57). We investigated whether circadian release of CD34⁺ CACs is altered in diabetic subjects. Peripheral blood was collected every 2 h for 24 h from both control and diabetic subjects. In agreement with previous studies (58–60), normal rhythmic oscillations were observed in control subjects with a clear peak of circulating CD34⁺ CACs cells in the middle of the night (resting phase), optimal time of regeneration in humans. Similar to our observations in diabetic rat model (7). This study revealed that circadian fluctuation of CD34⁺ CACs was disrupted with rhythmicity lost in diabetic individuals. Importantly, we have previously demonstrated that, similar to endothelial cells, the increase in ASM activity in CACs in diabetic animal models was associated with increased ceramide levels, decreased membrane fluidity and impaired migration. This impairment in migration, combined with diminished sympathetic signaling to BM may lead to increased CAC retention in the bone marrow

and loss of circadian release of the progenitor cells as demonstrated in this study.

This study underscores the deleterious effect of high ASM levels on the vascular repair potential of both mature retinal endothelial cells and circulating angiogenic cells in diabetes. Correcting this defect could treat vasodegeneration, enhancing vessel repair and thus preventing progression into PDR stage.

REFERENCES

REFERENCES

1. Hammes HP, Feng Y, Pfister F, Brownlee M. Diabetic retinopathy: Targeting vasoregression. *Diabetes*. 2011;60(1):9–16.
2. Lorenzi M, Gerhardinger C. Early cellular and molecular changes induced by diabetes in the retina. *Diabetologia*. 2001;44(7):791–804.
3. Wong K. Defining diabetic retinopathy severity. *Diabet Retin Evidence-Based Manag*. 2010;10:105–20.
4. Grant MB, May WS, Caballero S, Brown G a J, Guthrie SM, Mames RN, et al. Adult hematopoietic stem cells provide functional hemangioblast activity during retinal neovascularization. *Nat Med*. 2002;8(6):607–12.
5. Kocher AA, Schuster MD, Szaboles MJ, Takuma S, Burkhoff D, et al. Neovascularization of ischemic myocardium by human bone - marrow – derived angioblasts prevents cardiomyocyte apoptosis , reduces remodeling and improves cardiac function. *Nat Med*. 2000;7(4):430–6.
6. Kalka C, Masuda H, Takahashi T, Kalka-Moll WM, Silver M, Kearney M, et al. Transplantation of ex vivo expanded endothelial progenitor cells for therapeutic neovascularization. *Proc Natl Acad Sci U S A*. 2000;97(7):3422–7.
7. Busik J V, Tikhonenko M, Bhatwadekar A, Opreanu M, Yakubova N, Caballero S, et al. Diabetic retinopathy is associated with bone marrow neuropathy and a depressed peripheral clock. *J Exp Med*. 2009;206(13):2897–906.
8. Kusuyama T, Omura T, Nishiya D, Enomoto S, Matsumoto R, Takeuchi K, et al. Effects of treatment for diabetes mellitus on circulating vascular progenitor cells. *J Pharmacol Sci*. 2006;102:96–102.
9. Fadini GP, Pucci L, Vanacore R, Baesso I, Penno G, Balbarini A, et al. Glucose tolerance is negatively associated with circulating progenitor cell levels. *Diabetologia*. 2007;50(10):2156–63.
10. Hazra S, Jarajapu YPR, Stepps V, Caballero S, Thinschmidt JS, Sautina L, et al. Long-term type 1 diabetes influences haematopoietic stem cells by reducing vascular repair potential and increasing inflammatory monocyte generation in a murine model. *Diabetologia*. 2013;56(3):644–53.
11. Loomans CJ, de Koning EJ, Staal FJ, Rookmaaker MB, Verseyden C, de Boer HC, et al. Endothelial progenitor cell dysfunction: a novel concept in the pathogenesis of vascular complications of type 1 diabetes. *Diabetes*. 2004;53(1):195–9.

12. Loomans C, van Haperen R, Duijs JM, Verseyden C, de Crom R, et al. Differentiation of bone marrow-derived endothelial progenitor cells is shifted into a proinflammatory phenotype by hyperglycemia. *Mol Med*. 2009;15(5–6):152–9.
13. Caballero S, Sengupta N, Afzal A, Chang KH, Li Calzi S, Guberski DL, et al. Ischemic vascular damage can be repaired by healthy, but not diabetic, endothelial progenitor cells. *Diabetes*. 2007;56(4):960–7.
14. Segal MS, Shah R, Afzal A, Perrault CM, Chang K, et al. Nitric oxide cytoskeletal-induced alterations reverse the endothelial progenitor cell migratory defect associated with diabetes. *Diabetes*. 2006;55(1):102–9.
15. Tikhonenko M, Lydic TA, Opreanu M, Li Calzi S, Bozack S, McSorley KM, et al. N-3 Polyunsaturated Fatty Acids Prevent Diabetic Retinopathy by Inhibition of Retinal Vascular Damage and Enhanced Endothelial Progenitor Cell Reparative Function. *PLoS One*. 2013;8(1):1–10.
16. Tamarat R, Silvestre J-S, Le Ricousse-Roussanne S, Barateau V, Lecomte-Raclet L, Clergue M, et al. Impairment in ischemia-induced neovascularization in diabetes: bone marrow mononuclear cell dysfunction and therapeutic potential of placenta growth factor treatment. *Am J Pathol*. 2004;164(2):457–66.
17. Kern TS. Contributions of inflammatory processes to the development of the early stages of diabetic retinopathy. *Exp Diabetes Res*. 2007;2007:95103.
18. Kowluru RA. Role of interleukin-1 β in the pathogenesis of diabetic retinopathy. *Br J Ophthalmol*. 2004;88(10):1343–7.
19. Kowluru RA, Odenbach S. Role of interleukin-1 β in the development of retinopathy in rats: Effect of antioxidants. *Investig Ophthalmol Vis Sci*. 2004;45(11):4161–6.
20. Jousseaume AM, Poulaki V, Mitsiades N, Kirchhof B, Koizumi K, et al. Nonsteroidal anti-inflammatory drugs prevent early diabetic retinopathy via TNF- α suppression. *FASEB J*. 2002;16(13):438–40.
21. Jousseaume AM, Doehmen S, Le ML, Koizumi K, Radetzky S, Krohne TU, et al. TNF- α mediated apoptosis plays an important role in the development of early diabetic retinopathy and long-term histopathological alterations. *Mol Vis*. 2009;15(August 2007):1418–28.
22. Demircan N, Safran BG, Soylu M, Ozcan A, Sizmaz S. Determination of vitreous interleukin-1 (IL-1) and tumour necrosis factor (TNF) levels in proliferative diabetic retinopathy. *Eye (Lond)*. 2006;20(12):1366–9.
23. Jousseaume AM, Poulaki V, Qin W, Kirchhof B, Mitsiades N, Wiegand SJ, et al. Retinal vascular endothelial growth factor induces intercellular adhesion molecule-1 and endothelial nitric oxide synthase expression and initiates early diabetic retinal leukocyte adhesion in vivo.

Am J Pathol. 2002;160(2):501–9.

24. Adamiec-Mroczek J, Oficjalska-Młyńczak J. Assessment of selected adhesion molecule and proinflammatory cytokine levels in the vitreous body of patients with type 2 diabetes--role of the inflammatory-immune process in the pathogenesis of proliferative diabetic retinopathy. *Graefes Arch Clin Exp Ophthalmol*. 2008;246(12):1665–70.
25. Miyamoto K, Khosrof S, Bursell SE, Rohan R, Murata T, Clermont AC, et al. Prevention of leukostasis and vascular leakage in streptozotocin-induced diabetic retinopathy via intercellular adhesion molecule-1 inhibition. *Proc Natl Acad Sci U S A*. 1999;96(19):10836–41.
26. Semeraro F, Cancarini A, Dell’Omo R, Rezzola S, Romano MR, Costagliola C. Diabetic retinopathy: Vascular and inflammatory disease. *J Diabetes Res*. 2015;2015:1-16.
27. Liu P, Anderson RG. Compartmentalized production of ceramide at the cell surface. *J Biol Chem*. 1995;270(45):27179-85.
28. Mathias S, Younes A, Kan C, Orlow I, Joseph C, Kolesnick RN, et al. Activation of the Sphingomyelin Signaling Pathway in Intact EL4 Cells and in a Cell-Free System by IL-1 β . *Science*. 1993;259(5094):519–22.
29. Schutze S, Potthoff K, Machleidt T. TNF Activates Phospholipase Sphingomyelinase NF-KB by Phosphatidylcholine-Specific C-Induced “ Acidic ” Breakdown. *Cell*. 1992;71(5):765–76.
30. Santana P, Peña LA, Haimovitz-Friedman A, Martin S, Green D, McLoughlin M, et al. Acid sphingomyelinase-deficient human lymphoblasts and mice are defective in radiation-induced apoptosis. *Cell*. 1996;86(2):189–99.
31. Haimovitz-Friedman A, Cordon-Cardo C, Bayoumy S, Garzotto M, et al. Lipopolysaccharide induces disseminated endothelial apoptosis requiring ceramide generation. *J Exp Med*. 1997;186(11):1831-41.
32. Marathe S, Schissel SL, Yellin MJ, Beatini N, Mintzer R, Williams KJ, et al. Human Vascular Endothelial Cells Are a Rich and Regulatable Source of Secretory Sphingomyelinase. *J Biol Chem*. 1998;273(7):4081–8.
33. Opreanu M, Tikhonenko M, Bozack S, Lydic TA, Reid GE, McSorley KM, et al. The unconventional role of acid sphingomyelinase in regulation of retinal microangiopathy in diabetic human and animal models. *Diabetes*. 2011;60(9):2370–8.
34. Chakravarthy H, Navitskaya S, O’Reilly S, Gallimore J, Mize H, et al. Role of Acid Sphingomyelinase in Shifting the Balance Between Proinflammatory and Reparative Bone Marrow Cells in Diabetic Retinopathy. *Stem cells*. 2016;34(4):972-83.
35. Bhatwadekar AD, Yan Y, Qi X, Thinschmidt JS, Neu MB, Li Calzi S, et al. Per2 mutation

- recapitulates the vascular phenotype of diabetes in the retina and bone marrow. *Diabetes*. 2013;62(1):273–82.
36. Bhatwadekar AD, Yan Y, Stepps V, Hazra S, Korah M, Bartelmez S, et al. MiR-92a corrects CD34+ cell dysfunction in diabetes by modulating core circadian genes involved in progenitor differentiation. *Diabetes*. 2015;64(12):4226–37.
 37. Roy S, Sala R, Cagliero E, Lorenzi M. Overexpression of fibronectin induced by diabetes or high glucose: phenomenon with a memory. *Proc Natl Acad Sci U S A*. 1990;87(1):404–8.
 38. Grant MB, Caballero S, Tarnuzzer RW, Bass KE, Ljubimov a V, Spoerri PE, et al. Matrix metalloproteinase expression in human retinal microvascular cells. *Diabetes*. 1998;47(8):1311–7.
 39. Kowluru RA, Santos JM, Mishra M. Epigenetic modifications and diabetic retinopathy. *Biomed Res Int*. 2013;2013:635284.
 40. Busik J V., Mohr S, Grant MB. Hyperglycemia-Induced reactive oxygen species toxicity to endothelial cells is dependent on paracrine mediators. *Diabetes*. 2008;57(7):1952–65.
 41. Gulbins E, Grassmé H. Ceramide and cell death receptor clustering. *Biochim Biophys Acta*. 2002;1585(2–3):139–45.
 42. Marchesini N, Hannun YA. Acid and neutral sphingomyelinases: roles and mechanisms of regulation. *Biochem Cell Biol*. 2004;82(1):27–44.
 43. Opreanu M, Lydic T a, Reid GE, McSorley KM, Esselman WJ, Busik J V. Inhibition of cytokine signaling in human retinal endothelial cells through downregulation of sphingomyelinases by docosahexaenoic acid. *Invest Ophthalmol Vis Sci*. 2010;51(6):3253–63.
 44. Paris F, Fuks Z, Kang A, Capodiec P, Juan G, Haimovitz-friedman A, et al. Endothelial apoptosis as the the Primary Lesion Initiating Intestinal Radiation Damage in Mice. *Science*.2001;293(5528):293–7.
 45. Garcia-barros AM, Paris F, Cordon-cardo C, Lyden D. Tumor Response to Radiotherapy Regulated by Endothelial Cell Apoptosis.*Science* .2003;300(5622):1155–9.
 46. Schatteman GC, Hanlon HD, Jiao C, Dodds SG, Christy BA. Blood-derived angioblasts accelerate blood-flow restoration in diabetic mice. *J Clin Invest*. 2000;106(4):571–8.
 47. Asahara T, Masuda H, Takahashi T, Kalka C, Pastore C, Silver M, et al. Bone marrow origin of endothelial progenitor cells responsible for postnatal vasculogenesis in physiological and pathological neovascularization. *Circ Res*. 1999;85(3):221–8.
 48. Asahara T, Murohara T, Sullivan A, Silver M, Van R, Asahara T, et al. Isolation of

Putative Progenitor Endothelial Cells for Angiogenesis *Science*.1997;275 (5302):964–7.

49. Takahashi T, Kalka C, Masuda H, Chen D, Silver M, et al. Ischemia - and cytokine - induced mobilization of bone marrow- derived endothelial progenitor cells for neovascularization. *Nat Med*. 1999;5(4):434-8.
50. Tepper OM, Galiano RD, Capla JM, Kalka C, Gagne PJ, Jacobowitz GR, et al. Human endothelial progenitor cells from type II diabetics exhibit impaired proliferation, adhesion, and incorporation into vascular structures. *Circulation*. 2002;106(22):2781–6.
51. Chen Y, Lin S, Lin F, Wu T, Tsao C. High Glucose Impairs Early and Late Endothelial Progenitor Cells by Modifying Nitric Oxide – Related but Not Oxidative Stress – Mediated Mechanisms. *Diabetes*. 2007;56(June):1559–68.
52. Catapano ER, Arriaga LR, Espinosa G, Monroy F, Langevin D, López-Montero I. Solid character of membrane ceramides: A surface rheology study of their mixtures with sphingomyelin. *Biophys J*. 2011;101(11):2721–30.
53. Bhatwadekar AD, Guerin EP, Jarajapu YPR, Caballero S, Sheridan C, Kent D, et al. Transient inhibition of transforming growth factor- β 1 in human diabetic CD34+ cells enhances vascular reparative functions. *Diabetes*. 2010;59(8):2010–9.
54. Chakravarthy H, Beli E, Navitskaya S, O'Reilly S, Wang Q, Kady N, et al. Imbalances in mobilization and activation of pro-inflammatory and vascular reparative bone marrow-derived cells in diabetic retinopathy. *PLoS One*. 2016;11(1):1–21.
55. Wang Q, Navitskaya S, Chakravarthy H, Huang C, Kady N, Lydic TA, et al. Dual Anti-Inflammatory and Anti-Angiogenic Action of miR-15a in Diabetic Retinopathy. *EBioMedicine*. 2016;11:138–50.
56. Méndez-Ferrer S, Lucas D, Battista M, Frenette PS. Haematopoietic stem cell release is regulated by circadian oscillations. *Nature*. 2008;452(7186):442–7.
57. Wang CY, Wen MS, Wang HW, Hsieh IC, Li Y, et al. Increased vascular senescence and impaired endothelial progenitor cell function mediated by mutation of circadian gene *Per2*. *Circulation* 2008; 118(21):2166-73.
58. Tsinkalovsky O, Smaaland R, Rosenlund B, Sothorn RB, Hirt A, Steine S, et al. Circadian variations in clock gene expression of human bone marrow CD34+ cells. *J Biol Rhythms*. 2007;22(2):140–50.
59. Mendez-Ferrer S, Andrew C, Merad M, Frenette PS. Circadian rhythms influence hematopoietic stem cells. *Curr Opin Hematol*. 2009;16(4):235–42.
60. Abrahamsen JF, Smaaland R, Sothorn RB, Laerum OD. Variation in cell yield and proliferative activity of positive selected human CD34+ bone marrow cells along the

circadian time scale. *Eur J Haematol.* 1998;60(1):7–15.

Chapter 4. Summary and future perspectives

4.1 Summary

- The studies presented in chapter 2 are conceptually innovative, showing that not only does dyslipidemia participate in diabetic retinopathy but also it has a role in blood retinal barrier (BRB). We explore a novel concept that ELOVL4 plays an important role in the blood retinal barrier (BRB) maintenance via the production and incorporation into the tight junctions of specific species of ceramides previously found in skin permeability barrier; omega-linked acyl-VLC ceramides. We proposed that diabetes induced down-regulation of retinal ELOVL4 results in reduced production of very long chain ceramides. This in turn contributes to increased retinal vascular permeability.

Using Bovine retinal endothelial cells (BRECs) as a model of inner blood retinal barrier, overexpression of hELOVL4 using adenoviral vector system significantly decreased basal permeability and prevented VEGF and IL-1 β -induced increase in permeability. Importantly, hELOVL4 overexpression prevented VEGF-induced decrease in occludin expression and border staining of tight junction proteins; ZO-1 and claudin-5. Interestingly, knock down of ELOVL4 was associated with increased paracellular permeability. Ceramides were found to co-localize with tight junction complexes. Lipidomic analysis of tight junction isolates revealed the presence of VLC ceramides.

In order to determine the effect of ELOVL4 on diabetes-induced blood retinal barrier dysfunction in vivo, we used streptozotocin mouse model of diabetic retinopathy treated

with intravitreal injections of hELOVL4-AAV2. We demonstrated that AAV2 mediated delivery of hELOVL4 prevents diabetes-induced increase in retinal vascular permeability. These findings are consistent with the results obtained in BRECs, supporting the curative potential of hELOVL4 vector.

- Continuing the studies in Chapter 2 where we investigated the role of diabetes-induced dyslipidemia in retinal vascular permeability, Chapter 3 describes the effect of dyslipidemia on the function of both cell types involved in revascularization; mature retinal endothelial cells and circulating angiogenic cells (CACs).

Using primary cultures of human retinal endothelial cells (HRECs) isolated from control and diabetic donor tissue and human CD34⁺ CACs from control and diabetic patients. We demonstrated that diabetes induced ASM activation, a key enzyme of sphingolipid metabolism, in retinal endothelial cells and CD34⁺ CACs. Diabetes induced ASM upregulation has deteriorative effect on both retinal endothelial cell and CD34⁺ function. Where diabetic HRECs with high ASM showed defective ability to form blood-vessel-like tubular structure. Moreover, diabetic CD34⁺ CACs with high ASM showed defective incorporation into endothelial tubes.

- Collectively, these data indicate that dysregulation of retinal sphingolipid metabolism play role in the development of diabetic retinopathy. Normalizing the ratio between pro-barrier long chain ceramides and pro-inflammatory and pro-apoptotic short chain ceramides through the control of ELOVL4 and ASM may represent a novel

therapeutic strategy for the prevention of diabetic visual impairment.

4.2 Future perspectives

1. We demonstrated the presence of omega-linked acyl VLC ceramides in native tight junction. However, it is important to identify the changes in the abundance of these species of VLC ceramides in cells transduced with or without recombinant ELOVL4 and in ELOVL4 knock down cells.

2. Several studies have shown the protective anti-apoptotic effect of VLC ceramides. In this study we have postulated that ELOVL4 produced VLC ceramides may act as bridges between tight junction proteins stabilizing these proteins against degradation. However, it would be useful to identify if there are different mechanisms by which ELOVL4 can reduce paracellular permeability through neutralizing cytokine or growth factor induced increase in permeability.

3. The exact confirmation of VLC ceramides in the tight junction structure is not known. It would be important to visualize the tight junction structure in its native environment to show the exact configuration of lipid in interaction with tight junction protein. This can be achieved using the cryo-electron microscopy technique.

4. Our lab has previously demonstrated that increase in ASM activity in diabetic CACs in animal model was associated with accumulation of membrane short chain ceramides, thereby decreasing membrane fluidity and impairs migration of CACs. Hence it is important to confirm the effect of high ASM on membrane ceramide levels and membrane rigidity in human CD34⁺ CACs isolated from diabetic individuals.

The potential use of gene therapy using AAV serotype 2 as a vector for the treatment of different retinal diseases is being evaluated in several clinical trials. In this context, a gene-

based therapy involving intravitreal injection of AAV2 expressing hELOVL4 in diabetic patients during their preclinical stage could have significant utility in the treatment of diabetic retinopathy. We examined the beneficial effect of ELOVL4 in vitro, using the bovine retinal endothelial cells as model of the inner blood retinal barrier, and in vivo through STZ induced diabetic mice as a model of type I diabetes.

Before progressing to clinical trials in humans we need to perform additional, confirmatory preclinical studies addressing basic questions on AAV2-mediated hELOVL4 expression; dosing, safety, toxicity, tissue distribution after intravitreal administration. As we examined its protective effect on a type I diabetic model, it would be important to test its beneficial effect on several animal models of diabetic retinopathy; type II diabetic mice to confirm its effect in both types of diabetes. Then shifting to large animal model of Diabetic Retinopathy (DR), such as diabetic pigs. The pig model has the advantage that it possesses retinal vascular system very similar to that of humans. Most importantly, the pig model develops signs of DR within 18 weeks after induction of diabetes compared to the dog model and rhesus monkey model, which develop retinopathy after years of diabetes induction.

After these additional studies, including safety, tolerability and therapeutic dosing, a pilot study could be carried in small number of human subjects to ensure safety and tolerability before progressing into phase I clinical trial. The available evidence that rAAV mediated-gene therapy holds great promise in treatment of different retinal diseases with great safety and long lasting efficacy, suggests that delivery of hELOVL4 could serve as a novel gene therapeutic target for DR patients.

Overall, our studies indicate that correcting sphingolipid metabolism in diabetic retina and CACs could treat vasodegeneration, enhance vessel repair and thus prevent progression into PDR stage.